Physics 134

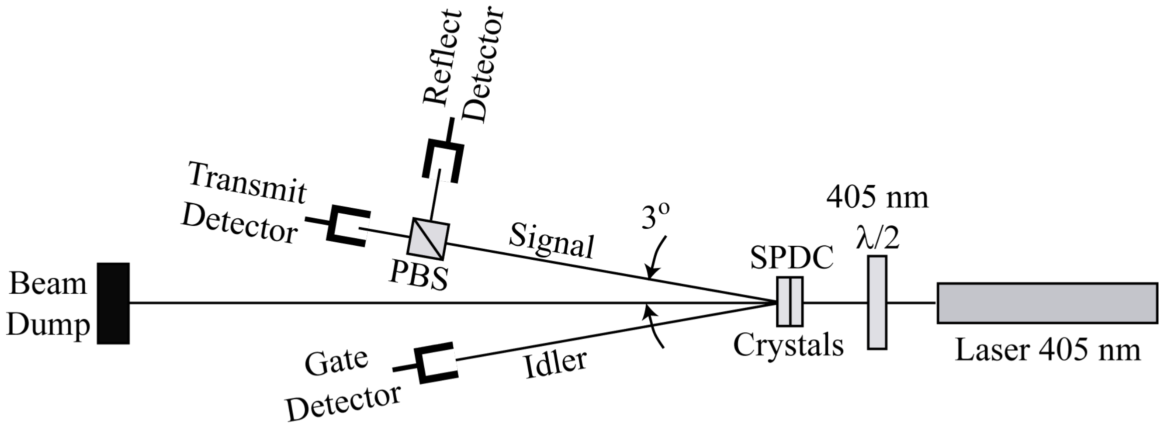

Optics Laboratory

Spring 2020

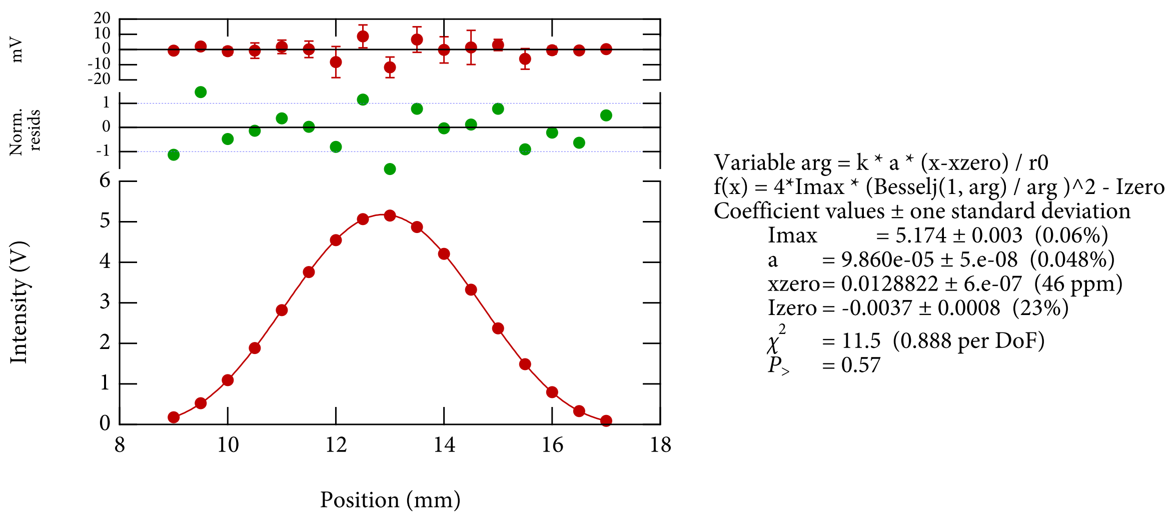

Semester Calendar

The notation “1–1” indicates the first experiment of the semester, and the first week of three weeks spent on that experiment. “3–2” means the third experiment of the semester, and the second of three weeks spent on that experiment.

Meeting	Week	Thursday	Friday
1	Mon, Jan 20 to Fri, Jan 24	1-1	1-1
2	Mon, Jan 27 to Fri, Jan 31	1-2	1-2
3	Mon, Feb 3 to Fri, Feb 7	1-3	1-3
4	Mon, Feb 10 to Fri, Feb 14	2-1	2-1
5	Mon, Feb 17 to Fri, Feb 21	2-2	2-2
6	Mon, Feb 24 to Fri, Feb 28	2-3	2-3
7	Mon, Mar 2 to Fri, Mar 6	3-1	3-1
8	Mon, Mar 9 to Fri, Mar 13	3-2	3-2
9	Mon, Mar 16 to Fri, Mar 20	Spring Break	
10	Mon, Mar 23 to Fri, Mar 27	3-3	3-3*
11	Mon, Mar 30 to Fri, Apr 3	TR-1	TR-1
12	Mon, Apr 6 to Fri, Apr 10	TR-2	TR-2
13	Mon, Apr 13 to Fri, Apr 17	TR-3	TR-3
14	Mon, Apr 20 to Fri, Apr 24	TR-4	TR-4
15	Mon, Apr 27 to Fri, May 1	Reports due	

* Because this meeting would occur on a school holiday (César Chávez Day), this meeting should be rescheduled individually with Prof. Lyzenga.

Caution

Summary reports are due **before noon two days before the first lab meeting for the next experiment**. Please aim to have the work submitted on time. To handle unavoidable time crunches, you will start with a bank of 5 late days, which can be used at any point during the semester without penalty. Once the bank is exhausted, your grade will be reduced for each day your report is late.

The 60-minute final exam will be given on Friday, May 8 at 1:30 PM.

Introduction

This laboratory/lecture course is designed to

1. reinforce and extend your skills in designing an experiment to test a hypothesis, and to fine-tune your expertise in rigorously analyzing the results of your measurements to determine if the hypothesis has been disproved or supported by your experimental studies;
2. extend your knowledge of theoretical optics and introduce new experimental techniques in optics;
3. engage you in performing interesting and challenging experiments in optics, pique your interest in experimental physics, and inspire you to pursue a career in science.

The course consists of 3 laboratory experiments, one technical report project, and roughly 20 lectures with two associated problem sets. There is also a 60-minute final exam. The experiments are to be chosen from eight possible experiments that are currently set up in the laboratory. The lectures will be given during the first half of the semester, at 10:00 on Monday, Wednesday, and Friday in of each week Shanahan 3465. **The first lab meeting will be a working session!** It is important that you read the lab manual and indicate to your instructor by email which experiment you would like to perform first.

A schedule of lab meetings appears on page ii. Three laboratory meetings are allotted for each of the experiments. The lab instructions leave a good deal of room for your own creativity, so you will need to think carefully about each experiment **before** coming to lab. References are given in the laboratory instructions to background reading material which can be found in the main laboratory, Jacobs B121. You are encouraged to browse through the books and read them in the lab, but **please do not remove these books from the lab**! If you photocopy the sections or chapters of interest, we can all share the books harmoniously.

Time in the laboratory will be tight unless you arrive well prepared. To encourage you to do this, we are requiring **reading logs**. That is, by noon of the day of the first lab meeting for each experiment, you must send your instructors an email message demonstrating that you understand the main point of the experiment. In addition, you should include any questions that have already occurred to you. At the discretion of your instructor, there may be additional reading logs required for later days in the experiment.

Laboratory notebooks are an important part of this lab course and will be primarily a diary of what you do in the laboratory; they should also include an informal summary of results, data analysis, and conclusions at the end of each week's work. At the end of each experiment, a formal summary with data plots, measured values with uncertainties, and any final insights should be integrated into a LaTeX document ("summary report"). These reports are typically 3–5 pages long in Physical Review format. The source files and a pdf version should be submitted on Sakai. These electronic "summary reports" will be archived and shared with future students who are pursuing topics that overlap with your work. Reports of an experiment are due two days before the first lab meeting of the next experiment, so that you will have time to prepare for the next experiment. That is, the Thursday section will submit reports on Tuesday before noon, and the Friday section will submit them on Wednesday before noon; see the calendar on page ii. A sample report is posted on Sakai.

There will be a multiple choice **final examination** given at the end of the semester. Questions on the exam will cover the material in the lectures, problem sets, and all experiments set up in the laboratory. However, the exam will be graded so that you can obtain a score of 100 even if you choose not to answer the questions pertaining to the experiments that you have not performed.

The grades on the three summary reports, the technical report, and the combined grades in the homework, reading logs, and final exam will be equally weighted (1/5 each) to derive the final grade in the course. **As a general rule, the grade for a late notebook writeup will be reduced based on how late the work is submitted**. Each student starts the semester with a bank of 5 late days. After those are exhausted, penalties accrue. Exceptions will of course be made for illness, natural disasters, or similar unusual circumstances. Please be sure to apprise your instructor of potentially extenuating circumstances.

This course carries two units of academic credit, and hence you should be devoting an **average** of 6 hours/week (absolute maximum average of 8 hours/week) to the course. This figure includes the 3-hour lab session and 1.5 hours of lecture (averaged over the semester) each week. If you find that you must spend more time than this to complete the work to your satisfaction, please notify your instructor. We intend this course to pique your curiosity and provide an outlet for your creativity, not to beat you senseless with a heavy load of required work. If you enjoy this course as much as the instructors do, it will be a high point of your semester.

Contents

Lab Reports as Scientific Papers

Your lab reports for Physics 134 may be quite different from the short lab summaries you have prepared for other courses. A Physics 134 report should be in the style of a scientific research publication: a self-contained exposition of the question, the approach you took to answering it, and the results you obtained. The report should be understandable and convincing to, let's say, a future junior physics major, without reference to either the lab manual or your lab notebook. Your lab report is both a scientific investigation *and* a piece of writing, so **good writing is important**.

Your report should respect the conventions described in the American Institute of Physics "Guide for Metric Practice," which is available on the department website at writing. **Please write in LaTeX using the documentclass revtex4-2 to use RevTeX 4.2**, the standard for submission to APS and AIP journals. See the Department LaTeX page for more information on getting started with LaTeX and for using RevTeX. A sample RevTeX report is posted on Sakai.

Suggestions for writing the report

- Remember your audience, and make sure your paper is clear and compelling to a reader who is unfamiliar with the Physics 134 experiments. You might ask a friend who isn't in Physics 134 to read your draft and tell you what they think they learned from it.

- The heart of a physics paper is the graph (or graphs) that summarize your principal results. Everything that appears in your paper before this figure leads up to the figure, and everything that appears after it discusses its significance. To lead up to your central figure, you must motivate your investigation (answer the "so what?" question), explain the approach you took in your investigation, and explain your setup and procedure in enough detail to clearly define all the data shown in the figure. To discuss the significance of your central figure, you must explain the logical or theoretical basis for your interpretation of the figure, interpret the figure (including uncertainties!) fairly, and suggest possible extensions and applications of your work.

- Refer to the specific content guidelines on the next page.

- Examine past lab reports or sample scientific articles, paying attention to style and format choices. For example, all figures should have figure numbers and informative captions. Figures should "float" to the top or bottom of a page, and should therefore be referenced in at least one appropriate place in the main body of the paper by number, *not position*. That is, do not reference the "figure below," since its position may shift during typesetting. Numbered in-text citations should refer to entries in a later "References" section. An example report is posted on Sakai in both source and PDF format.

- *Your lab report should be self-contained so that a reader can find it clear and convincing without referring to material that is only contained in the lab manual or your lab notebook. Figures should be made properly (see the section on Graphs below) and saved for inclusion in a vector graphics format (e.g., PDF), not a bitmapped format (e.g., PNG or JPG).*
- Reports should be submitted to your Sakai drop box, both in source and pdf format. Prepare a folder for each report, and place figures and source files (.tex or .ltx) in the folder.
- The scientific community and funding agencies place increasing importance on data archiving. In that spirit, you should upload your data to the same drop box folder that contains the corresponding report, in the format(s) you employ (typically spreadsheets and Igor experiment files).

Specific content guidelines

Except for the title and abstract, these are merely guidelines for the information your report should contain, NOT requirements or even suggestions for section headings within your report. Organize the main body of your report in any way that tells the story of your investigation clearly and logically. ***Focus on your own work, the choices you made, the approach you took, the data you took and its analysis.***

Title Your report should begin with a *title* .

Abstract Next comes a 2–5-sentence *abstract* saying what you set out to measure/investigate, what method you used, *and* what results you found. This is something like the thumbnail version of the rest of your report. After the abstract, start the text of the report itself; the main body should *not* refer back to the abstract.

Introduction/Motivation

- What question are you investigating? Do not assume that the reader is familiar with Physics 134 experiments already, so be sure to give some context.
- Why is this investigation interesting? (for example, illustration of an important principle? relationship to a technology? Discrepancies that many groups have seen and you can explain? Particular challenge? Other?)
- What if any expectations and/or hypotheses did you have as you started the datataking? Why?

Theory and Methods

- Write this for a reader who *does not know* what you did in lab or what equipment you had available to you. This should be a logical exposition of what you did to obtain the final result, and *why* each step was important or relevant. Attention to detail is important.

- Make sure all symbols are defined at their first use; use acronyms sparingly.
- Carefully labeled drawings are very helpful. These should be referenced from the text by Fig. # and pushed to either the top or bottom of the page.
- Consider presenting some theoretical background for your investigation. You need not show each step of a derivation, but the starting points (including approximations and assumptions) should be clearly set up, and the final result should be prominently reported.

Results/Discussion

- Make sure quantities are well defined. Units and errors are also important.
- It is neither necessary nor desirable to include all your raw data in the paper, but it should be clear how the raw data were processed to obtain the included graphs. For example, how many trials contributed to each data point and error bar? How were important quantities measured?
- Explain the source of any quoted uncertainty estimates (statistical variation, instrument precision, etc.).
- Data should be analyzed (plotted, fitted, compared with theory, etc.) logically and understandably. Graphs should include titles, axis labels, units, and error bars. Fit formulas should correspond to appropriate theory. Data should be properly combined to give final answers that address the original question as far as possible. Uncertainties should be reasonably treated.
- Clearly state comparisons to theory or to "known" values, and include source citations or derivations if necessary for the theory or known values. Discuss the statistical significance (or lack thereof) of your result(s).

Conclusions

- What light do your data and analysis shed on the original question/hypothesis?
- If there is a firm theoretical prediction, does the experiment agree with the theory? If so, with what precision can you confirm theory? If not, by how much is it off (relative to uncertainty)?
- If the experiment was designed to measure an unknown quantity or effect, what is your result? How precise can you claim it is?
- What are the major sources of systematic and random error in your experiment? What extensions/improvements suggest themselves if you had 1 or 2 more lab sessions?
- Point out the relevance of your work to future Physics 134 experimenters or to other situations if appropriate.

Cite references where appropriate e.g., lab manual, textbooks, and other sources of inspiration. Each reference you include in a list at the end of your paper should be cited at one or more particular points in the body of the paper.

A Word on Scientific Graphs

Scientific results are nearly always communicated with graphs rather than tables, which are reserved for lists of parameters or other catalogs. While it can be satisfying to prepare a data plot by hand (if you have no other choice and a gun to your head), you will undoubtedly use some public-domain or commercial software package. Common choices include spreadsheets, MATLAB, R, matplotlib, Igor, *Mathematica*, Origin, or even tikz or pgfplots in LaTeX. In my experience, the default properties of scatter plots in most programs leave much to be desired and need to be modified, ideally in a consistent way to permit direct incorporation of plots into notebooks, presentations, publications, and posters. My thesis advisor, Eric Mazur, developed a template in Adobe Illustrator in the late 1980s and still insists that his graduate students and postdocs produce plots consistent with that template and a restricted color scheme. Consistency makes it easy to produce presentations spanning different projects (and even eras) without having to remake figures. Doing it right the first time, particularly if you have scripts to take away the tedium, is the way to go.

Since we will be using Igor Pro a fair amount in this course, I will illustrate the procedure using Igor Pro 7 and the HMC menu, which contains routines I have written to simplify the fixes. Let's take a look using some excellent data on the Fraunhofer diffraction pattern of a circular aperture that was taken by Chris Moore ('05) when he took the course in 2004. If I just use Igor's defaults, either from the menu, or using the command

```
Display Iw vs xw
```

I get a graph in which the data points are shown connected, axes are not mirrored, tick marks

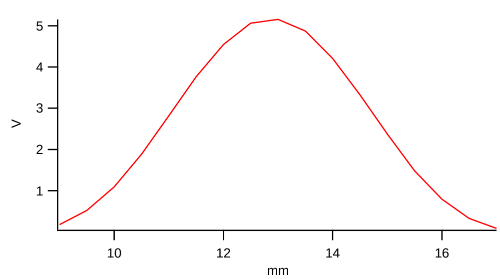

(a) Default graph format in Igor Pro.

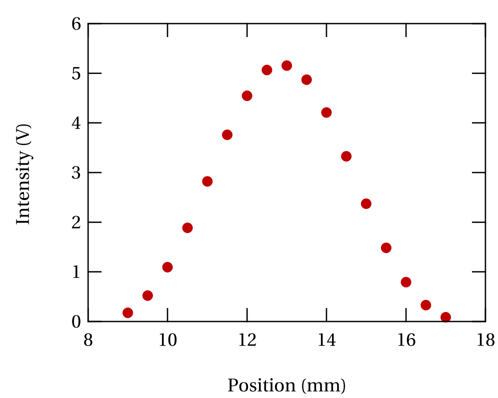

(b) After **FixGraph**.

Figure 1: The **FixGraph** command from the HMC menu performs a number of operations on a graph to put it more standard form, including setting the aspect ratio, displaying data points as discrete points, adding error bars if found, and labeling axes from the plotted wave names.

go out instead of in, and the font is a bit on the small size, as shown in Fig. 1a. It is preferable to represent discrete points with markers, not a continuous curve, unless they are quite numerous. If I now use the **Fix Graph** command from the HMC menu, these issues are corrected (Fig. 1b).

The graph isn't finished, however: we have not yet compared the data to theoretical expectations. In this case, the expected dependence of intensity on position x is given by

$$I(x) = I_0 + A\left(\frac{2J_1[ka(x-x_0)/r_0]}{ka(x-x_0)/r_0}\right)^2 \tag{1}$$

where x_0 is the position of the peak, $k = 2\pi/\lambda$, a is the radius of the aperture, and r_0 is the distance from the aperture to the detector plane. See Appendix A for details on how to define this fitting function in Igor Pro. After performing a nonlinear least squares fit and asking Igor to add the residuals to the plot, we get the rather inconvenient graph shown in Fig. 2a. However, running the **Add ChiSq Information** command from the HMC menu moves the fitting information to a more convenient location and adds important additional information, including the value of χ^2. Most of the graphs you will generate in the course will likely have this information displayed on them to guide your discussion of the extent of agreement between the data you have taken and theoretical expectations. For a formal publication, however, you would remove this information

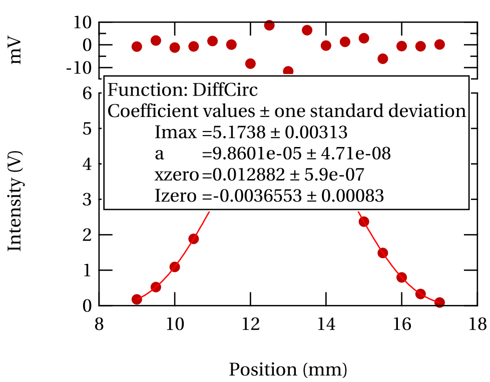

(a) After fitting

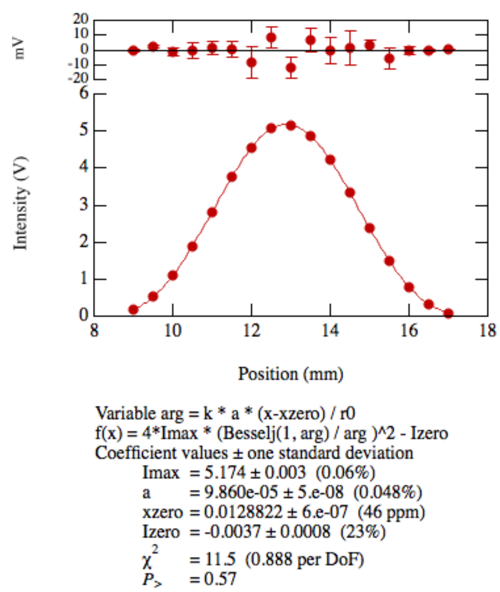

(b) After **Add ChiSq Information**.

Figure 2: The **Add ChiSq Information** command moves the fit information out of the way, includes the code for the fitting function, adds the values of χ^2 and $\tilde{\chi}^2$, and copies the error bars to the residuals. It also adds buttons at the top of the graph to move the fit information to the right side and to compute and display normalized residuals.

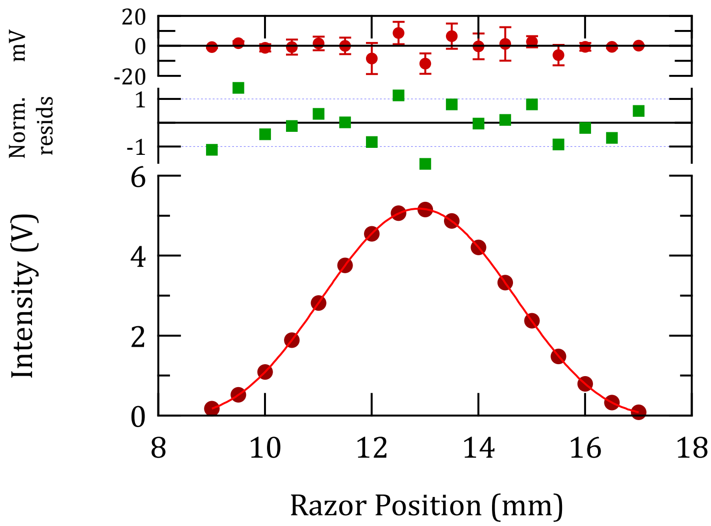

Figure 3: An example graph showing light intensity vs razor position for the Fraunhofer diffraction pattern from a circular aperture. Data taken by Chris Moore ('05) in 2004.

and summarize the necessary parts in the figure's caption. Figure 3 shows such a finished graph, to which a panel of normalized residuals has been added using the button at the top of the graph that is installed by the **Add Chisq Information** command. For your technical report, you should prepare clean graphs such as this one.

Experiment 1

Fraunhofer and Fresnel Diffraction
Diffraction Patterns of a Circular Aperture and a Straight Edge

References

- *Optics* by Eugene Hecht, Chapter 10
- *Introduction to Modern Optics* by Grant Fowles, Chapter 5
- *Principles of Optics* by Max Born and Emil Wolf, Chapter 8
- The following reference contains a superb treatment of Gaussian spherical beams: *An Introduction to Lasers and Masers* by A.E. Siegman, Chapter 8

1.1 Introduction

This experiment will extend your knowledge of Fraunhofer diffraction and introduce you to situations in which the more general Fresnel diffraction calculations are required. In Section I you will measure the Fraunhofer diffraction pattern produced by a circular aperture and compare your data with the predictions of scalar diffraction theory. In Section II you will spatially filter a helium-neon laser beam and study the famous Fresnel diffraction pattern of a straight edge.

In both parts of the experiment, you will want to begin by simply looking at the diffraction pattern you are attempting to measure. Then become familiar with the measurement capabilities and limitations of the experimental setup. With this knowledge you can then think and plan carefully to obtain the best possible measurements of your diffraction patterns in a reasonable amount of time.

Once you have taken your data appropriately (in Section I or in Section II), this experiment affords an excellent opportunity to witness the power of error analysis and nonlinear χ^2 fitting.

Take your results seriously and expect to obtain good fits with reasonable χ^2 values and random residuals. If you don't achieve them, you should investigate and understand any effects which keep you from getting them!

1.2 Fraunhofer Diffraction Pattern of a Circular Aperture

You should read carefully an account of the calculation of the Fraunhofer diffraction pattern produced by a plane wave incident upon a circular aperture. Most introductory optics texts include this calculation, and *you should write your own version in your notebook*. The references listed above have good treatments of scalar diffraction theory, although you are encouraged to consult any of the other optics texts available to you.

We would like to test the prediction that the intensity in the diffraction pattern is given by

$$I(\theta) = 4 I_{\max} \frac{[J_1(ka\sin\theta)]^2}{(ka\sin\theta)^2} \tag{1.1}$$

where θ is the angle of diffraction, $k = 2\pi/\lambda$, a is the **radius** of the aperture, and J_1 is the Bessel function of first order. The experimental setup includes a 5-mW helium-neon laser (JDS Uniphase Model 1125P, $\lambda = 632.8\,\mathrm{nm}$), a circular aperture with a *diameter* of roughly $200\,\mu\mathrm{m}$, and a photodiode detector with amplifier. **Do not touch the circular aperture; finger grease and dead skin cells severely degrade the quality of the diffraction pattern.** With this equipment you can record the intensity at a number of points in the diffraction pattern, and then fit the data to the functional form of Eq. (1.1). Appendix A at the end of the lab manual describes how to perform the nonlinear least squares fit to the circular aperture data using Igor Pro.

Start by directing the laser beam onto the 200-µm-diameter aperture. (See Fig. 1.1.) The diffraction aperture is mounted on an optical rail carrier with horizontal and vertical translation, so the aperture can be centered in the laser beam. At the output of the laser, the beam forms a waist (Gaussian spherical beam waist) with a spot diameter of $2w_0 = 0.83\,\mathrm{mm}$. In other words, the surface of constant phase of the electric field is a plane, and a circular aperture with a diameter of 0.83 mm will pass 86% of the beam power. The intensity of the beam falls off in the transverse direction (i.e., perpendicular to the beam propagation) as $\exp\left(-2r^2/w_0^2\right)$ where r is the distance from the beam axis. The finite diameter of the beam effectively forms an aperture through which the beam is continuously diffracting, so the beam is often described as "diffraction-limited." This process of diffraction leads to divergence of the beam as it propagates away from the laser output (in our case, along the optical rail); the beam divergence half-angle is $\theta_{1/2} = \lambda/\pi w_0 = 0.05\,\mathrm{mrad}$. Most treatments of Fraunhofer diffraction from a circular aperture assume a constant intensity over the aperture. **You will have to decide what distance s you want between the laser and the diffraction aperture so that the intensity over the area of the aperture is roughly constant.**

There are other considerations in arranging the experimental setup. The distance s from laser to diffraction aperture and the distance r from diffraction aperture to the photodiode detector

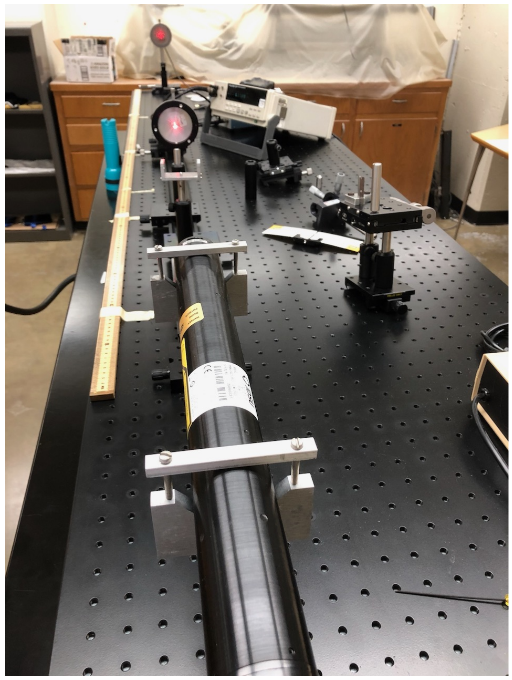

Figure 1.1: The experimental setup for measuring the Fraunhofer diffraction pattern of a circular aperture. The HeNe laser is at the bottom and its red beam impinges upon the 200-μm-diameter circular aperture to the right of the green flashlight. The diffraction pattern appears as a red blob on the photodetector at the top of the image.

should be chosen so that the following *Fraunhofer condition* is satisfied:

$$\frac{s}{d} \gg \frac{d}{\lambda} \qquad \text{and} \qquad \frac{r}{d} \gg \frac{d}{\lambda} \tag{1.2}$$

where $d = 2a$ is the diameter of the diffraction aperture. When this condition is satisfied (a ratio of 10 should do) the diffraction pattern formed on the detector aperture is the Fraunhofer pattern. The detector aperture (the aperture immediately in front of the photodiode) must be chosen judiciously. Larger apertures allow more light to hit the photodiode and hence give more signal, but they average over a larger area of the diffraction pattern. (Note that since the active area of the photodiode is roughly 2.5 mm in diameter, there is no point in using a detector aperture with a diameter larger than 2.5 mm.)

You should choose a detector aperture which is the optimal compromise between too little signal and too much spatial averaging. Of course, increasing the distance r between the diffraction aperture and photodiode also reduces the effect of spatial averaging and decreases the overall intensity on the photodiode.

Record the intensity at an appropriate number of points in the diffraction pattern. Uncertainties in the data points should be determined by forming a sample variance of several scans through the pattern.

The dependence of $I(\theta)$ in Eq. (1.1) on the fitting parameter a is certainly not linear. Bevington and Robinson §8.6 describe a computer program MARQUARDT which performs least squares fits to fitting functions which are nonlinear functions of fitting parameters. MARQUARDT is based on an algorithm published in 1963 by D. W. Marquardt (*J. Soc. Ind. Appl. Math.* **2**: 431–441 (1963)). This same algorithm, often called the Levenberg-Marquardt algorithm, is the basis of the nonlinear least squares fitting routines in the commercially available software packages, such as Igor Pro, Origin, or MATLAB. The Appendices at the end of the lab manual contain tutorials for these software packages.

The instructions in the Appendices will lead you step-by-step through the mechanics of fitting your data. The main challenge for you will be to apply your understanding of χ^2 fitting and error analysis in order to guide the fitting routine most efficiently and interpret its output sensibly.

Don't be upset if your value for the radius a of the aperture deviates from 100 µm. This value is a nominal value specified by the manufacturer with a tolerance of 10%. Concentrate on obtaining a good, self-consistent fit. *Aim to attempt a fit to your data while still in the laboratory, so that you can seek help from your instructor if you encounter difficulties using Igor Pro.*

1.3 Fresnel Diffraction by a Straight Edge

Read carefully an account of the calculation of the Fresnel diffraction pattern of a straight edge. Most optics texts treat this classic example; many students find the treatment in the reference by Fowles particularly clear. Astrophysicists measure the Fresnel diffraction pattern produced on the earth's surface by starlight as it passes the edge of the moon's disk (called lunar occultation). Deviations from the expected pattern for a point source enable them to deduce a value for the diameter of the star. The disk of the star is otherwise unresolvable by earth-bound telescopes.

You can create a point source with a substantial cone of light by spatially filtering the laser beam. The spatial filter consists of a microscope objective and a circular aperture, housed together. The microscope objective produces a focused waist of the laser beam shortly beyond the objective. The aperture transmits only the waist of the Gaussian spherical laser beam, and blocks stray reflections and imperfections in the beam. The final result is a beautiful cone of light with no peripheral imperfections — hence the name "spatial filter". Chapter 8 of the reference by Siegman contains an excellent description of Gaussian spherical beams.

Mount the spatial filter on the optical rail carrier with horizontal and vertical translation. (See Fig. 1.2.) Remove the 25-µm-diameter aperture from the spatial filter (after noting its orientation) and direct the laser beam through the microscope objective, using the horizontal and vertical translation of the carrier to center the objective on the laser beam. Replace the 25-µm-diameter aperture and use the horizontal and vertical micrometers on the spatial filter to maximize the intensity transmitted by the aperture. You may need to use the axial screw adjustment on the spatial filter to translate the microscope objective slightly forwards or backwards along

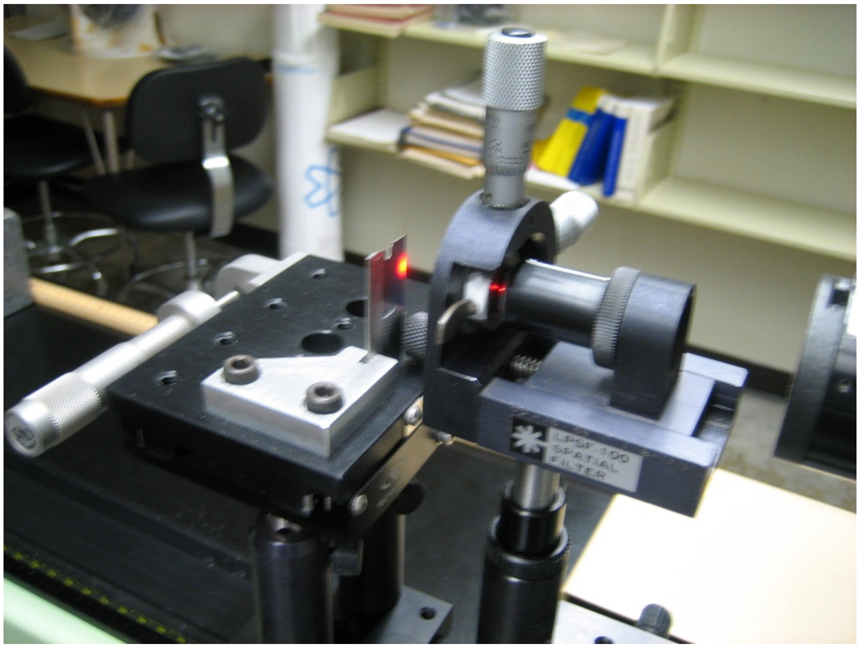

Figure 1.2: A spatial filter consists of a focusing lens (microscope objective) and a circular aperture. The laser beam is focused through the aperture while stray light from the laser resonator is caught by the edges of the aperture, leaving a very smooth and uniform beam incident upon the straight edge.

the beam path so that its focal plane coincides with the plane of the 25-μm aperture. When you have positioned the focused "waist" of the laser beam in the center of the 25-μm aperture, the transmitted intensity will be a maximum.

Direct the spatially filtered beam onto the razor blade, which is fastened to a micrometer-driven translator, which in turn is mounted on an optical rail carrier. Rather than translating the photodiode to scan the diffraction pattern, **you can simply translate the razor blade** using the micrometer. This procedure keeps the photodiode in the same portion of the spatially filtered beam. Use your ingenuity to devise a convenient geometry of spatial filter, razor blade, and detector. Compare your data with the predictions of Fresnel diffraction theory.

Some students in the past have become intrigued with the famous Poisson bright spot in the diffraction pattern of a ball bearing. In fact, if you point the spatially filtered beam at just about anything in the lab you'll see some fairly remarkable wave phenomena. You are certainly free to test any of the predictions of diffraction theory in addition to—or instead of—the examples suggested above, but be sure to clear your plans with your instructor.

1.3.1 Recording 2-D Diffraction Patterns with a CCD Camera

During the summer of 2012, the Physics Department purchased a CCD camera from Thorlabs (DCU224M, 1280 × 1024 pixels, B&W, sensitive area 5.95 mm × 4.76 mm, pixel area 4.65 μm × 4.65 μm, frame rate 15 fps, purchase price $2400). The camera communicates with a host computer via a USB 2.0 cable. This camera is available to us for recording 2-D diffraction patterns at speeds much, much faster than is possible by recording them point-by-point manually. And, of course, we can have a lot of fun fitting 2-D diffractions patterns or 1-D slices through these 2-D patterns with functions derived from Fraunhofer and Fresnel diffraction theory.

In Optics Lab during the spring of 2013, Peter Megson and Jaron Kent-Dobias (both HMC '14) used a red LED and crossed polarizers to demonstrate that the 1.3 megapixels of the DCU224M CCD camera respond linearly to incident light, and that the pixels are remarkably uniform across the entire array. (The tech reports of Peter and Jaron are available on the Sakai course site.) There is just one catch. A protective glass coverslip over the array results in an annoying interference pattern when a light source like a HeNe laser (with coherence length much longer than the thickness of the coverslip) is used to illuminate the camera. Jaron was able to reduce the effect of the interference pattern by a judicious normalization procedure, but we may want to explore ways to avoid the interference pattern altogether. For example, we could display a diffraction pattern of interest on a white screen and record the back-scattered light from the screen with the CCD camera. Or perhaps we could display the diffraction pattern of interest on a ground-glass screen and position the CCD camera to image the forward-scattered light transmitted through the ground-glass screen to the camera.

Actually, there is a second catch: the CCD camera's dynamic range is less than ideal for capturing in the same image the central maximum and the weaker peripheral rings in the diffraction pattern. You may need to develop a way to stitch together parts of the image with very different intensities.

There clearly is enormous potential for recording and fitting unusual 2-D diffraction patterns if we can successfully employ the CCD camera to record those patterns without artifacts. If you are interested in participating in the successful implementation of the camera to record and fit 2-D diffraction patterns, just chat with your instructor about how you can contribute to the mission! Work on the camera may replace some parts of Sections I and II if that seems appropriate, and there are certainly many opportunities here for ground-breaking technical report work!

Experiment 2

Grating Spectrometer

References

- *Optics* by Eugene Hecht. Section 10.2.8 contains a good discussion of gratings and grating spectroscopy.
- *Quantum Physics of Atoms, Molecules, Solids, Nuclei, and Particles* by Robert Eisberg and Robert Resnick.
- *Experimental Physics* by R.A. Dunlap. Chapter 10 contains a concise description of photomultiplier tubes.

2.1 Introduction

In this experiment you will become familiar with a research-quality grating spectrometer, the SPEX 500M, and use it to study the spectra of a variety of laboratory sources; e.g., Hg, Na, H, D, as well as the solar spectrum. There is considerable freedom to choose the measurements you will perform — just be sure to consult with your instructor regarding the light sources you are considering. The SPEX 500M is an impressive instrument with a resolution of 0.03 nm (0.3 Å) over a wavelength range 0–1500 nm, and it collects lots of light with an f-number of 4.0 (the *lower* the f-number, the better!).[1] The designation "500M" is shorthand notation for the 500 mm focal length of the spherical mirrors used in the instrument design. See the Appendix on page **??** for more details on the spectrometer design and components.

[1]A note on units. The SPEX 500M displays wavelengths in the non-SI unit of angstroms (10^{-10} m). While a lovely dimension, particularly as regards atomic radii, it is hardly more serviceable than the standard SI unit of nanometers when it comes to visible wavelengths. As a former employee of the National Institute of Standards and Technology (NIST), Prof. Saeta is duty-bound to eschew such archaisms. Hence, he wrote the Igor Pro software to work in nanometers, not angstroms.

Most of the first laboratory meeting will be needed to familiarize yourself with the instrument and to perform a calibration procedure with a cool (roughly room temperature) low pressure mercury source. Collision broadening of spectral lines in this source is negligible, and the Doppler width of lines is less than the resolution of the instrument. The narrow spectral lines of this source and the well-documented wavelengths of the mercury spectral lines make this source ideal for calibration.

The second and third lab meetings will be spent performing measurements of spectra of a number of different light sources. For example, the Balmer series in the hydrogen spectrum played a critical role in the development of modern quantum physics. You can perform measurements of this spectral series to test the predictions of the Bohr and Schrödinger theories of the hydrogen atom. With our SPEX 500M grating spectrometer the Rydberg constant can be measured to five or six significant figures. In addition, you can cleanly resolve the isotope shift in the hydrogen spectrum by comparing the spectra of hydrogen and deuterium which are present in the same special "Balmer tube" source.

Instead of studying the hydrogen spectrum, you may wish to study the spectrum of the Sun. While the general shape of the spectrum is that of a blackbody ($T \approx 5000°$C), there are many absorption lines due to cooler gaseous elements in the Sun's atmosphere. You are challenged to identify the spectral lines of as many elements as you can; for example, helium was first discovered during studies of the Sun's spectrum. Of course, some of the most famous solar lines are due to hydrogen. You may also wish to observe the Doppler shift in the Sun's spectrum due to solar rotation. It's not an easy measurement, but it's an exhilarating challenge!

All students are urged to measure the sodium doublet splitting using the low-pressure sodium street lamp. This splitting is the most famous example of spin-orbit coupling in elements of relatively low atomic number. Everyone is also urged to measure the width of the collision-broadened green line emitted by a high-pressure mercury source. The sodium doublet and the pressure-broadened mercury line are also studied in the Fourier transform spectroscopy experiment, so your observations in these two experiments will provide an interesting comparison of the two spectroscopic techniques.

2.1.1 The SPEX 500M Scanning Grating Spectrometer

Two top views of the optics of the spectrometer are sketched in Fig. 2.1. The entrance slit is located in the focal plane of the collimating mirror, and the exit slit is located in the focal plane of the focusing mirror. Hence, light emanating from a point in the entrance slit is collimated (parallel rays) onto the grating, and parallel rays diffracted from the grating at the correct angle are focused to a point in the exit slit. In the top panel of Fig. 2.1, light is incident upon the grating at an angle α, and the zero-order diffraction maximum ($m = 0$) is specularly reflected at an angle α and focused onto the exit slit. In the bottom panel of Fig. 2.1, the grating is rotated by an angle β so that light is incident upon the grating at an angle $\varphi = \alpha + \beta$. The light focused onto the exit slit must now be diffracted away from the specular reflection by an angle $\theta = 2\beta$. Hence the

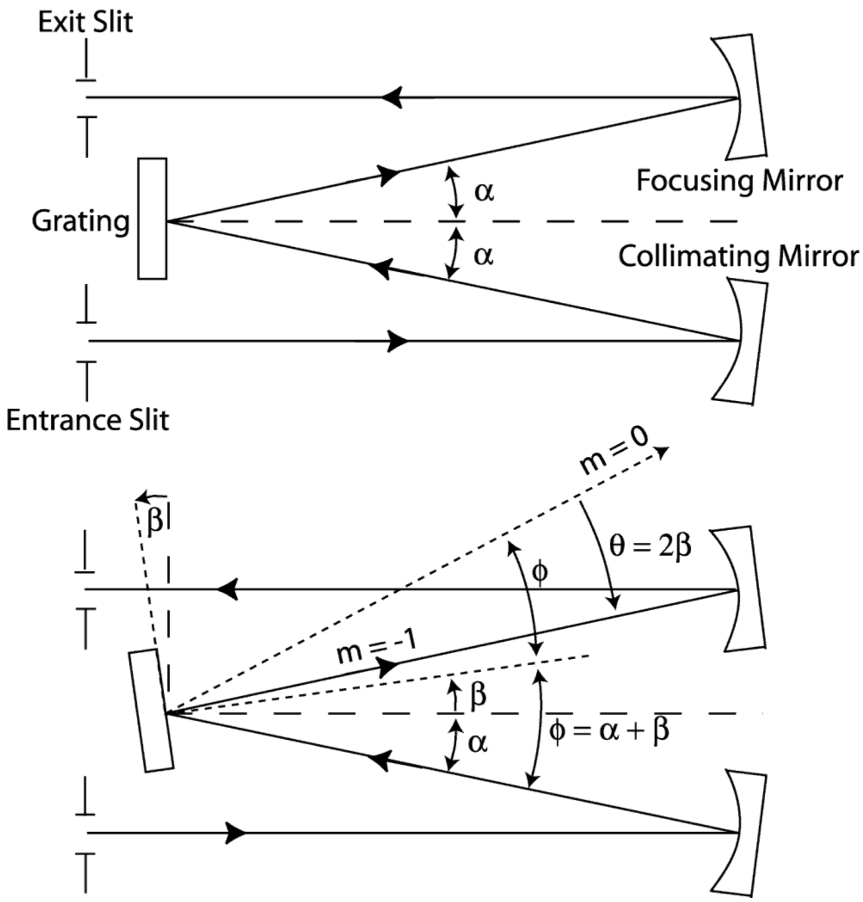

Figure 2.1: The design and operation of the SPEX 500M Spectrometer.

$m = -1$ diffraction maximum of wavelength λ appears at the exit slit, according to the relation

$$d \sin\varphi - d \sin(\varphi - \theta) = m\lambda \tag{2.1}$$

In Eq. (2.1), d is the grating period, m is the diffraction order, and λ is the wavelength.

Equation (2.1) can be derived readily by examining Fig. 2.2. In the left panel, two rays are incident upon the grating at angle φ with respect to the grating normal, and strike points a distance d apart, where d is the grating spacing. The upper ray travels a distance $d \sin\varphi$ further, as indicated in the figure. In the right panel, the two associated secondary spherical wavelets (from diffraction theory) are emitting in the direction of the focusing mirror at an angle of $\varphi - \theta$ with respect to the grating normal. This time the upper ray travels a distance $d \sin(\varphi - \theta)$ shorter. Considering the total path length to and from the grating, the upper ray travels a longer distance, $d \sin\varphi - d \sin(\varphi - \theta)$. When this extra distance is equal to an integer number of wavelengths $m\lambda$, the

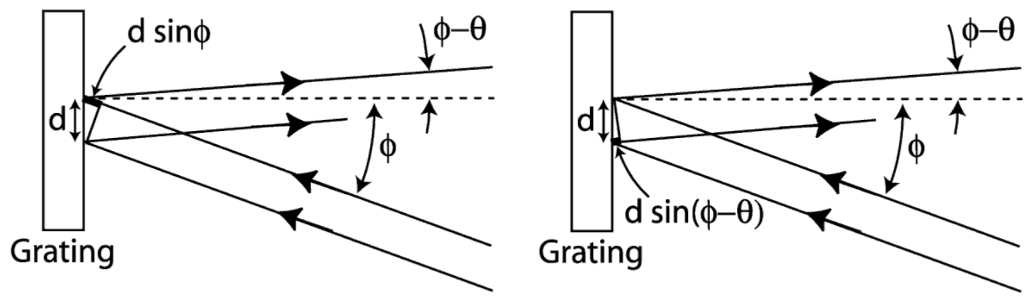

Figure 2.2: Derivation of the grating equation in reflection geometry.

diffraction maximum is focused onto the exit slit, in accordance with Eq. (2.1).

Using $\varphi = \alpha + \beta$ and $\theta = 2\beta$, Eq. (2.1) can be rewritten

$$d \sin(\alpha + \beta) - d \sin(\alpha + \beta - 2\beta) = m\lambda$$

which reduces to

$$2d \cos\alpha \sin\beta = m\lambda \tag{2.2}$$

Equation (2.2) relates the grating tilt angle β to the wavelength of the first order maximum that is focused onto the exit slit. Further information about the mechanics of the grating spectrometer, and a discussion of its resolution, are deferred to §2.5.

2.2 Calibration of the Spectrometer with the Mercury Source

The spectrometer system consists of an optical system, a scanning drive with mechanical readout (in angstroms), a photodetection system, and a controlling computer. (See the photo in Fig. 2.3, although the computer has been upgraded since the photo was taken.) We want to determine the precision of measurements performed using the complete system, so we must calibrate the entire system. Clearly, the resolution of the spectrometer system may be limited by components other than the grating, and we shall find that to be the case with our spectrometer.

The optical system consists of an entrance slit, a collimating mirror, the grating, a focusing mirror, and an exit slit (see Fig. 2.1). The scanning drive consists of a mini-step driver (MSD) which rotates the grating and can be operated either manually (local mode) or controlled by a computer (remote mode). Rotating the grating causes diffraction maxima of changing wavelengths to sweep by the exit slit. A mechanical readout indicates the wavelength (in angstroms) whose first-order maximum should be appearing at the exit slit. (See Fig. 2.4) The light that passes

Figure 2.3: The SPEX 500M grating spectrometer with controlling electronics and computer.

through the exit slit is detected by a photomultiplier tube, and the output current of the photomultiplier is measured by a microammeter. The microammeter displays the photocurrent reading on a front panel analog meter and provides an output voltage which is proportional to the photocurrent. The microammeter output voltage is fed into a multimeter for display and into an analog-to-digital converter board in the main chassis of the computer. The spectrum of a source can be recorded under computer control using a program written in Igor Pro and described in §2.6. A more detailed description of the spectrometer system is given in the Appendix (see page **??**).

Mount the low-pressure mercury source (housed in an aluminum cylindrical cap) on the entrance slit of the spectrometer. The glass envelope of this source is quartz and transmits the ultraviolet spectral lines of mercury, which prove useful for calibration. However, be careful not to turn the lamp on before it is mounted on the entrance slit of the spectrometer, because **the ultraviolet light can damage your eyes!** Set the widths of the entrance and exit slits to 6 μm. (One small division on the slit micrometers equals 2 μm.) A horizontal slide on the entrance slit has settings for slit heights of 2 cm, 1 cm, and 0.2 cm. There are also settings that superpose 1-mm-diameter circular apertures over the top, center, or bottom portions of the entrance slit. The "S" setting means "Shut". The height of the entrance slit should be set at 1 mm using the 1 mm aperture over the center of the slit. Power ON the high voltage on the photomultiplier tube (it is

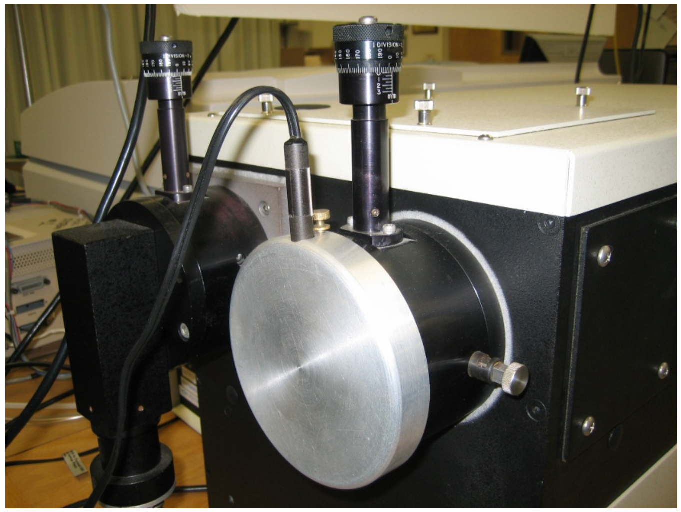

Figure 2.4: The entrance and exit slits of the SPEX 500M grating spectrometer.

set at −900 V). Use the 1-μA full-scale setting on the microammeter.

Instructions for scanning a spectral line under computer control have been placed with the computer. Perform a scan of the 546 nm line of Hg just to familiarize yourself with the spectrometer system.

Next scan the neighborhoods of the following eight spectral lines of Hg, which span the visible spectrum:

365.015 nm	546.074 nm
404.656 nm	576.959 nm
435.835 nm	625.132 nm (2nd order 312.566 nm)
507.304 nm (2nd order 253.652 nm)	730.030 nm (2nd order 365.015 nm)

In addition, you may want to check the calibration of the instrument across its entire range to 1500 nm by scanning the lines:

- 871.670 nm (2nd order 435.835 nm)
- 1092.148 nm (2nd order 546.074 nm)
- 1307.505 nm (3rd order 435.835 nm)

Measure the positions, full-widths-at-half-maximum (FWHM), and intensities of these lines. Make sure you understand the origin of the "lines" labeled as 2nd and 3rd order in the lists above. For instance, if you scan both the 365.015-nm line and the 730.030-nm line, how should you expect the two scans to compare to one another? After measuring the positions of the eight (or eleven) spectral lines, it is a good idea to spot check a few lines to see how repeatable your measurements are.

Notice that the computer always begins a scan by moving several nanometers below the starting wavelength, then rapidly approaches the starting wavelength and finally performs the scan slowly in the direction of increasing wavelength. This manipulation removes the "backlash" of the mechanical drive. *Backlash is present in all mechanical drives, and you should always take it into account.*

You may notice that your measured positions of the Hg spectral lines (based on the mechanical readout) deviate slightly from the above literature values (found also in published tables placed with the spectrometer). These deviations represent the limits of the precision of the spectrometer drive, though most of the deviations consist of a simple additive constant and a slight correction to the slope of the wavelength drive. The linear calibration described below is aimed at removing *most* of these deviations, leaving only nonlinearities which indeed represent shortcomings of the wavelength drive.

Some general advice is in order regarding the use of the photomultiplier tube at the exit slit of the spectrometer.

Caution

The spectrometer photomultiplier tube is a Hamamatsu R928 that has an extended red multialkali photocathode that is sensitive to light of wavelength 185 nm to 900 nm. **The anode current (measured with the microammeter provided) has an absolute maximum rating of 100 μA.** Should you exceed 100 μA, there is a good chance you will damage the photomultiplier tube irreparably.

Try to keep the photocurrent below 20 μA, using the microammeter front panel as a guide. You must narrow the widths of the slits, decrease the height of the entrance slit, or attentuate the source intensity to ensure that the photocurrent of each spectral line does not exceed this nominal 20-μA rating at any point in your scan across the spectrum. *Please be nice to our spectrometer PMT.*

Finally, use our linear least-squares method to fit a straight line to a plot of literature wavelengths versus measured wavelengths. Ideally the slope should be 1 and the y-intercept should be zero. The value of χ^2 should give some indication of the linearity of the spectrometer drive over the full visible spectrum spanned by our calibration lines. The linearity is even better over short wavelength intervals. Usually when an unknown spectral line is recorded, two bracketing calibration lines are also scanned, and the wavelength of the unknown spectral line is calculated by interpolation of the two literature wavelength values of the calibration lines.[2]

The χ^2 for your straight-line fit will be sensible only if you use sensible uncertainties for the measured positions of spectral lines. There are two contributions to the uncertainty of a mea-

[2] In practice, it is common to use a low-order polynomial, rather than a line, to calibrate a grating spectrometer. A polynomial of order greater than one can correct for slight errors in the definition of the origin of wavelengths and misalignments of the sine bar.

sured spectral line position. First, the uncertainty with which you can locate the center of a line is best measured by a sample variance technique. Second, the resolution of the instrument is reflected in the width of the spectral line (when the source is the low pressure mercury lamp). **You will have to think carefully about which of these two contributions is more appropriate for the linear regression procedure.** If the sample variance technique yields a number which is much larger than the half width at half maximum (HWHM), then clearly the sample standard deviation should be used. If, however, the sample standard deviation is much smaller than the HWHM (which is in fact the case), it may be that structure in the line is obscured by the resolution of the instrument, and the HWHM may be a reasonable number to use as an uncertainty in the position of a spectral line. (You will probably find that the quarter-width-at-half-maximum (QWHM) is a good uncertainty to use.)

You should also take data to measure the resolution of the instrument as a function of the slit widths. The information in the Appendix (see pages **??** through 18) will allow you to compare your measured line widths of a Hg spectral line with the theoretically expected values given the dispersion of the grating and the widths of the slits. It is a good idea to roughly analyze this data as you proceed, so you can be sure to take data over a reasonable range of slit widths.

What you have learned about the instrument in your experimentation so far should be used to guide your data-taking and analysis for subsequent parts of this experiment.

2.3 Measurement of the Hydrogen Spectrum or the Solar Spectrum

2.3.1 The Balmer Series of Hydrogen

Position the hydrogen "Balmer tube" source so that the source is imaged by the lens onto the entrance slit of the spectrometer. (Even if you decide to study the solar spectrum, you may want to use the Balmer tube as a comparison source when searching for hydrogen lines in the solar spectrum.) Your instructor can suggest an arrangement that has proven satisfactory. If you decide to devise your own arrangement, be sure to direct the fan onto the lower portion of the tube; cooling the tube by convection prolongs the life of the tube considerably. You should measure the position, FWHM, and intensity of as many lines of the Balmer series as possible (at least eight). If you plot the reciprocal of the wavelength of a series line versus $1/n^2 - 1/m^2$, where n and m are the final and initial principal quantum numbers of the transition, you can use a linear fitting procedure to deduce a value *and an uncertainty* for the Rydberg constant of hydrogen. In comparing your measured value with literature values, be sure to compare apples with apples and oranges with oranges. Literature values are often quoted for R_∞, the Rydberg constant assuming an infinitely heavy nucleus. When you have finished the data analysis, take a moment to muse on how beautifully a straight line fits your data. The fundamental postulates of quantum mechanics have led to predictions which agree awfully well with measured values, whereas classical mechanics and electromagnetism predict that atomic electrons should spiral into the nucleus.

You can measure another interesting feature of the hydrogen spectrum by replacing the hydrogen Balmer tube with the deuterium Balmer tube. Be sure to allow the hydrogen tube to cool; the operating temperature of the tubes usually renders them too hot to touch. The deuterium tube actually has enough hydrogen to give roughly equal intensity lines for the two isotopes. Measure the spectral lines of deuterium and deduce a value *and an uncertainty* for the Rydberg constant.

2.3.2 The Solar Spectrum

You will need a little luck with the weather (and even more luck if you have an evening section), but after all, this is sunny southern California! Use the heliostat and fiber optic cable to bring a little sunshine into the spectrometer. Your instructor will help you position the heliostat outdoors near the rear door of the building; the fiber optic cable and power cord for the heliostat motor should be carefully laid out through an open window in the lab. Position the fiber optic cable so that it is protected from sharp kinking or compression, which will quickly degrade its performance. The body of the heliostat must be correctly oriented (angled plate facing north) for proper operation. When focusing sunlight onto the fiber optic, be careful not to melt the cable cladding. The end of the fiber optic cable inside the lab can be held at the entrance slit of the spectrometer with the optical rider provided.

Leave the heliostat unplugged at first and watch it (outdoors) for a minute or so to see the focused sunlight spot drifting due to the Earth's rotation. Now realign the heliostat and plug it in; if you have oriented it correctly, the drift you observed before should be nearly eliminated by the tracking which is now taking place. Do not expect to see or hear rapid motion from the motor when the device is tracking properly!

The Sun's spectrum is, in general, a jumble of absorption lines superposed on a continuous blackbody spectrum. You will have to do a little reading on the solar spectrum and decide which prominent features you are going to try to observe. It may prove helpful to alternate or even superpose the spectra of the Sun and an appropriate laboratory source. You will have to think through your approach to these measurements and come to the laboratory prepared. Don't lose sight of the fact that elements in the Sun which are heavier than helium came from the same place that those elements in your body came from: exploding stars, or at least stars that are long dead!

If you decide to measure the solar rotation, it will be critical to show that the position of a solar spectral line depends on which portion of the Sun's disk is being imaged onto the optical fiber. As the Sun rotates, light emitted from one side of the Sun's equator will be blue-shifted because that portion of the Sun is moving toward the Earth, while light emitted from the other side of the equator will be red-shifted as a result of motion away from the Earth. If you power off the heliostat and simply allow the Sun's disk to pass over the optical fiber while you take spectra as quickly as possible, you should see a small but systematic shift in the position of a solar spectral line. It will be a *small* shift because the Doppler shift is considerably less than the resolution of the spectrometer, 0.03 nm! Be sure to perform all the calculations before you come to lab!

2.4 Measurements of the Sodium Doublet Separation and the Width of the Collision-Broadened Mercury Green Line

2.4.1 The Sodium Doublet

The low-pressure sodium source (the bulb is sold commercially as a street lamp) is sufficiently bright that it can simply be placed 20 cm to 1 m from the entrance slit of the spectrometer (it need not be imaged onto the slit). Like the street lamps, the source requires several minutes to reach full intensity. Measure the positions, FWHM, and intensities of the two lines. From this data you can deduce a value *and an uncertainty* for the spin-orbit coupling energy in this alkali "one-electron" atom. Compare your measured value with literature values. You should review the treatment of spin-orbit coupling given by Townsend in Chapter 11 and/or by Eisberg and Resnick.

2.4.2 The Mercury Line Width

The high-pressure mercury source also requires several minutes to reach full intensity, but is then sufficiently intense that it may simply be positioned 20 cm to 1 m from the entrance slit of the spectrometer. Measure the FWHM of the green line and obtain a detailed plot of the shape of the spectral line. The bulb operates at approximately nine atmospheres and 5000°C. The slight tail on the long wavelength side is characteristic of a collision- (or pressure-) broadened line. Our treatment in lecture of collision broadening does not account for the tail but does predict a Lorentzian lineshape. It would be interesting to see how well the measured lineshape can be fitted with a Lorentzian. Also, do you notice a hint of self-absorption in the spectral profile?

2.5 Appendix: the Sine Bar and Resolution

Figure 2.5 illustrates how a linear relation can be obtained between an easily controllable parameter and the wavelength at the output of the spectrometer. The grating is mounted on a rotatable table, and the end of a lever of total length L slides on the end surface of a translatable rod. The key point is that as the rod is translated and the distance x is varied, the end of the lever may slide on the end of the rod (slide left-right in Fig. 2.5). The relation between the tilt angle β of the grating and the distance x is clearly $\sin\beta = x/L$. The arrangement depicted in Fig. 2.5 is commonly referred to as a "sine bar" by mechanical engineers. Substituting this relation into Eq. (2.2) we get

$$\lambda = \frac{2d\cos\alpha}{mL}x \tag{2.3}$$

which is indeed a linear relation between λ and x. A stepping motor turns a threaded rod and hence varies x in a linear way. As a result, the number of revolutions executed by the motor is

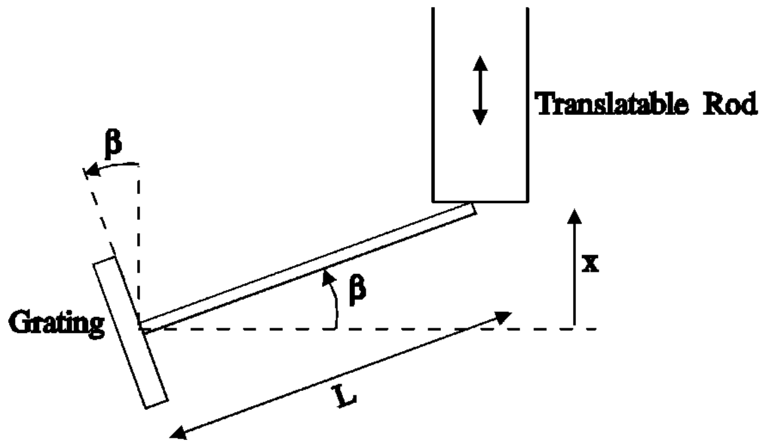

Figure 2.5: The sine bar.

linearly related to the wavelength at the output. A mechanical counter keeps track of the turns of the motor.

The dispersion of the spectrometer $D \equiv d\lambda/d\theta$ is the incremental change in the wavelength appearing at the exit slit for a given change in the angle θ of diffraction. The dispersion can be calculated by differentiating Eq. (2.1) with respect to θ while holding the angle of incidence φ constant:

$$\frac{\mathrm{d}\lambda}{\mathrm{d}\theta} = \frac{d\cos(\varphi - \theta)}{m} \tag{2.4}$$

The dispersion is often expressed as the change in wavelength in nanometers per millimeter of travel in the direction of the exit slit width. If y measures the distance along the slit width direction, the relation between y and θ is $y = f\,\theta$, where f is the focal length of the focusing mirror (f = 500 mm). Substituting the differential form $dy = f\,d\theta$ into Eq. (24), we get

$$\frac{\mathrm{d}\lambda}{\mathrm{d}y} = \frac{d\cos(\varphi - \theta)}{mf} \tag{2.5}$$

The grating employed in the SPEX 500M has 1200 grooves/mm, so the grating spacing is 1/1200 mm or 833 nm. If we set $\cos(\varphi - \theta) \approx 1$, then the dispersion in first order ($m = 1$) is according to Eq. (2.5)

$$\frac{\mathrm{d}\lambda}{\mathrm{d}y} = \frac{833\,\mathrm{nm}}{500\,\mathrm{mm}} \approx 1.67\frac{\mathrm{nm}}{\mathrm{mm}} \tag{2.6}$$

The upper limit on the resolution of the spectrometer can now be calculated by multiplying the dispersion by the slit width. For a slit width of 10 µm, this calculation yields (1.67 nm/mm) (10 µm) = 0.0167 nm ≈ 0.17 Å. This result is conventionally multiplied by 2 to account for the way the entrance slit is imaged onto the exit slit, giving a resolution of approximately 0.03 nm or 0.3 Å.

At a wavelength of 550 nm, a resolution of 0.03 nm gives a resolving power of

$$R \equiv \frac{\lambda}{\Delta\lambda} = \frac{550\,\text{nm}}{0.03\,\text{nm}} \approx 18,000 \tag{2.7}$$

This value is quite a bit less than the theoretical resolving power of the grating $R \equiv Nm$ where N is the number of lines in the grating. Since the grating has 1200 grooves/mm and has a ruled width of 110 mm, N is equal to 1200 times 110 or 132,000! The grating is large so that more light can be focused at the exit slit, rendering the spectrometer a "faster" instrument. Resolution and speed of a spectrometer are two quite different (sometimes opposing) design considerations. While our instrument has only modest resolution, its speed or f-number (4.0) is excellent.

2.6 Using Igor to Control the SPEX 500M Grating Spectrometer

These instructions describe the software that provides computer control of the SPEX 500M grating spectrometer. In this experiment, Igor interfaces a PC (a Dell Dimension 4600 computer named “Waller”) running Windows 7 to the MSD2 electronics that drives the stepper motor that rotates the grating in the SPEX 500M spectrometer. These instructions will guide you through a scan of a mercury line (546.074 nm), and help you produce a printed plot of the spectral line on the HP Color LaserJet Enterprise M553 printer (named “Scandal”, IP=134.173.33.114).

2.6.1 Recommended Startup Procedure

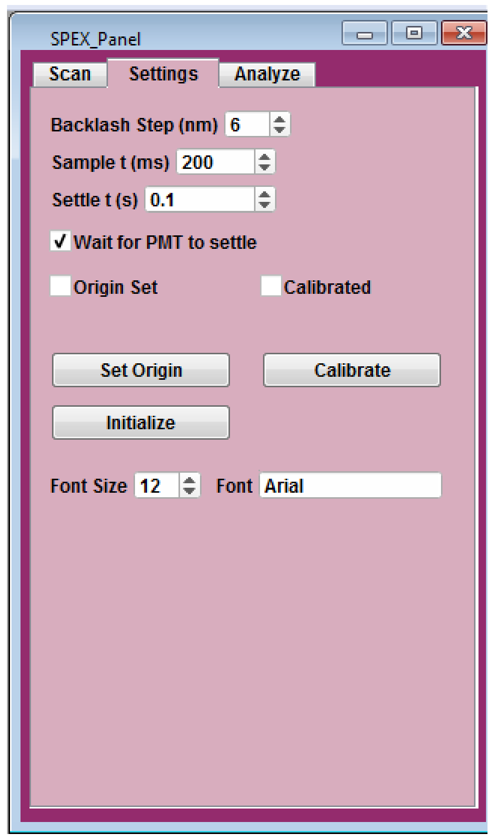

1. On the SPEX 500M grating spectrometer, set the widths of the entrance and exit slits to 6 μm, and set the height of the entrance slit to 1 mm using the middle 1 mm-diameter aperture.
2. Power ON the mercury calibration lamp and the photomultiplier tube high voltage (−900 V).
3. Power ON the MSD2 driver (power switch at right rear, local/remote switch on REMOTE).
4. Power ON the multimeter and the microammeter (full scale at 1 μA, multiplier at ×1).
5. Finally, power ON the computer main chassis and monitor.
6. As Windows 7 boots up, log in with the following account and password:

account name	**spex**
password	**grating**

7. Launch the program “Igor64.exe” using the shortcut on the desktop. If prompted, click Yes to install a newer version of HMC.ipf, and then click No to the question, “Do you want to save changes to experiment ‘untitled’?”
8. Once Igor has loaded, go to the **Expt** menu option and click **SPEX** on the pulldown menu. A window named “SPEX_Panel” should open in Igor, as illustrated above. Within that window, the **Settings** tab should be frontmost.
9. Click Initialize. The command line window should then write several line of output ending with “Communications with the SPEX established properly.” (See top of next page.)

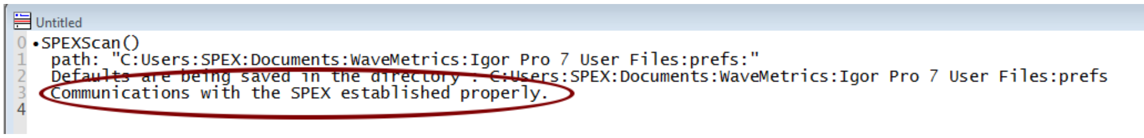

(If this does not occur, turn off the SPEX MSD2 controller, wait 10 seconds, turn it back on, and initialize again.)

10. Now click Set Origin under the **Settings** tab. You will be prompted to enter the current wavelength **in nanometers**. Do so, reading the spectrometer window display, *noting that the number on the instrument's display is reported in angstroms, not nanometers.*

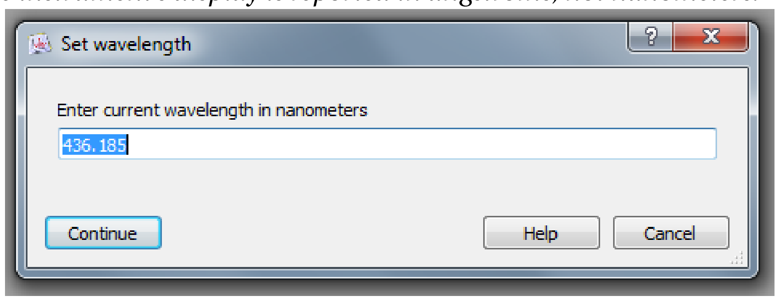

Click Continue. Note that the ☒ Origin Set box has been automatically ticked in the SPEX **Settings** panel.

2.6.2 Taking Spectra

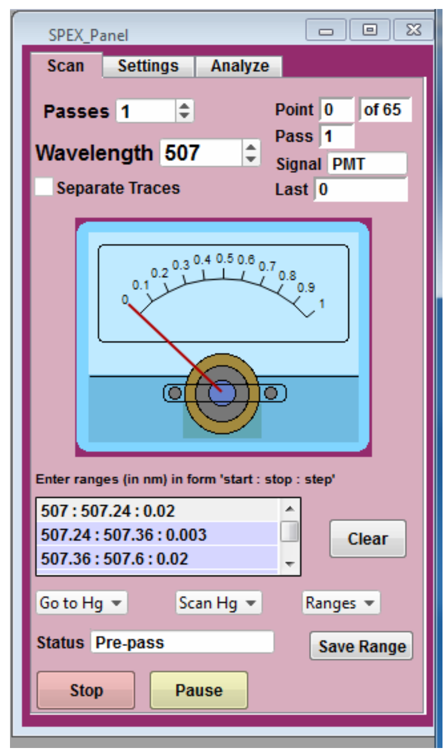

Go to the **Scan** tab and enter in the **wavelength (nm)** box a value smaller than that which you would like to scan. Press **enter** or click on the rose background outside the box; the spectrometer will move to the input wavelength. Verify on the front of the spectrometer that it has moved to the correct wavelength. Enter the range of your scan in the appropriate box using the "**start : stop : step**" syntax, as indicated above the box entry. You may enter a single range, as shown in the example here, or you may enter a range on each of several lines in the box. Note that the mercury lines are preloaded for you in the Go to Hg and Scan Hg menus. The green line at 546.074 nm is a good choice for a first scan, and a good step size to start with is 0.01 nm.

Enter a value for **Passes**, which corresponds to the number of passes over the specified wavelength range(s) you wish to make. A data point is taken at each specified wavelength on each pass. The point is obtained by sampling the signal voltage many times and averaging. The duration of averaging is set by the **Sample Time** variable on the **Settings** tab. If you choose one pass, Igor displays error bars using the standard error of the incoming data during the sampling time at each wavelength.

If you choose more than one loop, Igor uses the standard error of the repeated trials (passes) at each wavelength. Click **Start**. A new plot window with your data will automatically open. It is named for the time at which you begin the acquisition.

If you use more than 1 pass, you may check the ☒ Separate Traces box if you wish to see a separate trace for each pass through the wavelength range. At the end of each pass, a new curve is added to the lower half of the plot window, as illustrated in Fig. 2.6. In this example, there are actually five separate traces in the lower panel, but because of the excellent signal-to-noise ratio, they are virtually indistinguishable. The discrete points in the top panel of Fig. 2.6 have the normal averages and their standard errors, computed as described above, and updated after each measurement.

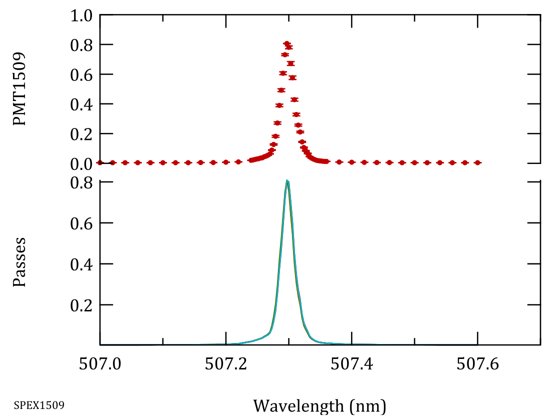

Figure 2.6: An example scan with separate traces for each pass.

2.6.3 Where are the Data?

Each spectrum is stored in its own data folder named after the date and time of the scan. At the start of each spectrum (run), an entry with the parameters of the scan is made in the Scan Diary, which is a standard Igor Notebook window. You can add your own notations to this window to help you keep track of any changes you may have made to the setup—such as amplifier gain, alignment, light source, etc.—and can even paste in copies of the graphs as a catalog. Each spectral entry shows the data folder holding the scan and then a line showing the number of passes requested in parentheses, followed by the wavelength range(s). An example Scan Diary window is shown in Fig. 2.7

You can see all the data waves using the **Data Browser**, which you can find in the **Data** menu. The figure at the right shows the Data Browser corresponding to the series of traces shown in Fig. 2.6. Notice that at the bottom left corner of the figure is the label SPEX1509, which tells you that the run was initiated at 15:09 (3:09 p.m.).

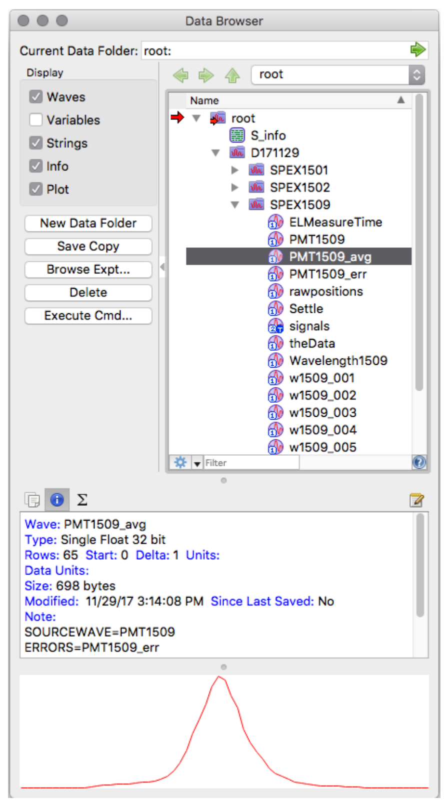

The PMT1509_avg wave (illustrated at the bottom of the Data Browser, since it is highlighted)

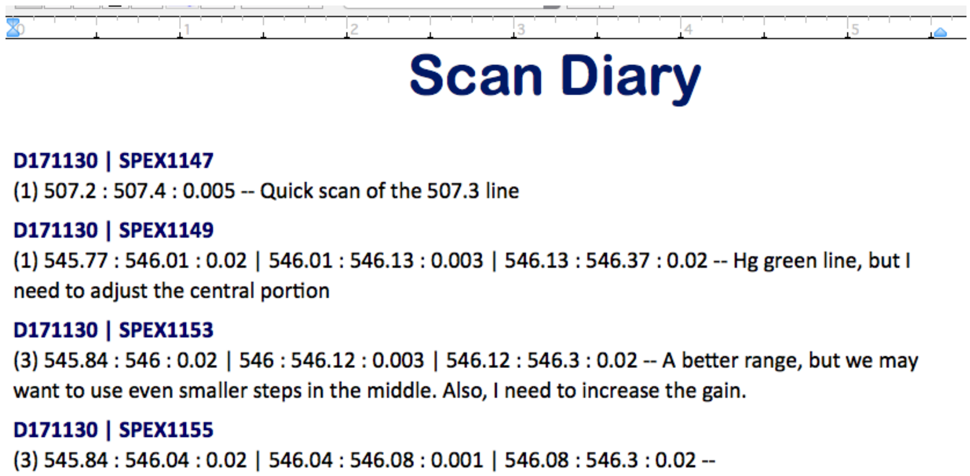

Figure 2.7: The Scan Diary window.

shows the average computed for the 5 passes (loops). The individual passes are labeled w0953_001 through w0953_005. The wave note contains further information about the data source: the SOURCEWAVE is PMT1509 and the ERRORS are in PMT1509_err. This means that to produce a "proper" plot of these data, you would display PMT1509_avg vs Wavelength1509 and add error bars from PMT1509_err.

The result is shown in Fig. 2.8, after changing the y axis to logarithmic display and shrinking the markers so the error bars can be seen. You can print a copy on the color printer Scandal using **File | Print Graphics. . .**

2.6.4 Remaking a Plot

If you have closed a spectrum plot and wish to regenerate it (or just find it, if it is buried on your display), select **SPEX Plot** from the **Expt** menu and choose the appropriate spectrum from the popup menu.

2.6.5 Working on Another Computer

The Igor SPEX software allows you to store all your scans in a single Igor Experiment file, organized by the date of the scan and the time it was begun. Make sure to save often. When you want to work with your data on another computer, copy the Experiment file to the other computer. You may see error messages that Igor cannot find some waves and/or procedure files. Just click to ignore those warnings. You should be able to access all of your data via the Data Browser.

If you would like the convenience of the **SPEX Plot** command, you can download the appropriate

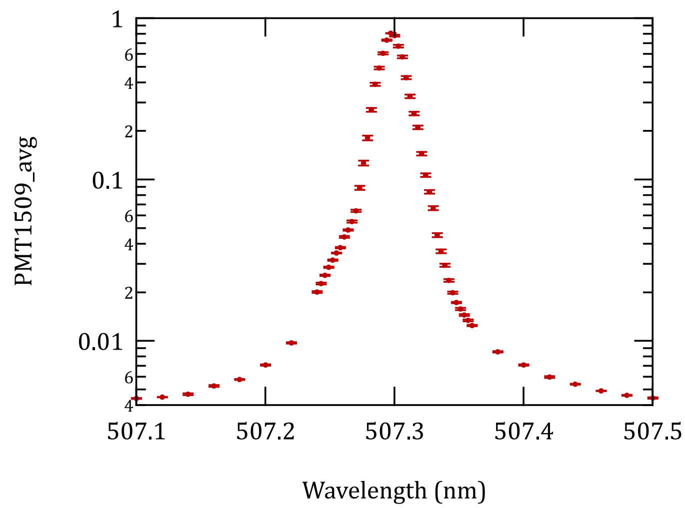

Figure 2.8: Sample Hg line, the $\lambda = 253.652\,\mathrm{nm}$ line at second order.

procedure file from the department server within Igor by typing the command

```
Install("SPEXPlot", targetFolder=''User Procedures'')
```

This will install the code in the **User Procedures** folder, which houses optional procedures that you may wish to use from time to time. You can make sure it is available in any particular experiment file by entering

```
#include "SPEXPlot"
```

in the Procedure Window (Cmd/Ctrl-M).

2.6.6 Calibration Lines

For easy reference, here are the mercury calibration lines.

365.015 nm		625.132 nm	(2nd order 312.566 nm)
404.656 nm		730.030 nm	(2^{nd} order 365.015 nm)
435.835 nm		871.670 nm	(2^{nd} order 435.835 nm)
507.304 nm	(2^{nd} order 253.652 nm)	1092.148 nm	(2^{nd} order 546.074 nm)
546.074 nm		1307.505 nm	(3^{rd} order 435.835 nm)
576.959 nm			

Experiment 3

Scanning Fabry-Perot Interferometer

References

- *Optics* by E. Hecht; See Section 9.6 for the Fabry-Perot interferometer, and Section 14.2 for an overview of lasers.
- *An Introduction to Lasers and Masers* by A. Siegman; see Chapter 8 for an excellent discussion of optical resonators; see Sections 9.2 and 9.4 for treatments of Doppler broadening, laser oscillation frequencies, and the Lamb dip.
- *Optical Electronics* by A. Yariv; Chapters 4 through 7 are highly recommended; Chapter 4 discusses Fabry-Perot interferometers and optical resonators, Section 6.6 contains an insightful comparison between homogeneous and inhomogeneous line profiles and the effect on lasing, Section 6.8 explains the Lamb dip, and Section 7.5 describes the helium-neon laser and includes a neon atomic energy level diagram.
- "Scanning Spherical-Mirror Interferometers for the Analysis of Laser Mode Structure" by D. Sinclair (a scanned pdf copy is available on the course Sakai website); this technical bulletin is distributed by Spectra-Physics and provides a good introduction to most of the measurements performed in this experiment.
- *Quantum Physics of Atoms, Molecules, Solids, Nuclei, and Particles* by Eisberg and Resnick. Section 10-6 describes the Zeeman effect using Na as an example. While Ne is a neighbor of Na in the periodic table, the excited states of Ne are described by j-l coupling rather than LS coupling.

3.1 Introduction

In this experiment a Fabry-Perot interferometer with a resolving power of 10^7 will be used to examine the spectral profiles of two helium-neon lasers and to measure the Zeeman splitting of neon in one of these lasers. Our Fabry-Perot instrument has an optical cavity formed by two spherical mirrors arranged in the confocal configuration. The term "confocal" means that a point midway between the mirrors is the focal point of both mirrors. The Fabry-Perot interferometer transmits light whose wavelength is resonant with the cavity. To scan a spectrum, the distance between the mirrors is varied slightly by applying a ramp voltage to a piezoelectric crystal on which the mirrors are mounted. As the separation of the mirrors is varied, the wavelength of light transmitted by the interferometer varies, and the photodiode at the rear of the interferometer measures the transmitted intensity. Thus the output of the photodiode plotted versus the ramp voltage applied to the piezoelectric crystal yields the spectral profile of the incident laser beam.

Our Fabry-Perot instrument is called a "scanning confocal spherical mirror Fabry-Perot interferometer," or sometimes just an "optical spectrum analyzer." This class of instruments is routinely used to monitor the operating characteristics of lasers. In addition to providing an introduction to Fabry-Perot interferometers, this experiment involves a fair amount of laser physics including the principles of optical resonant cavities. The observation of the Zeeman splitting in neon also involves a good deal of atomic physics. Because much of the material in this experiment will be new to you, you will have to consult the references listed above in order to be productive in the laboratory.

3.2 Examining the Output Beam of the Uniphase Model 1125P HeNe Laser

Most of the first laboratory meeting will be spent learning to operate the Spectra-Physics Model 470 Scanning Fabry-Perot Interferometer (let's call it the "SF-P" for short). You will use the SF-P to examine the output of the Uniphase Model 1125P helium-neon laser. The Model 1125P has a plane-polarized, 5-mW output at 632.8 nm. The specifications say that more than 95% of its output power is in the TEM_{00} transverse (spatial) mode. The TEM_{00} mode possesses the familiar Gaussian distribution of intensity. (The intensity is proportional to $\exp\left(-2r^2/w^2\right)$ where r is the distance from the center of the beam spot and w is called the spot size (radius).)

A photo of the laser-interferometer setup appears in Fig. 3.1, and a sketch with electrical connections is included in Fig. 3.2. Power **On** the Hewlett-Packard Model 54603B digital oscilloscope and the Model 1125P laser. (The *unpolarized* Model 1125 should be housed inside the solenoid, and the *polarized* Model 1125P is probably sitting on the optical rail next to it.) Make sure the cable connections between the oscilloscope, the Spectra-Physics Model 476 Interferometer Driver (let's call it the Driver for short), and the SF-P agree with the connections sketched in Fig. 3.2. In order to familiarize yourself with the function of the Driver controls, perform the following

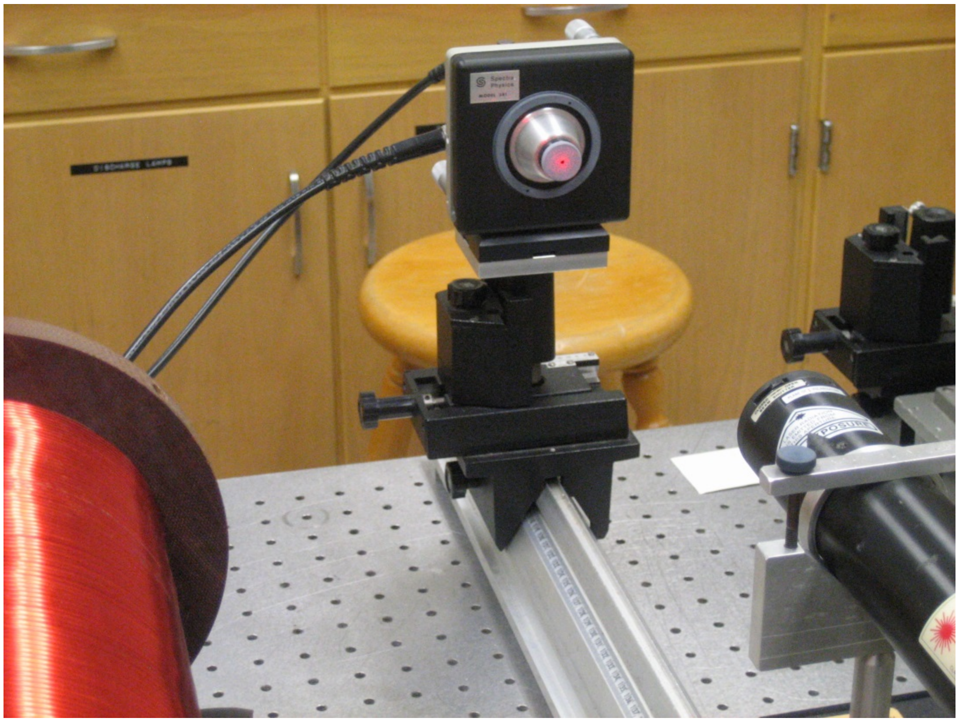

Figure 3.1: Photogaph of the Fabry-Perot (center-top) illuminated by the Uniphase 1125P (polarized) HeNe laser (bottom-right). The solenoid is visible at the lower left and houses the Uniphase 1125 HeNe laser.

exercises. (A copy of the Driver manual has been placed with the experimental equipment.)

1. Observe the high-voltage ramp applied by the Driver to the piezoelectric crystal; this ramp varies the spacing between the mirrors of the SF-P. To make this observation, disconnect the Driver high voltage output (200 to 300 volts) from the SF-P as sketched in Fig. 3.2, and connect it to the input of the 100× attenuator (the small box that is probably located on the oscilloscope cart). Connect the output of the attenuator to input 1 of the oscilloscope and change the horizontal display to “Main” instead of “XY” which is the setting used in Fig. 3.2. (Press “Main/Delayed” and select “Main” in the submenu appearing on the oscilloscope screen.) Now power **On** the Driver. Set the Driver SWEEP to FREE RUN and the SWEEP TIME to 0.01 sec (turn the TIME knob fully clockwise). Set the Driver DISPERSION to X2 with the VARIABLE knob set at midrange. Set the vertical gain of the scope to 1 V/div, and set the horizontal sweep to 5 ms/div. Observe the attenuated ramp on the oscilloscope screen. Play with the Driver CENTERING knob and notice that its effect is simply to increase or decrease the DC level of the high voltage ramp. Play with the Driver DISPERSION settings and notice that they control the amplitude of the ramp. When you think you understand the function of the DISPERSION and CENTERING controls on the Driver, power **Off** the Driver. Reconnect

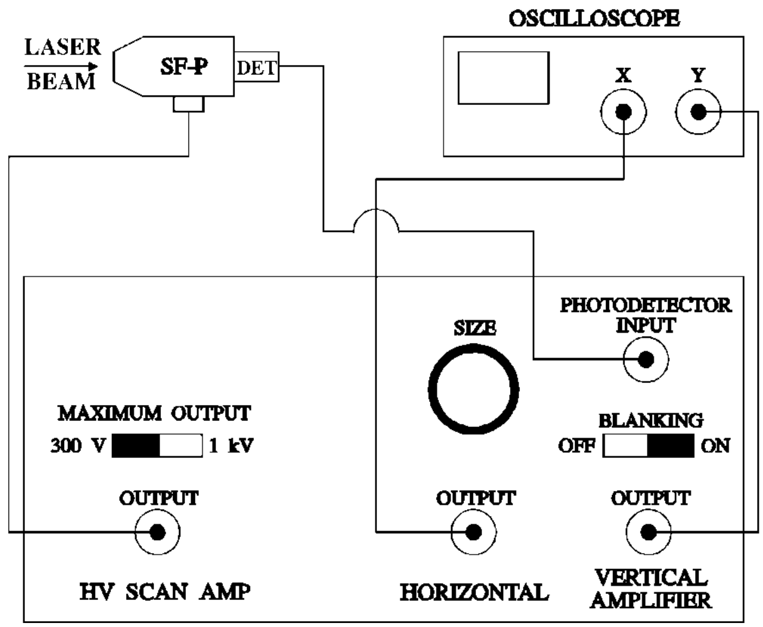

Figure 3.2: Electrical connections between the Spectra-Physics Model 470 Scanning Fabry-Perot Interferometer, the Hewlett-Packard Digital Oscilloscope, and the rear panel of the Spectra-Physics Model 476 Interferometer Driver.

the Driver high voltage output to the SF-P crystal input as indicated in Fig. 3.2, and reset the oscilloscope sweep to XY. (Press "Main/Delayed" and select "XY" in the screen menu.) Power **On** the Driver.

2. Set the Driver controls on the front panel:

   VERTICAL GAIN 100 with VARIABLE knob at mid-range
   SWEEP FREE RUN with TIME knob fully clockwise
   DISPERSION X2 with VARIABLE knob at mid-range
   CENTERING mid-range

3. Set the oscilloscope controls to:

   HORIZONTAL SWEEP XY
   X Gain 1 volt/div
   Y Gain 1 volt/div

4. Check again to see that the cable connections are as sketched in Fig. 3.2. Adjust the SIZE knob on the Driver rear panel so that the "non-blanked" portion of the oscilloscope sweep covers 10 divisions in the horizontal direction. The "non-blanked" portion is simply the raised portion of the displayed signal. The HORIZONTAL OUTPUT on the rear panel of the Driver is just an attenuated version of the high voltage ramp; the SIZE knob is a fine control on the attenuation factor. Be sure to understand what you're doing!

While you may already see a spectrum of the laser output displayed on the screen (see Fig. 3.3), you should now carefully center the laser beam on the SF-P aperture and align the beam with the optical axis of the SF-P. To do so, perform the following exercise.

5. Translate the SF-P horizontally and vertically using the translators on the optical rail rider. Make sure the laser beam enters cleanly the SF-P aperture. Now rotate the SF-P using the micrometer adjustments on the SF-P mount. Direct the beam reflected from the SF-P mirrors back toward the laser output. When the reflected beam hits the laser output mirror, the subsequent reflection from the laser mirror can be seen on the SF-P aperture. This "reflection of a reflection" indicates that the alignment is close enough. In fact, you may be too close, because light reflected from the SF-P back into the laser resonant cavity can interfere with and destabilize the radiation in the cavity.

By now you should see the spectrum of the laser output displayed on the oscilloscope. Two or three modes should be lasing under the Doppler-broadened profile of the neon transition, and this spectrum should appear twice because the scan includes more than one free spectral range of the SF-P. Fine-tuning the micrometer rotation adjustments should narrow the laser modes to essentially vertical lines.

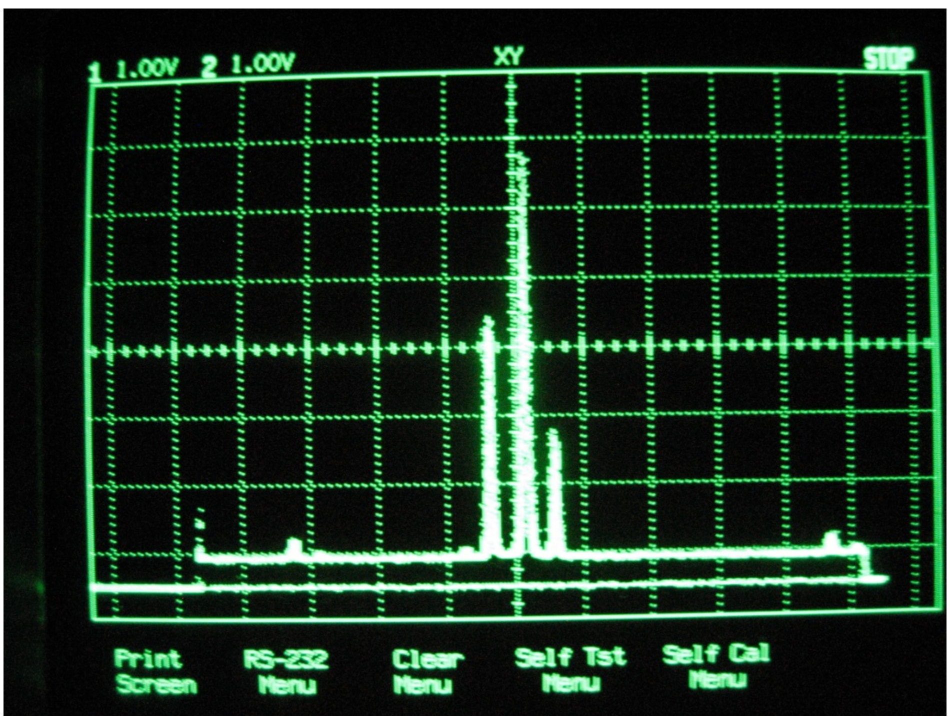

Figure 3.3: Photograph of the oscilloscope screen displaying three laser modes with a Doppler-broadened envelope. Just one free spectral range is shown.

We must discuss in more detail what is really meant by a "**free spectral range**" (FSR) in the context of a scanning interferometer. The multiple copies of the laser spectrum displayed on the oscilloscope screen are present because of the scanning feature of the SF-P. For a given wavelength λ, the condition for resonant transmission of a *confocal* SF-P is given by

$$d_{\mathrm{SF-P}} = d_0 = m\lambda/4 \tag{3.1}$$

where $d_{\mathrm{SF-P}}$ is the instantaneous mirror separation, m is an integer (e.g., 10^6), and d_0 is the mirror separation, let's say, at the beginning of a piezoelectric scan. As the piezoelectric drive increases the mirror separation, a resonant transmission occurs again at

$$d_{\mathrm{SF-P}} = d_0 + \Delta d^{(\mathrm{FSR})} = (m+1)\lambda/4 \qquad \Longrightarrow \qquad \Delta d^{(\mathrm{FSR})} = \lambda/4 \tag{3.2}$$

In other words, for a wavelength of 632.8 nm, transmission occurs each time the piezoelectric drive increases the mirror separation by 158.2 nm, a mighty small displacement. (Note that the factor of 4 in the denominators of Eq. (3.1) and Eq. (3.2) is replaced by a 2 for non-confocal interferometers, like a laser resonant cavity. While you should be able to justify the 2 by very simple physical arguments, the correction to 4 for a confocal cavity is a subtle point which you can use without deriving for now.)

The distance between copies of the laser spectrum provides a convenient calibration of the SF-P. We have just seen that the wavelength λ is transmitted when $d_{\mathrm{SF-P}} = d_0 = m\lambda/4$ and when $d_{\mathrm{SF-P}} = d_0 + \Delta d^{(\mathrm{FSR})} = (m+1)\lambda/4$, but it is also true that a longer wavelength $\lambda' \equiv \lambda + \Delta\lambda^{(\mathrm{FSR})}$ is transmitted when $d_{\mathrm{SF-P}} = d_0 + \Delta d^{(\mathrm{FSR})} = m\lambda'/4$. Combining the conditions

$$d_{\mathrm{SF-P}} = d_0 + \Delta d^{(\mathrm{FSR})} = (m+1)\lambda/4 = m\lambda'/4$$

with the definition $\lambda' \equiv \lambda + \Delta\lambda^{(\mathrm{FSR})}$ yields

$$\lambda = m\Delta\lambda^{(\mathrm{FSR})}$$

Substituting $m = 4d_0/\lambda$ from Eq. (3.1), we get

$$\Delta\lambda^{(\mathrm{FSR})} = \frac{\lambda^2}{4d_0}$$

It is convenient to express this result in terms of frequency:

$$\Delta\nu \approx \left|\frac{\mathrm{d}\nu}{\mathrm{d}\lambda}\right| \Delta\lambda \qquad \Longrightarrow \qquad \Delta\nu^{(\mathrm{FSR})} = (c/\lambda^2)\Delta\lambda^{(\mathrm{FSR})} = \frac{c}{4d_0}$$

The nominal mirror separation of our SF-P is $d_0 = 9.375\,\mathrm{mm}$, so that $\Delta\nu^{(\mathrm{FSR})} = 8.0\,\mathrm{GHz}$. We conclude that the distance between copies of the laser spectrum also corresponds to a frequency difference of 8.0 GHz which is called the "free spectral range" (FSR) of the SF-P. We shall make use of this number in our measurements with the SF-P.

The two or three active laser modes appearing on the oscilloscope screen usually drift back and forth under the Doppler profile of the neon transition, because the length of the laser cavity is thermally expanding and contracting. Recall from your reading in the references that the resonant wavelengths of the laser cavity (*not* a confocal arrangement) satisfy the relation $d_{\text{laser}} = m\lambda/2$ where d_{laser} is the mirror separation and m is an integer. The resonant frequencies are therefore $mc/2d_{\text{laser}}$, and hence the frequency separation of adjacent modes is $c/2d_{\text{laser}}$. The frequency separation $c/2d_{\text{laser}}$ is usually called the **mode spacing** or the **mode separation**, but can also be referred to as the free spectral range of the laser cavity. When the laser is first powered **On**, the plasma tube warms up, d_{laser} increases, and the allowed frequencies decrease in time. The result is a rather rapid movement of lasing modes under the Doppler profile whose center frequency is, of course, dependent only on atomic structure. When the laser reaches thermal equilibrium, the motion of the laser modes slows considerably. You may want to power the laser **Off** for a few minutes so that you can observe the warming effect when you power it back **On**.

If the Fabry-Perot is too well aligned, as mentioned above, you may see instability in the modes far beyond the smooth thermal effect described above. Deliberately misalign the interferometer slightly, if necessary, to keep light from reflecting back into the laser cavity and destabilizing the lasing action in this way.

3.2.1 Measuring the Mode Separation

Using the fact that the free spectral range (FSR) of the SF-P is 8 GHz, adjust the DISPERSION VARIABLE knob so that the laser spectrum repeats after 8 divisions on the oscilloscope horizontal scale; 1 division now equals 1 GHz. Measure the frequency separation of adjacent modes of the Model 1125P laser. The storage feature of the H-P 54603B oscilloscope provides a convenient method for measuring the frequency separation and obtaining a hard copy of the laser spectrum. Press **Stop** on the H-P oscilloscope, followed by **Erase**. The oscilloscope screen should now be clear. Press **Auto-store** on the oscilloscope and then quickly press **Stop**. A few traces of the laser spectrum should be superposed on the screen. A hard copy of this spectrum can be obtained on the Epson printer that is connected by serial port to the HP oscilloscope. The most efficient way to measure the mode separation is to employ the cursor features of the H-P oscilloscope. Use a sample variance technique to obtain an uncertainty for your measured value of the frequency separation. It may be useful to switch the Driver DISPERSION setting to $\times 5$ and $\times 10$, and use different portions of the piezoelectric length-versus-voltage curve. You will probably notice that the piezoelectric crystal has small nonlinearities in its length/voltage response. Do the best you can; all the random errors will be included in your sample uncertainty. *After* you have finished, compare your measured value with the nominal frequency separation quoted in the Uniphase Model 1125P Manual.

3.2.2 Measuring the Width of the Doppler Envelope

Also measure the apparent full-width-at-half-maximum (FWHM) of the Doppler envelope. Again use the storage feature of the H-P oscilloscope, but Store long enough to allow the thermal drift of the modes to trace out the Doppler envelope. Do not Store longer than necessary, however, as the slower thermal drift of the Fabry-Perot interferometer may complicate your measurements in that case. Again a sample variance technique will give you a good sense of your uncertainty. Interpret your measured FWHM in terms of a temperature for the helium-neon plasma. As we will derive (or have derived) in lecture,

$$\text{FWHM (in Hz)} = 2\sqrt{2\ln 2}\sqrt{\frac{kT}{m}}\frac{1}{\lambda}$$

Your deduced temperature will probably be below room temperature, indicating something is fishy. The resolution of this puzzle lies in the low level of pumping provided by the discharge through the plasma tube. The resonant modes of the laser cavity which lie in the wings of the Doppler profile don't have enough gain to actively lase. To put it another way, there aren't enough excited neon atoms with large velocities to enable the modes in the wings of the Doppler profile to provide enough gain to overcome the cavity round-trip loss. You are observing just the tip of the Doppler profile, and your measured FWHM is probably just the full width at 3/4 or 7/8 maximum. Examination of the Doppler profile near its base will reveal that, indeed, it is shaped like the cut-off top of a Gaussian rather than a full Gaussian. Unfortunately, we can't increase the plasma tube voltage (and hence current) to increase the number of excited neon atoms without damaging the power supply.

3.2.3 Measuring the Width of the Lamb Dip

As the active modes of the laser drift through the Doppler profile, you will notice that the amplitude of a mode dips slightly as it passes through the center frequency of the Doppler profile. The dip is called the Lamb dip, and is best observed by sweeping just one active mode through the Doppler profile by translating (usually piezoelectrically) one mirror. While there are two or three active modes in the Model 1125P laser, the effect is still rather obvious. When an active mode lies above the center frequency of the Doppler profile, the mode radiation field recruits photons from excited neon atoms by stimulating them to emit in the direction of their motion along the laser cavity axis (e.g., the z axis). Neon atoms with a range of velocities, $+v_z$ to $+v_z + \Delta v_z$, can contribute to the active mode, where Δv_z is determined by the contribution of collision and lifetime broadening to the total width of the neon transition. Collision and lifetime broadening are called *homogeneous* broadening mechanisms (which affect all atoms) and contribute much less to the total width of the neon transition than does the *inhomogeneous* mechanism of Doppler broadening (in which subpopulations of atoms participate). Moreover, neon atoms with velocities $-v_z$ to $-v_z - \Delta v_z$ can also contribute to the active mode, because the mode field can stimulate these atoms to emit photons along the negative z axis. Hence, two slices of the atomic velocity distribution with total width $2\Delta v_z$ can contribute to the active mode when it lies above (or, by similar argument, below) the center frequency of the Doppler profile. However, as the mode approaches the center frequency, only atoms with velocities $-\Delta v_z/2$ to $+\Delta v_z/2$ can be stimulated to emit photons (in either direction). Hence the amplitude of the mode dips when it reaches the center frequency. See the references for more thorough discussions of the Lamb dip.

Measure the width of the Lamb dip. Again use the storage feature of the oscilloscope. The thermal drift of the laser modes should trace out the Doppler envelope complete with Lamb dip. You may have to turn the laser off for a few minutes and then turn it back on to increase the rate of thermal drift. As in the Doppler width measurement, remember that your goal is to observe the drift of the laser modes without letting the slower thermal drift of the SF-P complicate or wash out your measurements! As usual, use a sample variance approach. (This is not an easy measurement; expect 10% to 20% precision.) The mean lifetimes of the initial and final states of the 632.8 nm neon transition are approximately 100 ns and 10 ns, respectively. The corresponding contribution of lifetime broadening to the width of the transition profile is

$$\text{FWHM (in Hz)} = \frac{1}{2\pi}\frac{1}{10^{-8}\,\text{s}} = 16\,\text{MHz}$$

From your measured width of the Lamb dip, does collision broadening contribute significantly to the homogeneous broadening of the neon transition?

Finally, place the polarizing prism between the laser and the SF-P and rotate it while you observe the amplitudes of the two or three active modes. You should see all of the active modes vary in amplitude together, because they are all polarized in the same plane. The Model 1125P probably uses a Brewster window on one end of the plasma tube to introduce losses for the unwanted polarization state. You will want to contrast this behavior with that of the modes of the "randomly" polarized Model 1125 laser.

3.2.4 Measuring the Polarization of the Uniphase Model 1125 Helium-Neon Laser

Carefully move the SF-P to the optical rail which supports the Model 1125 laser housed in the solenoid. See Fig. 3.4. The output beam of the Model 1125 is 5 mW and is "unpolarized". Repeat the alignment procedure and display the spectrum of the Model 1125 on the oscilloscope. Using the polarizing prism, examine the polarization of the active modes. (A quarter-wave plate for 633 nm is also available with the optical setup.) What do you see? Do you think that the output polarization of this laser should be described as "random"?

3.3 Measuring the Zeeman Splitting of Neon

In 1896 Zeeman observed that an atomic spectral line splits into several lines when the atom is placed in a magnetic field. We now know that the effect is due to the alignment of the atomic magnetic dipole moment in the applied magnetic field. Initially the magnetic sublevels of the atomic states involved in the transition have the same energy (are degenerate), but when the field is applied the degeneracy is removed according to the Hamiltonian

$$\hat{H}_{\text{Zeeman}} = -\hat{\boldsymbol{\mu}}_{\text{atom}} \cdot \mathbf{B}_{\text{external}} \tag{3.3}$$

The atomic magnetic dipole moment is determined by the orbital and spin angular momenta of the electrons:

$$\hat{\boldsymbol{\mu}}_{\text{atom}} = -\sum_i \frac{g_l \mu_{\text{B}}}{\hbar} \hat{\mathbf{L}}_i - \sum_i \frac{g_s \mu_{\text{B}}}{\hbar} \hat{\mathbf{S}}_i \tag{3.4}$$

where the sum is over the electrons. Because the angular momenta are quantized, the dipole moment is quantized, and the magnetic sublevels separate into discrete energy levels. If we take the z axis to be along the magnetic field, the Zeeman shift of each magnetic sublevel can be written

$$\Delta E_{\text{shift}} = \langle n l j m_j | -\hat{\mu}_z B | n l j m_j \rangle = g m_j \mu_{\text{B}} B \tag{3.5}$$

(The result in Eq. (3.5) is *not* obvious; but a little group theory and quantum mechanics can be used to derive it.) In Eq. (3.5), g is called the "g-factor" (which is the same for all magnetic sublevels but may be different for different atomic states), m_j is the quantum number for the z component of the total angular momentum, and μ_{B} is the Bohr magneton. Transitions between

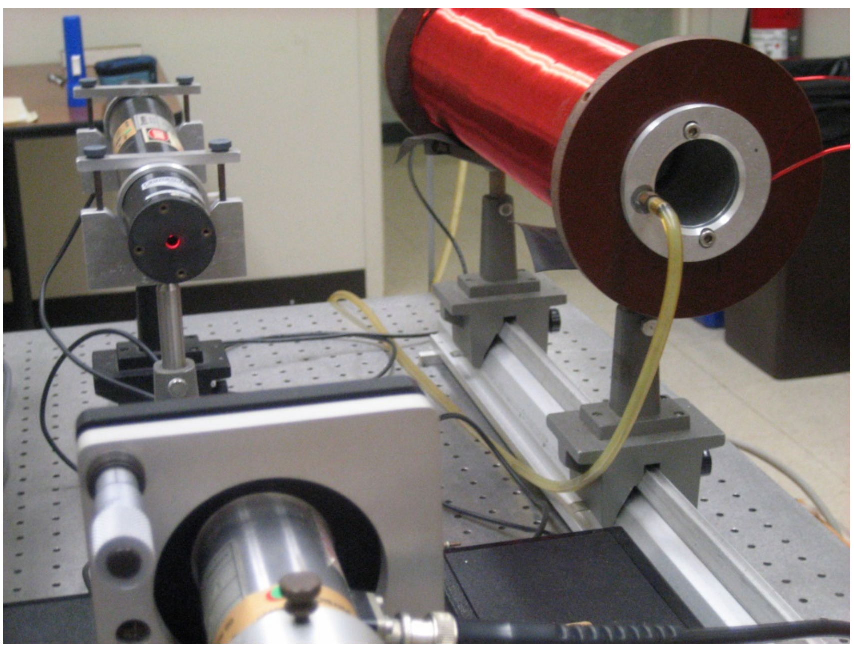

Figure 3.4: Photograph taken from the perspective of the Fabry-Perot interferometer (bottom-center-left). The Uniphase 1125P HeNe laser (top-left) illuminates the Fabry-Perot, and the solenoid (upper right) houses the Uniphase 1125 (unpolarized) HeNe laser.

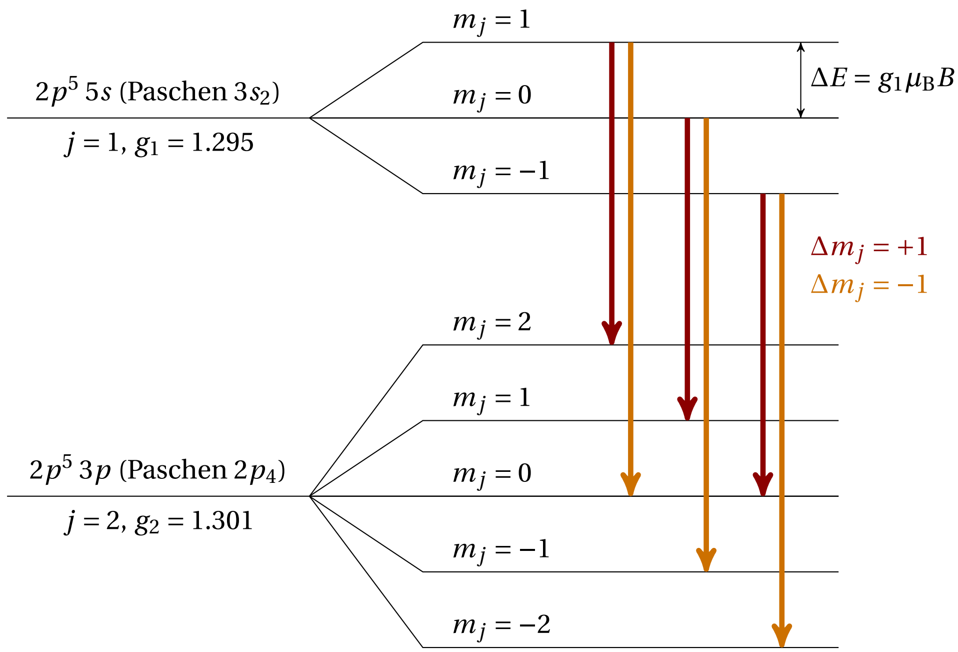

Figure 3.5: Zeeman splittings of the upper and lower Ne states involved in the 633 nm transition. The allowed transitions have $\Delta m_j = \pm 1$. Although the transitions with $\Delta m_j = 1$ have slightly different energy shifts from the energy in the absence of a magnetic field ($\Delta E/\mu_B B = \{g_1 - 2g_2, -g_2, -g_1\}$), our instrument cannot resolve these tiny differences. Curiously, if we average over the three transitions with $\Delta m_j = 1$ and compare to the average of the three transitions with $\Delta m_j = -1$, the splitting we observe depends only on g_2 of the lower lasing level.

different magnetic sublevels of the initial and final states result in the splitting of a spectral line into several lines, the number of lines depending upon the angular momenta of the initial and final states. See the reference by Eisberg and Resnick for an instructive treatment of the Zeeman effect in Na.

Ordinarily the observation of the Zeeman effect is an experimental *tour de force*. However, our scanning spherical-mirror Fabry-Perot interferometer has a resolving power of about 10^7 and allows us to observe the Zeeman splitting in neon with an applied magnetic field of just 500 gauss. For example, the Zeeman splitting between adjacent magnetic sublevels ($g\mu_B B$ in Fig. 3.5) corresponds to a frequency of 0.91 GHz with a magnetic field of 500 gauss. Futhermore, because we will be observing the laser beam traveling along the direction of the magnetic field, and because the selection rule $\Delta m_j = \pm 1$ applies, we will see the Doppler envelope split into two envelopes separated by twice the Zeeman splitting, or about 1.8 GHz at 500 gauss. See Fig. 3.5 for an example of the resulting transitions with an applied magnetic field.

The goal of this section of the experiment is to measure the Zeeman separation of the Doppler envelopes as a function of magnetic field. From this data, a value for g of the final state in the

633-nm transition can be deduced and compared with the literature value (1.301).

As a starting point, apply a magnetic field of about 500 gauss. The rear end of the laser head should be protruding about 3/4" from the rear end of the solenoid. This centers the lasing plasma in the solenoid and maximizes the spatial uniformity of the field. Use the HP 6574A Power Supply to generate a solenoid current of 10 A (the conversion factor is 49.9 gauss/A). Be sure to use the cooling water for the solenoid.

Caution

When using currents of 10 A or more, be sure to return the current to zero within one minute. Check the solenoid windings to make sure they are not hot. We don't want a melt-down! The power dissipated at 60 V and 20 A is 1.2 kW! Use the cooling water for the solenoid.

The instructions for using the HP 6574A are placed with the instrument.

At 10 A (499 gauss) you should see two Doppler envelopes that are fairly well separated, but the envelopes may not be perfectly symmetric. Any asymmetry in the Doppler profiles can easily lead to systematic errors in measuring the separation of the centers of the two envelopes. Previous students have found that symmetry is maximized when the separation of the envelopes is equal to an integer number of laser mode separations ($c/2d_{\text{laser}}$). This condition means that a Lamb dip occurs simultaneously in the two envelopes. It is suggested that you measure the Zeeman separation of envelopes at strengths of the magnetic field that yield symmetric envelopes.

You will probably find it convenient to normalize your measured Zeeman separation of envelopes by the laser mode separation. You can store a snapshot of the laser modes in one half of the H-P 54603B Digital Oscilloscope memory, and store a longer smear of the Doppler envelopes in the second half. Then you can use the oscilloscope cursors to measure both spacing and separation directly on the oscilloscope screen rather than dumping the screen to the Epson printer and analyzing the hard copy later. Of course you will probably want an occasional hard copy for your own records, but the transfer of the oscilloscope screen to the Epson printer is painfully slow (about 40 seconds). Use your time wisely.

Plot the Zeeman separation (expressed in mode spacings) versus solenoid current (or magnetic field). The slope of a linear fit of this plot can yield the g value for the final state of the 633-nm transition. Be sure to use a sample variance technique to determine uncertainties in the data, and propagate these uncertainties through to the value for g using a least-squares fitting procedure with a χ^2 criterion for goodness of fit.

3.3.1 More Advanced Measurements Using the Scanning Fabry-Perot Interferometer

The measurements described above serve as a great introduction to the use of our optical spectrum analyzer. However, there are many additional topics that can be explored with the same basic experimental setup, and some may appeal to you as potential directions for a technical report. Here are some examples that you may wish to discuss with your instructor.

Polarization state of photons in the presence of a magnetic field When a magnetic field is applied along the axis of the "unpolarized" Uniphase 1125 HeNe laser, the output spectrum is split into two "Doppler envelopes", one of which is expected to be right-circularly polarized and the other left-circularly polarized. Measurements performed by Optics Lab students have revealed that the polarization state of one of the Doppler envelopes is well-described by mostly right-circular polarization with a little bit of left-circular polarization, and the other Dopper envelope is mostly left-circular polarization with a little bit of right-circular polarization. In each case the electric field of the small unexpected polarization is accompanied by a phase shift, and this phase shift seems to be a function of the strength of the applied magnetic field. It would be *very interesting* to see if the dependence of the phase shift on field strength is linear, as might be expected from the Faraday effect, perhaps due to circular birefringence of the neon plasma in the laser. This is a very intriguing, ongoing research project!

Transverse spatial modes of a laser A demonstration laser is placed with the experimental setup and can be used to investigate the transverse modes (TEM_{00}, TEM_{01} or TEM_{10}, TEM_{11}, etc.) of the laser beam. An intra-cavity iris diaphragm is an integral part of the laser resonant cavity, and when the iris is expanded, higher order spatial modes are allowed to lase, with energy distributed at greater radii from the optical axis. A fast silicon photodiode and an electrical spectrum analyzer are also available and can be used to measure the beat frequencies between the various transverse modes. This is a great visual *and* quantitative way to learn more about laser resonant cavities and their operation!

Nonlinear mode frequency pulling The HP electrical spectrum analyzer provides high precision measurements of the beat frequency between adjacent laser modes. It is possible to see that as a mode drifts toward the center of the Doppler envelope (toward the resonance frequency of the atomic transition), the frequency of the mode is pulled toward the resonance frequency. Physically, mode frequency pulling is due to the nonlinear change in the refractive index as the mode frequency approaches the resonance frequency of the atomic transition, and the change in refractive index causes a change in the wavelength associated with a particular frequency. Because a mode is defined by its wavelength (its wavelength must fit into twice the mirror separation an integer number of times), the frequency of a mode is seen to deviate in a nonlinear way from the frequency expected under the assumption of a constant index of refraction for the plasma filling the laser resonant cavity.

The effect leads to a dramatic shift in beat frequency depending on whether a mode lies exactly at the resonance frequency, with modes symmetrically situated on either side of it, or whether the resonance frequency lies midway between two adjacent modes. Using a beam splitter to send some laser light to the Fabry-Perot and the rest to the fast silicon detector and the HP spectrum analyzer, one can watch a fascinating transition from one beat frequency when a mode lies at the center of the Doppler envelope, to another beat frequency when two adjacent modes lie symmetrically on either side of the center frequency. The difference in beat frequency is small — just 100 kHz out of 435 MHz, but the precision of the HP spectrum analyzer makes the shift in frequency easy to detect and display on the screen of the spectrum analyzer. It is truly mesmerizing! And a great study of resonance behavior at the atomic level!

Experiment 4

Michelson Interferometer

References

- *Optics* by E. Hecht, Section 9.4.2
- *Fundamentals of Optics* by F. Jenkins & H. White, Chapter 13, Sections 8 through 15, and Chapter 14, Section 13
- *An Introduction to Interferometry* by S. Tolansky, Chapter 8
- *Light* by R. W. Ditchburn, Section 5.21
- *The Feynman Lectures on Physics* by R. P. Feynman, R. B. Leighton, and M. Sands, Volume I, Sections 30.7, 31.1, 31.2, 31.3.

4.1 Introduction

In this experiment a Michelson interferometer will be used to observe white light interference fringes (§4.2), measure the wavelength of the output beam of a helium-neon laser (§4.3), and measure the index of refraction of air (§4.4). The Michelson interferometer that will be used is sketched in Fig. 4.1, and a photograph appears in Fig. 4.2. The compensator plate is necessary to observe white-light fringes, but it is not an essential component of the interferometer for the measurements in §4.3 and §4.4 of this experiment.

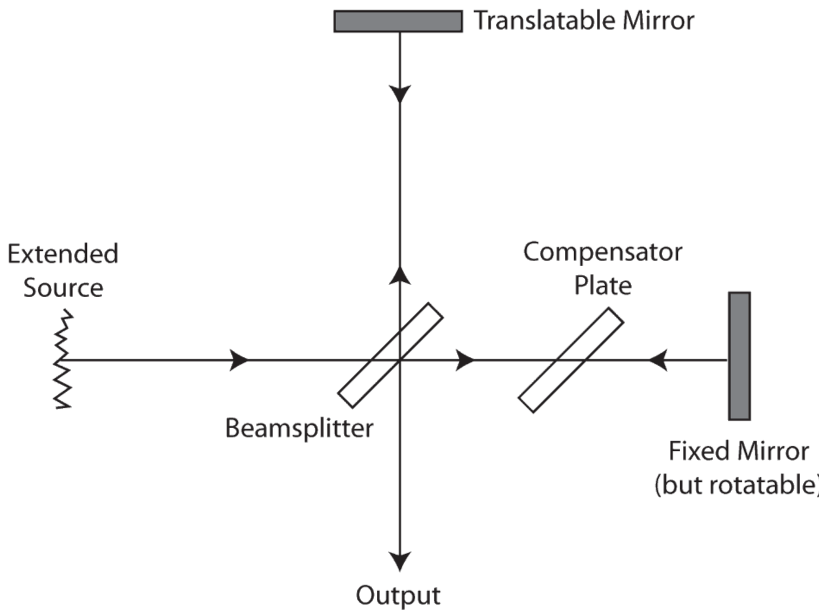

Figure 4.1: The Michelson interferometer.

4.2 Visual Observation of White-Light Fringes

In the first part of this experiment, you will adjust a Michelson interferometer so that white-light fringes are seen at the output. The spectral width of light incident upon the interferometer is increased from a narrow spectral line to a broad "white" spectrum in two convenient steps with the help of optical interference filters. These stepwise increases in the width of the incident spectrum result in a decreasing range of movement of the translatable mirror over which interference fringes can be observed. In other words, the broader the incident spectrum, the narrower the "coherence function." In effect, the equal path setting of the interferometer is located with increasing precision in two "bite-sized" steps. Without the use of the optical filters, an inexperienced person might require an hour or two to produce white-light fringes, but with the aid of the filters, the white-light fringes can be located in perhaps fifteen minutes. Part I of the experiment may take an entire laboratory session.

In addition to the interferometer, the laboratory station is supplied with a mercury arc lamp, an optical filter that has a 10-nm bandwidth centered at 546 nm that is used to isolate the green line of the mercury lamp, another optical filter with a 25-nm bandwidth centered at 550 nm, and a white-light source.

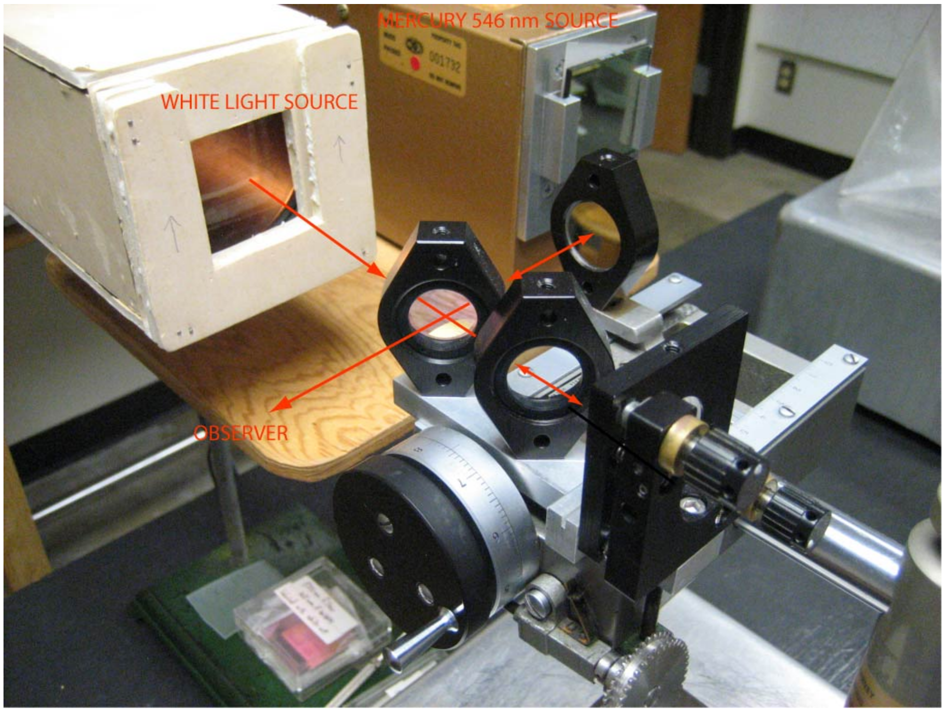

Figure 4.2: Photograph of the Michelson interferometer. The observer is out of view to the lower left and sites along the emerging beam.

Caution

The mercury arc lamp is a strong source of ultraviolet light (UV) and must be covered *at all times* by either an optical filter or a glass diffusing screen. Damage to the eyes may result if the bulb is viewed directly!

The following six steps outline a suggested procedure for bringing the interferometer into adjustment to observe white-light fringes. You should not feel obliged to follow this suggested procedure, but rather you should understand the motivation behind each step and, if desired, you may shortcut the procedure or improvise another. As Mr. Michelson himself once observed, "The key to success with the hands is to employ the head."

1. Your micrometer has a main, coarse translation screw and also a fine-motion screw which can be engaged and disengaged by tilting the translation screw assembly. Make certain the fine motion is disengaged and translate the carriage until the distances of each mirror from the beam splitter are roughly equal. A simple measurement with a ruler is sufficient for this step.
2. Place a pointed object at the input of the interferometer. If the instrument is not in good

adjustment, you will see two images of the object when looking into the output of the interferometer. Rotate the fixed mirror until the two images coincide.

3. Place the mercury lamp (with 10-nm-bandwidth green interference filter mounted on the front) in position to illuminate the field of view. Fringes should be visible when you look into the output of the interferometer. If they are not, repeat the adjustment described in (2). When fringes are seen, rotate the fixed mirror to produce circular fringes in the field. The manipulations required to accomplish this are much better learned by practice than by a long description. However, practice by itself without understanding will be tedious at best, and impossible at worst. *Be sure you understand the origin of the interference fringes.* See the references listed above.

4. Engage the fine translation screw and turn it (or use the coarse screw and turn *slowly*) in the direction that will make the fringes disappear into the center of the field. You should understand from your reading that this is the direction toward the equal path length position. Continue until only a few fringes are in the field. It may be necessary to rotate the fixed mirror slightly to keep the circular fringes centered as this operation is carried out.

5. When there are only a few circular fringes in the field, rotate the fixed mirror about a vertical axis so that the center of curvature of the fringes moves off to one side out of the field of view. Rotate until there are from 5 to 10 vertical, slightly curved fringes in the field of view. Continue translating the carriage in the same direction as before until the fringes appear to be straight. For a complete treatment of these "fringes of equal thickness" you'll need to see Section 5.21 of Ditchburn as well as Section 13.10 of Jenkins & White.

6. Replace the mercury source with the white-light source and transfer the 10-nm-bandwidth green interference filter to the white-light source. **Be careful; don't drop the filter and please handle the filter by its *edges.*** Continue translating the carriage in the same direction. If all the steps have been followed correctly, interference fringes should soon appear. Record the range of positions of the translatable mirror over which these fringes are visible (which should be a distance of roughly 20 μm). The range of visible fringes is called the "width of the coherence function." *Never attempt a single measurement that involves translating the carriage back and forth with reversals of direction, as the gears have significant mechanical backlash and in fact may take time to "engage" fully when the direction is reversed.*

7. Repeat (6) with the 25-nm-bandwidth filter, and notice that fringes are visible over a narrower range—record this range. Finally remove the interference filter and observe white-light fringes near the center of this range. Estimate and record the range over which these white-light fringes occur. You should see that the broader the incident spectrum, the narrower the coherence function, with a simple inverse relationship.

Looking directly into the interferometer, play with these white-light fringes and record your observations in your notebook. The condition for white-light fringes is, of course, the condition for equal path lengths. Since no source is completely monochromatic, fringes produced by any source will be strongest near this position. This would, in principle, apply even to a laser, but the helium-neon laser you will use in the second and third weeks of this experiment has a coherence length of about 10 cm, so in practice path differences large enough to wash out the laser fringes are not encountered often. Circular fringes are best for the measurement of wavelength and wavelength difference. When using circular fringes, it is necessary to begin measurement at a point slightly removed from the position of equal path lengths. The fringes are otherwise too broad to be clearly seen. Note the scale reading and direction of approach for the white-light fringes before proceeding.

Notice in Fig. 4.1 that, without the compensator plate, the path to and from the translatable mirror would include two traverses through glass (the beam splitter) which would not be included in the path to and from the fixed mirror. Since the optical path length equals the geometrical path length times the refractive index, and since the refractive index varies with wavelength, it follows that without the compensator plate the position of equal path lengths would not be the same for all wavelengths. If the compensator plate thickness equals the beam splitter plate thickness, there will be equal optical thicknesses of glass in the two legs for all wavelengths, and white-light fringes can be observed. If the thicknesses of the two plates are not equal, the white-light fringes are degraded. **Calculate the difference in the thicknesses of the two plates if the position of equal lengths for red light (say 650 nm) corresponds to a half-wave difference for blue light (say 450 nm).** (The famous *Handbook of Optics* lists the refractive index of BK7 optical glass as 1.5253 at 450 nm and 1.5145 at 650 nm.) You should now have some appreciation for the importance of the compensator plate.

4.2.1 Measuring the group refractive index and dispersion of glass or water

You may have time at the end of the first lab meeting, or perhaps during the second, to use the Michelson interferometer to measure the group refractive index of either a glass microscope slide or of water placed in a small cuvette. The group refractive index is the ratio of the free-space velocity of light c to the group velocity in the medium (glass or water in our case). It is related to the ordinary or phase refractive index by

$$n_\mathrm{g} = n_\mathrm{p} - \lambda \frac{\mathrm{d}n_\mathrm{p}}{\mathrm{d}\lambda} \tag{4.1}$$

where n_g is the group refractive index, n_p is the phase refractive index, and $dn_\mathrm{p}/d\lambda$ is called the dispersion of the medium. (You can derive this result from $v_\mathrm{g} = d\omega/dk$.) The method for measuring n_g is a natural extension of our method for finding the position of the white-light fringes, and is described below. If the phase index n_p is known for the material, then a measurement of n_g also provides a value for the dispersion $dn_\mathrm{p}/d\lambda$ through the relation Eq. (4.1). For glass and water, the group and phase refractive indexes differ by about 2% for visible wavelengths.

To measure the group refractive index, first find the position of the white-light fringes. Next place a microscope slide in the path of the fixed but rotatable mirror using one of the two aluminum holders provided. The slide will cover just the bottom half of the field of view. It will be very difficult, if not impossible, to find white-light fringes now because the dispersion of the slide will broaden the coherence function and reduce the visibility of the fringes. (See the paragraph above concerning the importance of the "compensator plate.") However, if you cover the white-light source with an interference filter, e.g., the 546-nm filter with a 10-nm bandwidth, you will be able to find green fringes by moving the translatable mirror, though the contrast or visibility of the fringes will be reduced from that which you observed without the slide in place. The visibility is reduced because the dispersion of the slide, even over the narrow 10-nm bandwidth, will broaden the coherence function and reduce its amplitude (i.e., the visibility of the fringes). If d is the distance that the translatable mirror must be moved in order to observe green fringes, then the group refractive index of the slide for 546 nm is given by

$$2d = 2(n_\mathrm{g} - 1)\,t \qquad \text{or} \qquad n_\mathrm{g} = 1 + \frac{d}{t} \tag{4.2}$$

where t is the thickness of the microscope slide and can be measured with the micrometer available in the lab. It makes a certain amount of intuitive sense that a measurement of the displacement of fringes due to a group or band of wavelengths is related to the group refractive index, not the ordinary phase index, and this result can be derived rigorously. The wavelength at which you measure n_g can be varied by using the assortment of interference filters available in the lab (435 nm, 546 nm, and 656 nm).

If you don't have time to perform measurements of the group refractive index during the allotted three laboratory sessions, you may want to pursue this path of investigation as a tech report. Adam Pivonka (HMC '05) was the first to perform these measurements, and his tech report from the spring of 2004 is available in the lab. Please note that Adam was not fully aware of the difference between the group and phase refractive indexes, but his tech report has a very nice description of the measurements.

4.3 Measurement of the Wavelength of a HeNe Laser

The second laboratory session will be spent measuring the wavelength of a helium-neon laser by translating the mirror and recording the movement of fringes at the output of the Michelson interferometer. The mirror may be translated with the motor drive provided. The interferometer should be adjusted to produce circular fringes at the output, and a photodiode should be placed at the center of the fringe pattern (counting fringes by eye can be *very* tedious). The photodiode should be placed sufficiently far from the interferometer so that the central fringe (spot) covers the photodiode. Note that for a given distance from the interferometer to the photodiode, the central spot will increase in diameter as the translatable mirror approaches the equal path length position. The oscillations of the output of the photodiode amplifier can be counted with the frequency counter and/or the LabView software provided. Instructions for data acquisition in Labview are provided next to the computer in the Michelson interferometry lab.

Use your ingenuity to devise a procedure to measure the wavelength of the laser with a precision of better than 1%. Do not *guesstimate* uncertainties; use a *sample variance technique* to determine them rigorously!

4.4 Measurement of the Index of Refraction of Air

When you have completed §4.3, notify your instructor so that the vacuum chamber may be positioned in one leg of the Michelson interferometer. (It's better to let your instructor shatter the glass windows of the chamber and knock the interferometer onto the floor.) The refractive index difference between air and vacuum will be measured by varying the pressure (density) of air in a chamber of constant length while recording the movement of fringes with the photodiode and computer data acquisition system.

A mechanical vacuum pump is used to evacuate the chamber which comprises 2.0165 ± 0.0005 inches of one leg of the interferometer. A mechanical gauge is used to measure the air pressure in the chamber. When the chamber has been evacuated, the valve connecting the vacuum pump and the chamber may be closed and the pump turned off. This will eliminate vibrations transmitted from the pump through the vacuum hose to the chamber. These vibrations can lead to jitter in the photodiode record, because there is some light reflected from the chamber windows. If the needle valve connecting the chamber with room pressure is opened slightly (be gentle, it's a delicate needle valve), the chamber pressure will rise slowly and the fringes will move. The incoming air molecules scatter light, and hence they increase the refractive index and increase the optical path length of that leg of the interferometer. See the reference by Feynman for a beautiful discussion of the origin of the index of refraction.

The following technique is suggested for recording and analyzing the pressure change and fringe movement. Each time the chamber pressure increases by, for example, 10 cm of Hg, make a mark at the corresponding point on the fringe signal recorded by the computer data acquisition system. (You can make this mark by briefly interrupting the laser beam.)

The particular method you devise for data acquisition and analysis should use a sample variance technique to determine the uncertainty in your measured value of $n-1$. Discuss your proposed method with your instructor *before* taking serious data.

Your technique for data analysis should yield a plot of the number of fringes recorded since the valve was opened versus the change in chamber pressure since the valve was opened. (The pressure change should range from, for example, 10 cmHg to 70 cmHg.) The plot should be linear. A least squares fit of the data to a straight line should yield a y intercept of zero (within uncertainty), and the slope of the fit can be used to deduce a value of $n-1$ for air at atmospheric pressure. Compare your value for $n-1$ with the value tabulated in, for example, the CRC Handbook. You will have to take into account the difference of the laboratory temperature from the temperature at which the tabulated value was measured. A thermometer is provided with the laboratory equipment. Convert your measured value of $n-1$ to a value at the temperature quoted in the literature (e.g., 15°C). (The ideal gas law is adequate for this purpose.)

4.5 Using Igor to Record Fringes

These instructions describe a small Igor program to record photodiode output in a virtual strip chart. It is installed on a Windows PC (Purcell, IP = 134.173.33.90) and uses a National Instruments multifunction board to digitize the data. It is quite straightforward to use.

1. Power on the computer, then log in with the account and password

account name	**michelson**
password	**fringes**

2. Launch the program "Igor64.exe" using the shortcut in the taskbar. If prompted, click Yes to install a newer version of HMC.ipf, and then click No to the question, "Do you want to save changes to experiment 'untitled'?"
3. From the **Expt** menu select **Chart**.
4. Click Start to begin recording data. You'll see a virtual strip chart recorder something like the one shown in Fig. 4.3.
5. When you are finished with a scan, click Stop.
6. ⚠If you want to keep the data, click the Save button. Otherwise, it will be erased when the next scan starts. Saved scans are named after the time at which the scan started, with a name such as **S150427** (meaning it started at 3:04:27 pm).

When you click the Save button, the program automatically makes a graph, such as the one shown in Fig. 4.4. By default, the graph has two cursors activated (shown in green and blue in

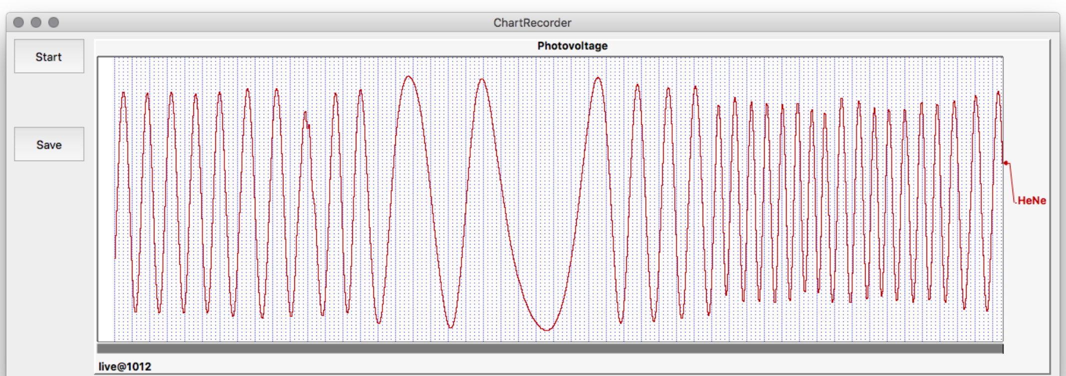

Figure 4.3: Igor's virtual strip chart recorder.

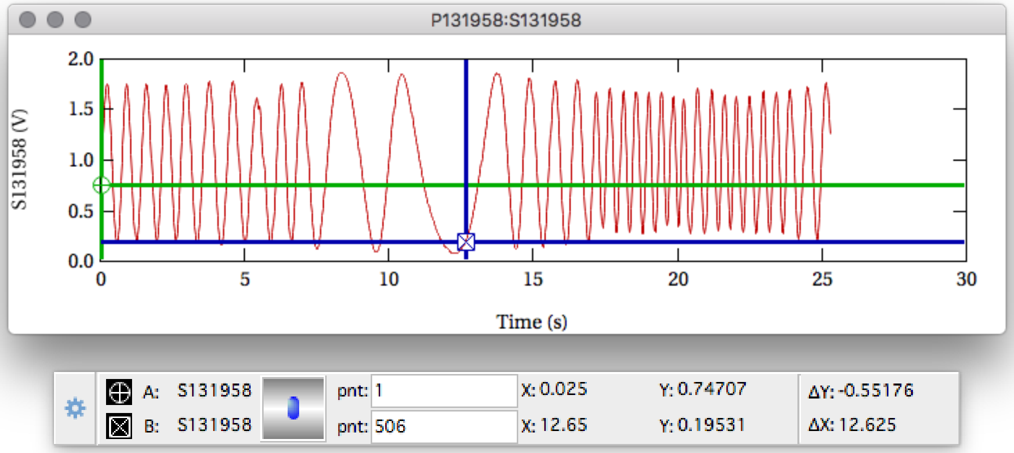

Figure 4.4: Sample scan plot created when clicking the Save button. If you close the plot (or just can't find it), you can make it reappear using the **Plot Scan** submenu.

Fig. 4.4). You can use the cursors to read data from the curve in the information box beneath the graph.

To learn more about how cursors work in Igor, open up the help system and navigate as illustrated below.

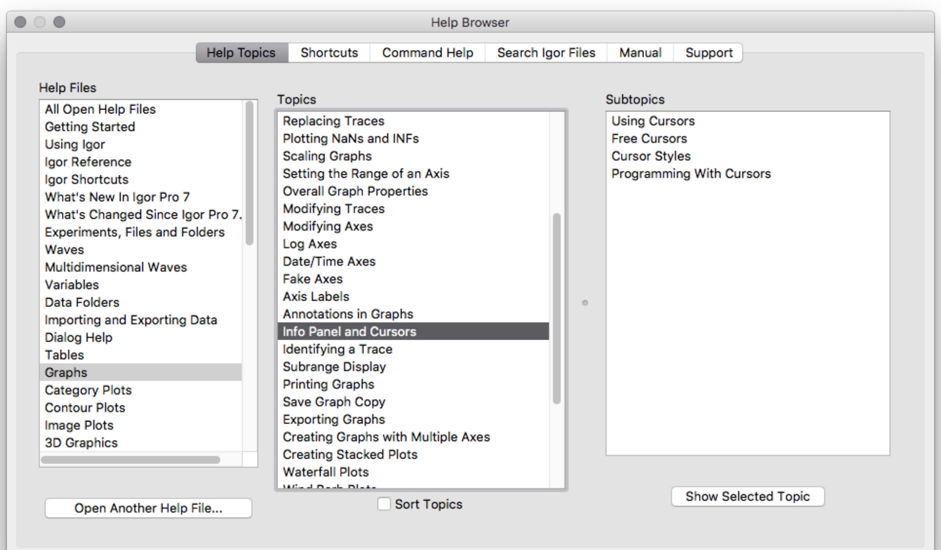

Experiment 5

Fourier Transform Spectroscopy

References

- *Optics* by Miles Klein, Chapter 6, Sections 1 and 2
- *Introductory Fourier Transform Spectroscopy* by Robert J. Bell
- *Optics* by Eugene Hecht. Chapter 12 contains an introduction to coherence theory.

5.1 Introduction

Traditional dispersive techniques for observing the spectrum of a light beam have employed gratings (dispersion by diffraction) and prisms (dispersion by refraction). In the more recently developed technique of Fourier transform spectroscopy, the output intensity $I(\tau)$ of a Michelson interferometer is measured as a function of the optical path difference $2d$ between the two legs of the instrument ($\tau = 2d/c$). The Fourier transform of this output intensity yields the spectrum of the light beam incident on the interferometer. The relationship can be expressed as

$$P(\omega) = \frac{2}{\pi}\int_0^\infty \left[\frac{I(\tau)}{\langle I\rangle} - 1\right]\cos\omega\tau\,\mathrm{d}\tau \tag{5.1}$$

where $P(\omega)$ is the normalized spectral distribution of the light beam incident on the interferometer; i.e.,

$$\int_0^\infty P(\omega)\,\mathrm{d}\omega = 1$$

$I(\tau)$ is the output intensity of the Michelson interferometer when the optical path difference between the two legs of the instrument is $2d$, or when the difference in time of light propagation is $\tau = 2d/c$. $\langle I \rangle$ is the average output intensity over the full range of τ. The integral in Eq. (5.1) is the Fourier cosine transform. The inverse Fourier cosine transform relationship is

$$\frac{I(\tau)}{\langle I \rangle} - 1 = \int_0^\infty P(\omega) \cos\omega\tau \, \mathrm{d}\omega \tag{5.2}$$

Equations (5.1) and (5.2) express the fact that $P(\omega)$ and $[I(\tau)/\langle I \rangle - 1]$ comprise a Fourier cosine transform pair.

A Michelson interferometer that has been modified and fine-tuned for this technique is called a Fourier transform spectrometer (see Fig. 5.2), and the resolving power of the spectrometer depends in principle on the maximum optical path length difference that can be introduced between the two legs of the instrument. Fourier transform spectrometers with half-meter mirror movements have been built with resulting resolving powers on the order of 10^6, which is truly state-of-the-art. With such an instrument, and sufficiently fine sampling of the intensity vs. path length difference, a reliable spectrum can be obtained by full Fourier transform techniques.

Often the general shape of the spectrum of the incident beam is known, but the magnitude of a particular spectral parameter is unknown. For example, the incident spectrum may consist of two spectral lines of roughly equal intensity whose spacing is to be measured; e.g., the yellow doublet of the sodium discharge lamp. Or the incident spectrum may consist of a single line with Lorentzian shape whose half-width-at-half-maximum (HWHM) is to be measured, e.g., the pressure broadened green line of the mercury discharge lamp. In these cases the explicit Fourier transform of the output intensity data need not be calculated, since the functional forms of the relevant Fourier transform pairs are well known. For the sodium doublet, $P(\omega)$ may be written approximately as the sum of two equally weighted delta functions

$$P(\omega) = \frac{\delta}{2}\left(\omega - \omega_{\text{avg}} - \frac{\Delta\omega}{2}\right) + \frac{\delta}{2}\left(\omega - \omega_{\text{avg}} + \frac{\Delta\omega}{2}\right) \tag{5.3}$$

where $\Delta\omega$ is the doublet separation, and ω_{avg} is the average angular frequency of the doublet. The corresponding output intensity $I(\tau)$ is then

$$I(\tau) = \langle I \rangle \left[1 + \cos\left(\frac{\Delta\omega}{2}\tau\right)\cos\left(\omega_{\text{avg}}\tau\right)\right] \tag{5.4}$$

You should verify that equations (5.3) and (5.4) are consistent with equations (5.1) and (5.2).[1]

For the pressure-broadened green line of the mercury discharge lamp, $P(\omega)$ may be written as the Lorentzian spectral profile,

$$P(\omega) = \frac{1}{\pi}\frac{(1/\tau_{\text{p}})}{(\omega - \omega_0)^2 + (1/\tau_{\text{p}})^2} \tag{5.5}$$

[1] You'll find the following identities useful:

$$2\cos\omega_1\tau\cos\omega_2\tau = \cos(\omega_1 + \omega_2)\tau + \cos(\omega_1 - \omega_2)\tau \qquad \delta(\omega - \omega_0) = \frac{2}{\pi}\int_0^\infty \cos\omega_0\tau\cos\omega\tau\,\mathrm{d}\tau$$

where the HWHM is $(1/\tau_p)$, and ω_0 is the angular frequency corresponding to $\lambda = 546\,\mathrm{nm}$. The parameter τ_p is the mean time between collisions of mercury atoms. The corresponding $I(\tau)$ is

$$I(\tau) = \langle I \rangle \left[1 + \exp\left(-\tau/\tau_p\right)\cos(\omega_0 \tau)\right] \tag{5.6}$$

Again you should verify that equations (5.5) and (5.6) are consistent with equations (5.1) and (5.2). Hints: when evaluating the integral in Eq. (5.1), use the first identity in the footnote and then express (for example) $\cos(\omega - \omega_0)\tau$ as $\mathrm{Re}\left(\exp[i(\omega - \omega_0)\tau]\right)$. The resulting integral is straightforward. Please note, however, that the integral in Eq. (5.1) yields two terms, one of which is always negligibly small and does not appear in Eq. (5.6). When evaluating the integral in Eq. (5.2), note that the limits can be extended to $-\infty$ to $+\infty$ because the width of the line $(1/\tau_p)$ is many orders of magnitude smaller than the center frequency ω_0. Now the integral becomes a great application of the residue theorem from complex analysis!

In both of the examples in equations (5.4) and (5.6), the output intensity $I(\tau)$ consists of a rapidly fluctuating fringe term, $\cos\omega_{\mathrm{avg}}\tau$ or $\cos\omega_0\tau$, which is modulated by a slow envelope, $\cos(\Delta\omega\tau/2)$ or $\exp\left(-\tau/\tau_p\right)$, respectively. In these cases and in other similar situations, the value of a spectral

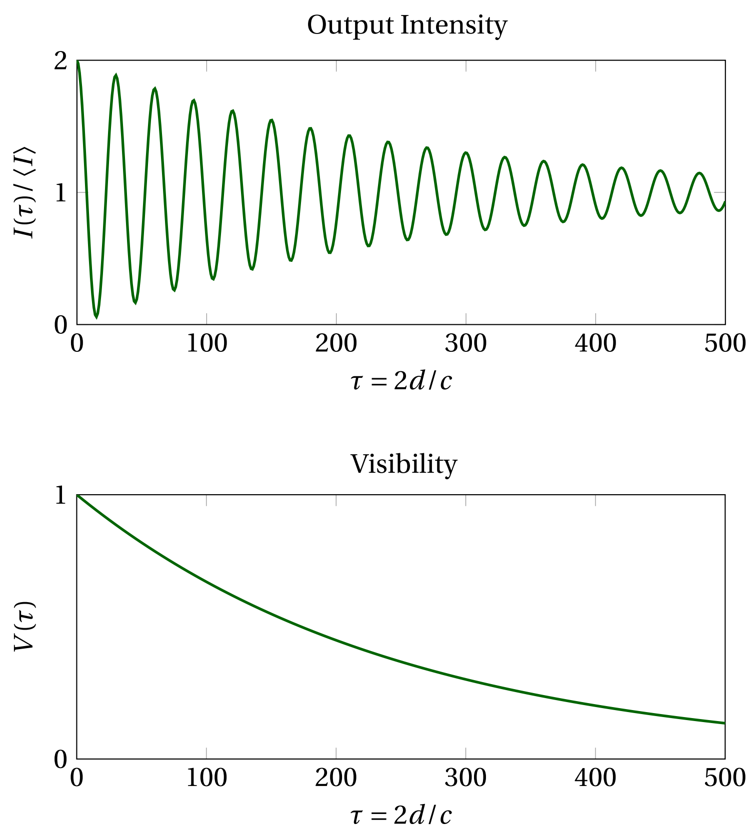

Figure 5.1: Representative plots of output intensity and visibility for a Lorentzian spectral line.

parameter can be obtained simply by measuring the so-called visibility $V(\tau)$ of the fringes as a function of mirror position. The **visibility** of the fringes is defined to be the zero-to-peak amplitude of the fast fringes divided by the average output intensity $\langle I \rangle$; i.e., just the magnitude of the slow envelope of the fringes. Hence for the sodium doublet and the mercury green line, the visibilities $V(\tau)$ are $|\cos(\Delta\omega\tau/2)|$ and $\exp(-|\tau|/\tau_\text{p})$, respectively. Figure 5.1 illustrates $I(\tau)$ and $V(\tau)$ for the mercury green line. Measurements of $V(\tau)$ for these two cases will therefore yield directly the spacing of the sodium doublet and the mean time between collisions of mercury atoms.

5.2 Measurement of the Sodium Doublet Separation

The experimental apparatus consists of a sodium discharge lamp, an optical interference filter that eliminates all spectral lines except the yellow doublet, a homemade Fourier transform spectrometer, a photodiode and amplifier, an electrical filter, and a digital oscilloscope (see Fig. 5.2). The electrical filter is necessary to suppress the 120-Hz (and higher harmonics) fluctuation of the lamp intensity due to the 60-Hz stimulating voltage. Center the circular fringes formed at the output of the spectrometer on the photodiode. If you don't see the fringes at the output, try translating the mirror to make sure the visibility of the fringes, $|\cos(\Delta\omega\tau/2)|$, doesn't simply happen to be zero. If you still don't see fringes, use the following steps to bring the instrument into proper adjustment:

(1) Use a ruler to position the translatable mirror at the equal path length position ($\tau = 0$).

(2) Place a pointed object at the input of the instrument and look into the output of the instrument. Rotate the fixed mirror until the two images coincide.

(3) With light from the sodium lamp incident upon the instrument, look into the output of the instrument. You should see fringes. If you don't, repeat (1) and (2). Rotate the fixed mirror to form circular fringes, or at least strong fringes. Now place a white card at the output to view the fringes.

When you have centered the circular fringes, visually check the alignment of the lamp, interference filter, and interferometer. A crooked light path can cause subtle problems later. When you have centered the fringes on the photodiode, translate the mirror by turning the micrometer drive and note qualitatively the periodic appearance and disappearance of the fringes. Be careful not to go too far from the $\tau = 0$ position because the nonzero width of the spectral lines comprising the sodium doublet leads to an eventual washout of the fringes ($V(\tau) \to 0$ as τ becomes large). While viewing the fringes by eye, you should measure roughly the distance from one visibility minimum to the next. Compare your measured value with the value you calculate using the literature value for the spacing of the sodium doublet. If the values agree, you know what you're looking at!

The goal of §5.2 is to measure the doublet separation $\Delta\omega$ with a precision better than 1%. Many students are able to achieve this goal simply by observing visually several successive visibility

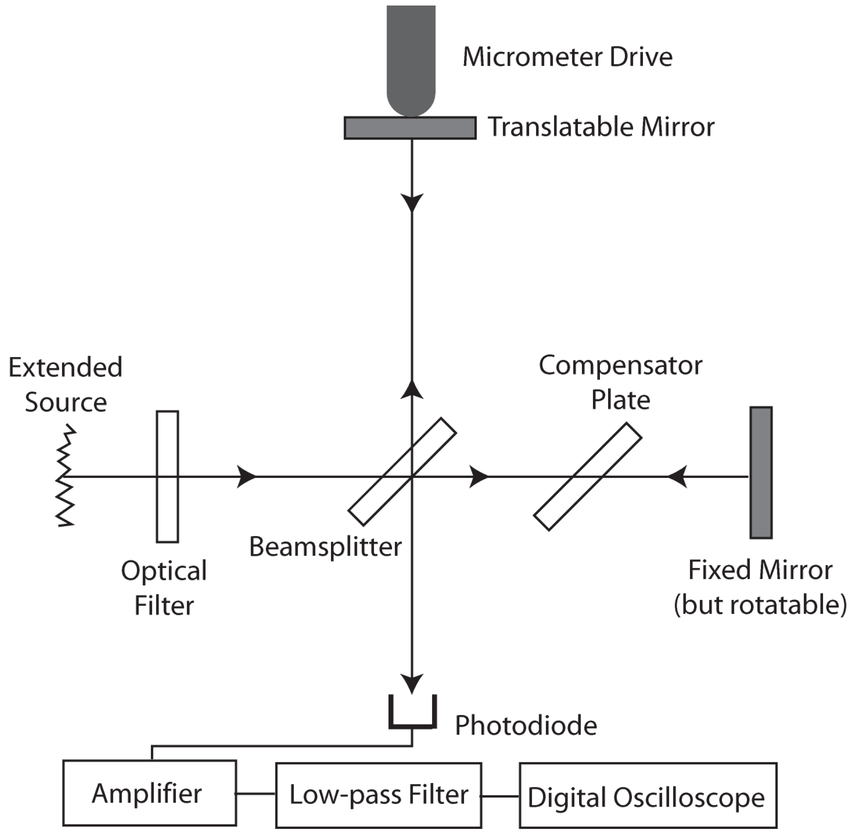

Figure 5.2: Experimental setup for FTS measurements.

minima (up to 6 or more) while recording the micrometer readings at the minima. A plot of the micrometer readings versus minimum number (simply an integer) should be a straight line. A least-squares fit should yield a slope (with uncertainty) from which the doublet splitting can be deduced. If you use this technique, be sure to use a sample variance technique to assign uncertainties to the positions of the minima.

Alternatively, you can measure the visibility using the photodiode. *Lightly* touch the translatable mirror mount or *gently* press on the optical rail or table that support the interferometer. A *light* touch or *gentle* press will cause the fringe pattern to shift by a few fringes, which in turn causes the output intensity $I(\tau)$ measured by the photodiode to vary through a few cycles of the rapid fluctuation term $\cos\omega_{\text{avg}}\tau$. If the digital oscilloscope is in its Store mode, and the horizontal time scale is set to a few milliseconds per division, then the fluctuating output of the photodiode amplifier will result in a band of brightness on the scope screen. The bottom and top of the bright band correspond to the minimum and maximum values of $I(\tau)$ for τ in an interval small enough for the visibility $V(\tau)$ to be constant. Hence from the vertical height of the bright band and the vertical position of its midpoint, a value of $V(\tau)$ may be calculated. By advancing the micrometer, repeating the "*light* touch" or "*gentle* press" maneuver, and recording again the band of brightness, values for the visibility may be obtained at chosen values of τ. An interpolation technique can be used to find the positions of successive minima. Again, be sure to use a sample variance technique to determine an uncertainty in the distance between successive minima, and propagate this uncertainty through to an uncertainty in the doublet separation.

Convert your measured value for the sodium doublet separation $\Delta(\omega)$ into a difference in wavelength (assume the average wavelength is 589.3 nm). Compare your measured value with the literature value—it should be roughly 0.6 nm (or 6 Å). Note that 1% of 0.6 nm is 0.006 nm. Take a moment to muse on the magnitude of 0.006 nm.

An alternative approach to measuring the visibility of the fringes would be to use an imaging detector, such as the CMOS sensor in a digital camera, and to analyze the image of the fringes to deduce their visibility. The advantage of this approach is that you don't have to touch the instrument lightly to slightly vary the path length. The down side is that you have more work to do to convert the images to visibility readings. Such an investigation might be an interesting project for a technical report.

5.3 Measurement of the Width of the Mercury Green Line

Replace the sodium discharge lamp with the mercury discharge lamp. Be sure to replace the sodium doublet interference filter with the interference filter for the 546-nm mercury green line. After centering the fringes on the photodiode, translate the mirror of the spectrometer and notice the decrease in the visibility of the fringes as the mirror is translated in either direction from the $\tau = 0$ position. The photodiode technique (as described in §5.2) will be particularly helpful here even if you did not use it previously. Remember, though, that the width of the bright band in this technique tells you only $(I_{\mathrm{max}} - I_{\mathrm{min}})$, and you will need to know the overall offset from zero in order to calculate and plot the fringe visibility.

You should measure the visibility of the fringes as a function of $\tau = 2d/c$. Be sure to take data in both directions from the $\tau = 0$ position, and check to see that the data is symmetric about $\tau = 0$. Think hard about what might give rise to an asymmetry between positive and negative τ.

For a Lorentzian spectral line, a plot of $\ln[V(\tau)]$ versus τ should be linear with a slope of $(-1/\tau_{\mathrm{p}})$. Using a linear regression technique, calculate a value and an uncertainty for τ_{p}, the mean time between collisions of mercury atoms. Your uncertainty in τ_{p} should be the result of sample uncertainties in measured parameters. Convert $(1/\tau_{\mathrm{p}})$, the HWHM of the spectral line (in rad/s) to a width in nanometers and compare this width with the center wavelength of 546 nm. If you have performed the grating spectrometer experiment, compare your two values for the width of this line. If you haven't performed the grating spectrometer experiment, indicate the necessary resolving power of a grating which could detect the nonzero width of this line. Are such gratings available commercially?

Experiment 6

Quantum Optics

References

- *The Quantum Challenge* by G. Greenstein and A. G. Zajonc (1997, or 2$^{\text{nd}}$ edition 2005). The first two chapters of this book set the stage for the test of the quantum nature of light. The book as a whole is an intriguing review of recent tests of quantum theory, and suggests many elaborate experiments with our setup — tests of Bell's inequality, quantum erasers, quantum coherence theory, etc. Strongly recommended background reading!
- "The Nature of Light: What is a Photon?", *Optics and Photonics News Trends* Oct 2003. This is a special issue of *OPN Trends* focusing on the current notion of a "photon". There are five articles by renowned experts in the field of quantum optics, and the one by Arthur Zajonc and another by Rodney Loudon are particularly relevant for us.

6.1 Introduction

The particle-wave duality of light has sparked heated debate throughout the history of science. In the early 20$^{\text{th}}$ century, it became clear that the particle-wave duality applied to "particles" as well as light, and this of course refueled the debate leading to even deeper controversy. Not only were scientists faced with the job of reconciling in one theory the aspects of Newton's particles and Maxwell's waves, but the whole notion of physical reality as described by the new quantum theory seemed to be dragged into the fray. The Einstein-Podolsky-Rosen paradox seemed to epitomize the difficulties that many scientists encountered in constructing an appropriate view of physical reality. Quantum theory certainly seems to be successful, but the word "strangeness" is now a popular term used to describe some of its predictions — and most of these predictions have been verified experimentally!

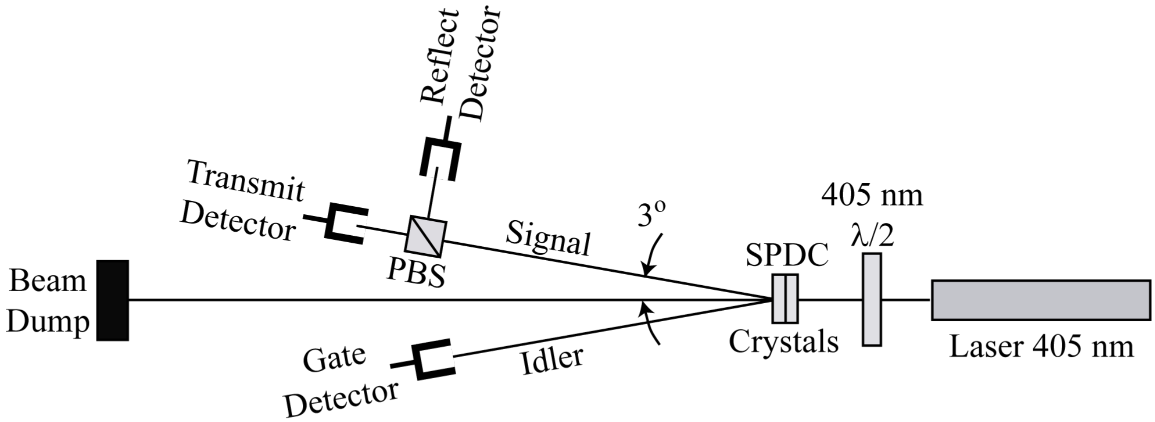

Figure 6.1: Experimental setup for the study of the quantum nature of light. (PBS = polarizing beam splitter; SPDC = spontaneous parametric down-conversion.) According to quantum theory, a signal photon incident upon the polarizing beam splitter (PBS) is either transmitted or reflected, so no GTR triple-coincidence counts should be recorded.

The setup associated with this experiment consists of a source of entangled photon pairs, some standard optical components, and four photon-counting silicon photodetectors. (See Fig. 6.1) A wide array of measurements can be performed with this equipment, including: (1) a confirmation of the quantum nature of the photon—i.e., light exists in quanta, (2) a study of single-photon interference, (3) a demonstration that photons are bosons, (4) a test of Bell's inequalities, and (5) a demonstration of a "quantum eraser."

Beginning in the Fall of 2005 and the Spring of 2006, students in Advanced Lab and Optics Lab have performed experiment (1) and confirmed the quantum nature of the photon, though it is an experiment that has been recently enhanced by new, faster data acquisition hardware (field programmable gate array — FPGA) that makes possible new measurements with classical light sources that serve as important control experiments. The measurement exploits the properties of a pair of entangled photons and employs time-coincidence techniques to show that a photon incident upon a beam splitter is either transmitted or reflected but does *not* go in both directions as classical electromagnetic theory would predict. The experiment goes to the heart of the field of photon statistics and quantum optics.

Students have also performed experiment (4) by examining a situation in which the predictions of quantum mechanics are confirmed but those of hidden variable theories are clearly violated. The entangled polarization state of photon pairs is produced in the "spontaneous parametric down-conversion" process which forms the core of the "single photon source", a key component of the experimental setup. The experiment is very reminiscent of the Einstein-Rosen-Podolsky (EPR) paradox that started all the intellectual hubbub in the mid-20$^{\text{th}}$ century. These Bell inequality tests have been performed several times, though recently we have acquired a "pre-compensation" quartz crystal that should improve the "purity" of the entangled polarization state of photon pairs and hence accentuate the failure of hidden variable theories to account for the measurements. A similar pre-compensation crystal produces highly entangled photon states in the Lynn research lab (see Julien Devin's senior thesis, 2012), but so far we have not succeeded in reproducing that result in the optics/advanced lab setup. Carefully reviewing the theory, the crystal specifications, and the experimental setup should enable us to solve this puzzle!

Finally, in the Fall of 2010, Advanced Lab students assembled an optical setup that comprises (5) a quantum eraser, and preliminary results were dramatically successful! This experiment includes an interferometer in the path of the "signal" photon which produces interference fringes, so (2) single photon interference is involved in this experiment as a delightful bonus! The measurement consists of first demonstrating fringes at the output of an interferometer in the "signal" photon path, with the polarization optics in the "idler" photon path having appropriate settings. Then a half-wave plate in the idler photon path is rotated by 22.5°, and suddenly the fringes generated in the "signal" photon path disappear because polarization now offers *which-way* information on a signal photon's path through the interferometer. When the idler half-wave plate is rotated back to its original position, the which-way information is "erased," and fringes reappear. The finges are controlled by an adjustment that is potentially space-like separated from the fringe measurement! A DC servo motor actuator has been installed to automate the collection of fringes, and fringes have been observed with the revised setup. However, the fringes do not entirely disappear, so this experiment offers the challenge of uncovering the flaw(s) in the setup and successfully observing the complete disappearance and recovery of fringes to confirm the predictions of quantum mechanics.

Choosing one of three experimental paths: You must decide which of these three types of measurements to pursue — (i) the confirmation of the quantum nature of light, (ii) tests of Bell's inequalities (with possible investigation of the pre-compensation crystal), or (iii) demonstration of a quantum eraser. You can't do all three, and you can't go wrong no matter which you choose! Each experimental path is described in more detail in a sequel document accessible wherever you found this introductory document. Enjoy the journey!

6.2 The Quantum Nature of Light

References

- "Observing the quantum behavior of light in an undergraduate laboratory," by J. J. Thorn, M. S. Neel, V. W. Donato, G. S. Bergreen, R. E. Davies, and M. Beck, *American Journal of Physics* **72**(9) 1210-1219 (2004). This paper from Mark Beck's group at Whitman College describes the experiment that Adam Pivonka and Tera Bell replicated in 2004-2005 to confirm the existence of quanta of light. In fact, Prof. Beck generously guided us as we purchased the components of our current experimental setup, and he also made available to us everything on his website, including the LabVIEW VIs that we use to acquire data. This paper is a MUST read!
- "Studying the Quantum Nature of Light," by Adam Pivonka, senior thesis, May 2005. A copy is placed with the lab reference material, and an electronic version is available on the course Sakai site. Adam describes the use of the setup to confirm the quantum nature of the photon. ALL of the details are there!
- "Comparing measurements of $g^{(2)}(0)$ performed with different coincidence detection techniques," by M. Beck, *J. Opt. Soc. Am. B* **24**, 2972-2978 (2007). This paper by Mark Beck is particularly useful if you are attempting to do a control experiment, measuring the autocorrelation function for a classical source of light. The paper explains how the limitations of our NIM counting and coincidence electronics influence the count rates and render them difficult to interpret when working with a very high single-detector rate (roughly above 50,000/s); the Whitman College group ultimately adopted FPGA data acquisition modules to overcome these limitations, and so have we! An FPGA module is available and awaits use by Optics Lab and Advanced Lab students to measure $g^{(2)}(0)$ for a classical source (as well as a single-photon source).

6.2.1 Introduction

Adam Pivonka and Tera Bell (HMC '05) pursued a study of the quantum nature of light as their senior research project. They used coincidence techniques to show that a photon incident upon a beam splitter is either transmitted or reflected, but not both at the same time! They pointed out that classical theories of the electromagnetic field cannot explain this result. In fact, even a semi-classical theory, in which atoms are quantized and the EM field is described as a classical wave, predicts a strong correlation between transmitted and reflected beams, or at least no correlation, rather than the strong anti-correlation observed (a photon counted in the transmitted beam means **no** count in the reflected beam).

The work of Adam and Tera has been repeated and confirmed by members of the Advanced Lab and Optics Lab courses, and also by Andy Fischer and Travis McQueen (HMC '06) as part of their senior thesis project. In addition, many participants in Optics Lab have conducted con-

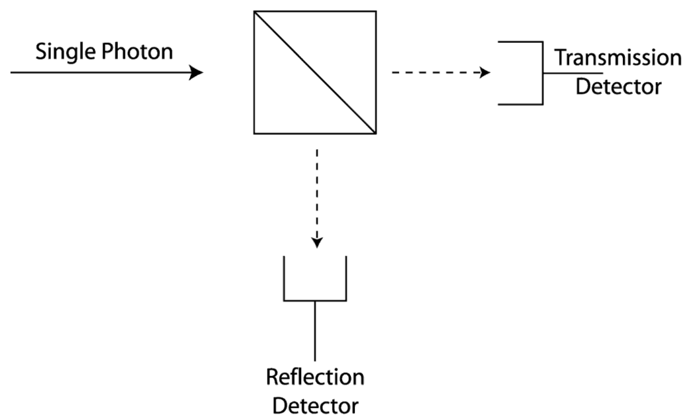

Figure 6.2: A single photon is incident upon a beam splitting cube, and photon-counting detectors look for a photon at the transmitted and reflected outputs.

trol experiments to demonstrate, as well as possible with our current NIM electronics, that our measurement scheme when applied to a classical light source yields no correlation rather than anti-correlation between the transmitted and reflected beams (see the 2007 paper by Beck). Extensive work has been performed on the data acquisition hardware in this experiment, and there is now the possibility of employing FPGA (Field Programmable Gate Array) modules to collect data with photon count rates at least 10 times higher. These higher count rates facilitate measurements of $g^{(2)}(0)$ for a classical light source with far better statistics and precision.

6.2.2 Demonstrating the Quantum Nature of Light

The conceptual scheme of our experiment is sketched in Fig. 6.2. We assume for the moment that we have a reliable source of single photons. Using this light source, we throw a steady stream of single photons at a beamsplitting cube. Photon-counting detectors are placed at the transmission and reflection outputs of the beam splitter. (See Fig. 6.3 for a photo of the experimental equipment. The detectors are housed in a light-tight box, and the photons are led to them by multimode optical fiber.) If the photon is really an indivisible particle, then either the transmission detector will record a photon, or the reflection detector will record a photon, but not both simultaneously! If the beam splitter has a 50%-50% splitting ratio, then half the time the transmission detector records the photon and half the time the reflection detector records the count. This is in sharp contrast with the classical view of this experiment.

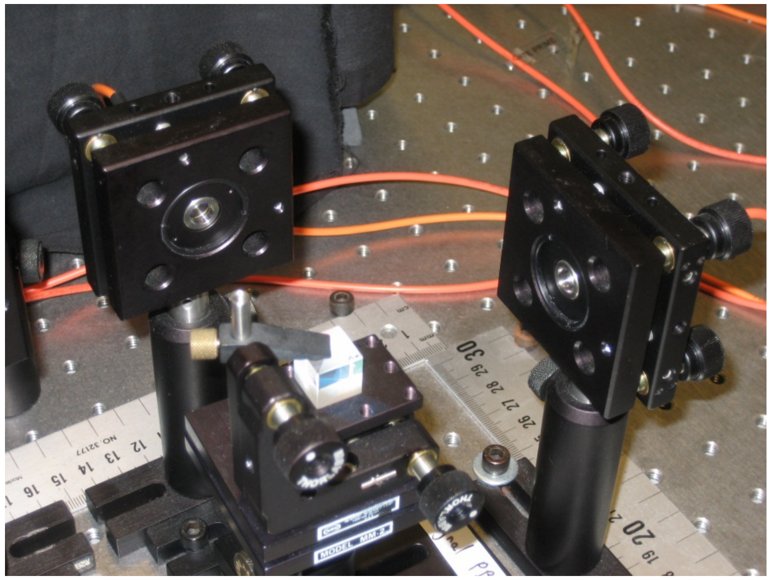

Figure 6.3: Photograph of the polarization beam splitter in the signal photon path. A vertically polarized photon incident upon the beamsplitting cube is reflected toward the "Reflect" fiber coupler, while a horizontally polarized photon is transmitted to the "Transmit" fiber coupler.

Classical Theory

The correlation between the transmitted and reflected intensities can be characterized quantitatively by the degree of second order coherence of the electric fields at the two outputs:

$$g_{TR}^{(2)}(0) = \frac{\langle I_T(t) I_R(t)\rangle}{\langle I_T(t)\rangle \langle I_R(t)\rangle} \tag{6.1}$$

We have evaluated $g_{TR}^{(2)}(\tau)$, sometimes called the "normalized intensity correlation function," at a time delay τ of zero, since we will be looking at the transmitted and reflected outputs at the same time. The angle brackets in Eq. (6.1) indicate that the time average is taken. Notice that the numerator is the time average of the product of the transmitted and reflected intensities. As mentioned above, if we do not expect the transmission and reflection detectors to produce outputs at the same time, then the numerator will be zero. In contrast, if we define transmission and reflection coefficients, T and R, then the transmitted and reflected intensities will be $I_T = TI_0$ and $I_R = RI_0$, where I_0 is the incident intensity. In our classical view, we regard the incident intensity as a continuous variable, and a portion is transmitted and a portion reflected, so that Eq. (6.1) becomes

$$g_{TR}^{(2)}(0) = \frac{\langle I_T(t) I_R(t)\rangle}{\langle I_T(t)\rangle \langle I_R(t)\rangle} = \frac{\langle TI_0(t) RI_0(t)\rangle}{\langle TI_0(t)\rangle \langle RI_0(t)\rangle} = \frac{\left\langle [I_0(t)]^2\right\rangle}{\langle I_0(t)\rangle^2} \tag{6.2}$$

The Cauchy-Schwartz inequality implies that $\left\langle [I_0(t)]^2 \right\rangle \geq \langle I_0(t)\rangle^2$, so that classically we have

$$g^{(2)}_{TR}(0,\text{ classical}) = \frac{\langle I_T(t) I_R(t)\rangle}{\langle I_T(t)\rangle \langle I_R(t)\rangle} = \frac{\left\langle [I_0(t)]^2 \right\rangle}{\langle I_0(t)\rangle^2} \geq 1 \tag{6.3}$$

The Whitman College group (Thorn et al., 2004) and also Adam Pivonka (HMC senior thesis) have shown that Eq. (6.3) holds also in the semi-classical view. In this theory, the energy states of atoms are quantized so that energy is absorbed from the electromagnetic field in quanta, but the electromagnetic field itself is treated classically as a continuous field.

Quantum Theory

When the electromagnetic field is quantized (quantum electrodynamics or QED), the transmitted and reflected intensities in Eq. (6.1) become operators (denoted with hats)

$$g^{(2)}_{TR}(0) = \frac{\left\langle : \hat{I}_T \hat{I}_R : \right\rangle}{\left\langle \hat{I}_T \right\rangle \left\langle \hat{I}_R \right\rangle} \tag{6.4}$$

In Eq. (6.4), the colons indicate normal ordering of the creation and annihilation operators that are implicit in the intensity operators. The Whitman group and Adam Pivonka present a careful evaluation of Eq. (6.4) with the result

$$g^{(2)}_{TR}(0,\text{ quantum}) = \frac{\left\langle : \hat{I}_T \hat{I}_R : \right\rangle}{\left\langle \hat{I}_T \right\rangle \left\langle \hat{I}_R \right\rangle} = 0 \tag{6.5}$$

We shall not repeat their derivation here, but simply note that that the result agrees with our intuitive expectation that a particle-like photon will be detected by the transmission detector or by the reflection detector, but not by both at the same time.

Theory Summary

When the transmitted intensity is completely uncorrelated with the reflected intensity, the average of the product in the numerator of Eq. (6.1) is equal to the product of the averages, and $g^{(2)}_{TR}(0) = 1$. This is the case for laser sources. It is also true that photons are distributed in a laser beam such that the number of photons detected in a time interval Δt is distributed according to the Poisson distribution. (See Eq. (6.6) below.)

When the transmitted intensity is positively correlated with the reflected intensity, so that both detectors are likely to be detecting photons at the same time (in bunches), then $g^{(2)}_{TR}(0) > 1$. This is the case for "thermal" or "chaotic" sources like fluorescent lights or incandescent light bulbs. If the detectors are fast enough to follow the fluctuations of these sources, then $g^{(2)}_{TR} = 2$. In this case, the numbers of photons detected in a time interval Δt are distributed according to the Bose-Einstein distribution.

Only when the transmitted intensity is perfectly *anti*-correlated with the reflected intensity does $g^{(2)}_{TR}(0) = 0$. In this truly quantum case, the photon distribution is called "sub-Poissonian" because the variance of the number of photons detected in a time interval Δt is less than the mean number.

Single-Photon Light Sources

Up to this point we have assumed that we possess a single photon light source with which we can launch a steady stream of photons toward the beam splitting cube in Figures (6.1) and (6.2). It is tempting to imagine constructing such a light source simply by attenuating a laser beam so that, on average, only one photon is in the vicinity of the beam splitter at any given time. The probability of detecting n laser photons in a time interval Δt is given by the Poisson distribution

$$P(n, \Delta t) = \frac{\langle n \rangle^n}{n!} e^{-\langle n \rangle} \tag{6.6}$$

where $\langle n \rangle$ is the average number of photons recorded in Δt . Using Eq. (6.6), it is easy to show that the ratio of probabilities of detecting 2 photons to just 1 photon in a time interval Δt is

$$\frac{P(2, \Delta t)}{P(1, \Delta t)} = \frac{\langle n \rangle}{2} \tag{6.7}$$

If Δt is the time taken by light to travel through the vicinity of the beam splitter, and if the laser is attenuated so that $\langle n \rangle \ll 1$, then there will be usually just one photon in the vicinity of the beam splitter. However, the probability of having any photons at all in the vicinity of the beam splitter is now small, since $P(1, \Delta t) \approx \langle n \rangle \ll 1$. It is tricky to attenuate the laser just enough to be fairly certain that only one photon is in the vicinity of the beam splitter at a time, and yet not too much so that count rates are still high enough to be usable. In any case, a more fundamental objection to this strategy is that $g^{(0)}_{TR}(0)$ is normalized by the average count rates in such a way that its value would still be 1 for an attenuated laser beam! We clearly need a non-classical single-photon light source if we are to demonstrate the particle nature of the photon.

6.2.3 The Experimental Setup

Our experimental setup for studying the quantum nature of light is sketched in Fig. 6.4. The entangled photon-pair source comprises a 50-mW violet laser (405 nm) illuminating a pair of barium borate (BBO) crystals cut to facilitate type-I spontaneous parametric down-conversion (SPDC). In this nonlinear process an occasional incident 405-nm photon is converted into a pair of 810-nm photons with linear polarization orthogonal to the linear polarization of the incident beam. The two BBO crystals are cut at the same angle to their optic axes but then oriented at 90° to one another, so that the two different crystals yield SPDC photons with orthogonal polarizations. The half-wave plate provides a means for rotating the polarization of the incident beam

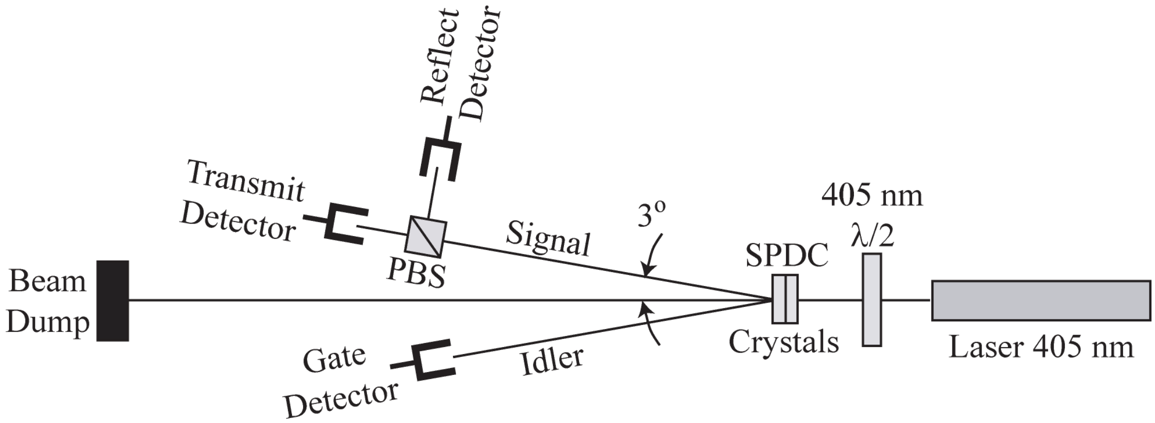

Figure 6.4: Experimental setup for the study of the quantum nature of light. (PBS = polarizing beam splitter; SPDC = spontaneous parametric down-conversion.)

so that roughly equal numbers of horizontally and vertically polarized 810-nm photons are produced in the SPDC process. Conservation of momentum and energy imposes constraints on the two 810-nm photons, so that they are entangled in energy, direction, and polarization.

One of the 810-nm photons is called the **idler** photon and is used as a gate for coincidence circuitry, while the other 810-nm photon is called the **signal** photon and is directed toward a beam splitter. In effect, gating with the idler photon allows us to conduct measurements in the signal path only when we know there happens to be a single photon in that path. This type of setup is known as an *a posteriori* source of single photons, as opposed to the desirable but technically daunting *a priori* source which would produce single photons on demand.

The idler and signal photons are captured by lens/optical-fiber combinations called "fiber couplers." The optical fiber transports the photons to silicon **avalanche photodiodes** (APDs) that are capable of detecting single photons with 60% quantum efficiency. The 20-ns-wide TTL pulses from the photodetectors are sent to three time-to-amplitude/single-channel-analyzer (TAC/SCA) modules that record two-way and three-way coincidences. The two-way coincidences are between the gate and transmission detectors (GT) and between the gate and reflection detectors (GR). The three-way coincidences involve all three detectors (GTR). See Fig. 6.5 for a schematic of electrical connections.

It is important to understand the operation of the TAC/SCA modules. In fact, setup and understanding of these may well occupy you for more than one full lab session. Let us consider the GT TAC/SCA module, in which the gate pulse is connected to the START input and the transmission pulse is connected to the STOP input. The TAC circuitry generates an output pulse with an amplitude that is proportional to the delay between the START pulse and the STOP pulse. We have inserted a little extra cable in the transmission and reflection pathways (10 ft and 20 ft, re-

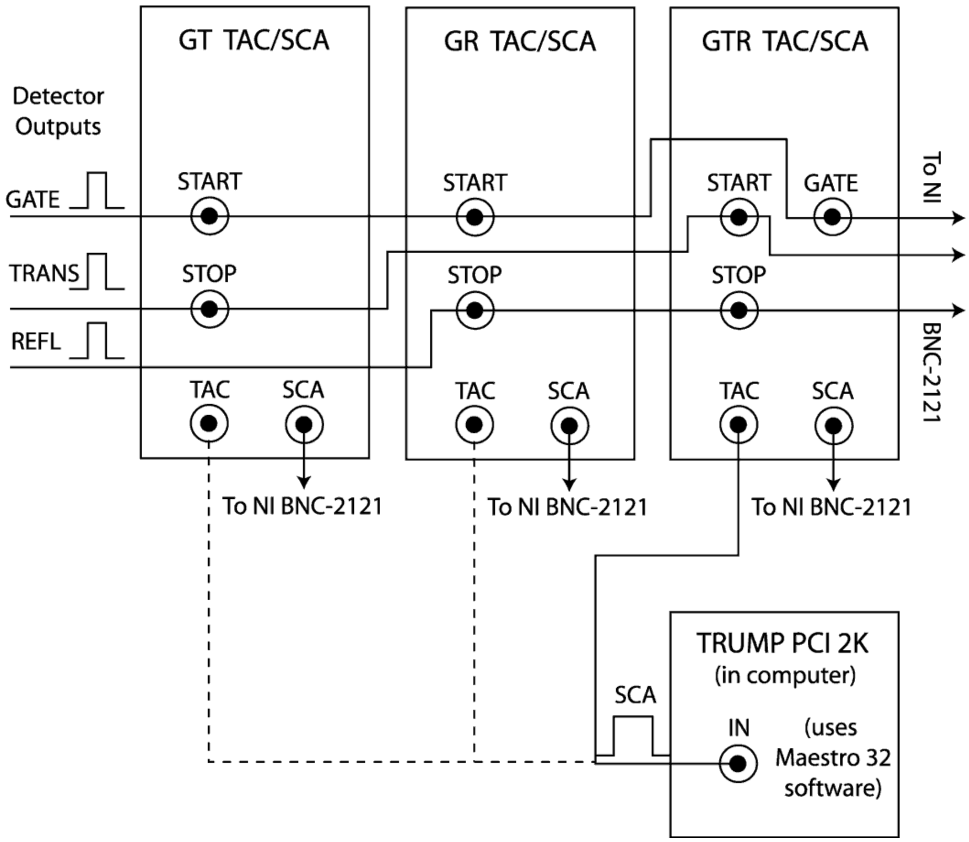

Figure 6.5: Output pulses from the three detectors are routed to three Ortec 567 Time-to-Amplitude/Single-Channel-Analyzer (TAC/SCA) modules and to the National Instruments 6602 Counter/Timer board through the BNC-2121 Connector Accessory. See Fig. 6.6 for the connections to the BNC-2121 Connector Accessory. The TAC outputs are connected to the Ortec TRUMP PCI 2K pulse height analyzer board for analysis of the timing of the photon pulses using the Maestro 32 software.

spectively) so that the transmission pulse is conveniently delayed by ~15 ns, and the reflection pulse is delayed by ~30 ns. As a result, when gate and transmitted photons are received by the detectors simultaneously, the GT TAC circuitry outputs a 3-μs-wide pulse with an amplitude of about 3.0 V (10 V corresponds to 50 ns delay, so 3 V corresponds to 15 ns). The SCA circuitry on the GT module is set so that TAC pulses ranging from 2.6 to 3.4 volts will generate an SCA output pulse (about 3-μs wide) which is then counted by the NI 6602 counter board. See Fig. 6.6 for a schematic of connections to 6 of 8 counters on the NI 6602 board. The TAC output, in addition to being passed internally to the SCA circuitry, can be sent to the TRUMP PCI 2K pulse height analyzer (PHA) card. The Maestro 32 software can be used to examine the amplitudes of TAC pulses and hence the time delays between the START and STOP pulses, and this information greatly simplifies the setting of the window of the SCA.

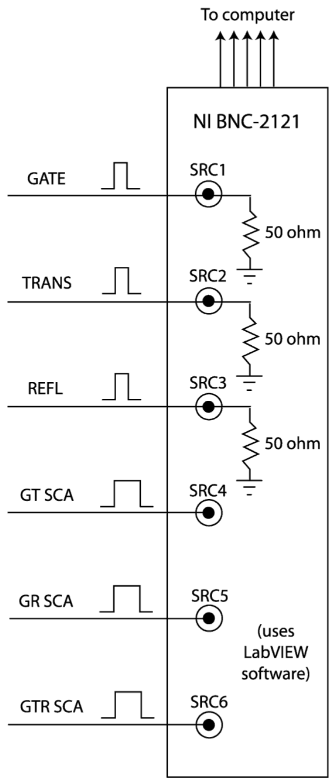

Figure 6.6: Signals are routed by the National Instruments BNC-2121 connector accessory to the National Instruments 6602 Counter/Timer Board which is inserted into the chassis of the computer. The NI 6602 has 8 counters, and we use 6 of them. The board is controlled by LabVIEW software.

How Can We Measure $g^{(2)}(0)$?

We need to relate measurable count rates to the definition of $g^{(2)}_{TR}(0)$ in Eq. (6.1). You can probably convince yourself of the following expression:

$$g^{(2)}_{TR}(0) = \frac{\langle I_T(t) I_R(t)\rangle}{\langle I_T(t)\rangle \langle I_R(t)\rangle} = \frac{P_{TR}}{P_T P_R} \tag{6.8}$$

Here P_{TR} is the probability of recording a transmitted photon and a reflected photon in the same time interval Δt , and P_T and P_R are the probabilities of recording a transmitted photon or a reflected photon in a time interval Δt, respectively. However, in order to implement our single photon source, we condition the recordings of transmitted and reflected photons on the reception of a simultaneous gate photon (idler photon). We must rewrite the expression in Eq. (6.8) so that it is relevant to our use of a single photon source, obtaining

$$g^{(2)}_{TR}(0) = \frac{\langle I_T(t) I_R(t)\rangle}{\langle I_T(t)\rangle \langle I_R(t)\rangle} = \frac{P_{GTR}}{P_{GT} P_{GR}} \tag{6.9}$$

where, for example, P_{GTR} is the probability of recording counts in all three detectors in a time interval ΔT. With a little more thought, you can probably convince yourself that these conditional probabilities can be expressed in terms of recorded counts,

$$P_{GT} = \frac{N_{GT}}{N_G} \qquad P_{GR} = \frac{N_{GR}}{N_G} \qquad P_{GTR} = \frac{N_{GTR}}{N_G} \tag{6.10}$$

where N_{GT} is the number of GT coincidence counts recorded in a given time interval, and N_G is the number of singles counts recorded by the gate detector in the same time interval. Three subscripts indicate triple coincidences. Combining Eqs. (6.9) and (6.10) we have

$$g^{(2)}_{TR}(0) = \frac{\langle I_T(t) I_R(t)\rangle}{\langle I_T(t)\rangle \langle I_R(t)\rangle} = \frac{P_{GTR}}{P_{GT}P_{GR}} = \frac{N_{GTR}N_G}{N_{GT}N_{GR}} \tag{6.11}$$

Our job then is to measure these coincidence counts and singles counts and discover if indeed our value for $g^{(0)}_{TR}(0)$ is close to zero as we would expect for a single photon source, or if it is nearer to 1.0 as we would expect from a classical perspective.

6.2.4 Measurements During the First Lab Meeting

You will want to begin your labwork by checking on optical alignment and instrument settings, and doing so will help to familiarize yourself with the experimental setup. But first a few words of caution:

Caution

- Wear the laser safety goggles when you turn on the blue laser
- Turn off the room lights before powering on the photodetectors

The first cautionary note is for your own safety, and the second is for the protection of our photon-counting silicon avalanche photodiodes. The module of four detectors costs $12,000! On the other hand, *your eyes are priceless!!*

To begin, have your instructor or an experienced colleague show you how to mount the BBO crystals in their mirror mount. The crystals are hygroscopic (suck up moisture from the air), so we store them with desiccant in a container on the optical table when not in use. We also blow dry nitrogen gently across one face of the crystals while they are in use on the optical table. They are not severely hygroscopic, so don't stress out about it, but it is prudent to keep them in a dry atmosphere at all times. That's not too hard to do in a good lab in southern California! While your instructor or experienced colleague is still in the area, have them show you the long-pass filters and photodetector module in the light-tight box on the optical table. Then button everything up and get ready for the festivities!

Put your goggles on and pull the curtain around the experimental setup to protect others in the main lab area from stray laser reflections. Power **On** the 405 nm laser. Adjust the BBO crystal mirror mount so that the back-reflection of the laser goes right back on itself (centered on the iris diaphragm). This should be a small adjustment. You will probably want to check the general alignment of the optical setup — the 405 nm laser beam should pass through the center of the iris diaphragm in front of the laser, and also through the center of the iris diaphragm in front of the beam stop. But before making any adjustments to the alignment, please consult your instructor. Everything should already be fairly well aligned. If not, we will need to think carefully about how to proceed!

Power **On** the NIM bin containing the TAC/SCA modules, and power **On** the HP digital oscilloscope sitting on top of the NIM bin. Turn off all lights and darken the area as much as possible, and then use the flashlight to power **On** the three power supplies for the photodetector module. You should disconnect the gate cable at the GTR TAC/SCA module and hook it up to the oscilloscope for viewing. The gate detector output should be 4 V high and about 20 ns wide. To observe the pulse successfully you will need to terminate the coax cable with 50 Ω to prevent ringing (reflections up and down the cable). Reconnect the gate cable to the GTR TAC/SCA module. Notice that the ends of the detector cables in this configuration are already terminated with 50 Ω just before they connect to the BNC-2121 input to the counter board (see Fig. 6.6).

Power **On** the PC computer "Mehta" (Dell Dimension 3000) and login under the account name "**quantum**" and password "**photon**". There should be a few sheets of instructions placed with the experimental setup that will help you use the Maestro 32 software to check on the SCA windows, and help you use LabVIEW to record coincidence counts and singles counts. You should play around for a bit, performing reality checks. For example, you will want to block the laser beam and measure the detector dark counts. In complete darkness, these are about 300 to 400 counts/sec.

Recording Counts While Rotating the Incident Polarization A great way to check on the performance of the entire system is to rotate the 405-nm half-wave plate (see Fig. 6.4) and record the singles and coincidence counts at say, 10° increments. As the half-wave plate is rotated by θ, the plane of polarization of the laser light incident upon the BBO crystals rotates by 2θ. Hence the contributions of the two BBO crystals to the down-converted 810 nm beam varies, and their contributions have orthogonal polarization. The beam splitter in the signal photon path in Fig. 6.4 is a polarizing beam splitter, which means that vertically polarized photons are reflected and horizontally polarized photons are transmitted. So as the half-wave plate is rotated by θ, the GT and GR coincidence counts should vary as $\sin^2(2\theta)$ and $\cos^2(2\theta)$, respectively, with of course some arbitrary phase offset. The sum of GT and GR coincidence counts should be approximately constant. Use a sample variance approach to data acquisition, and fit your data rigorously to obtain a value for the reduced χ^2 goodness of fit.

A plot of your data should make it clear that our alignment is not perfect, or our photodetectors have very different quantum efficiencies (not likely). In any case, this will be valuable information for your next measurements.

6.2.5 Testing the Quantum Nature of Light

When you are finally ready to measure $g_{TR}^{(2)}(0)$ for our single-photon source, there are a couple of checks on equipment that you should perform first. Assuming you believe that photons behave like indivisible particles, you probably expect to measure no triple coincidences (GTR). There are lots of ways to measure zero. For example, you might just forget to power ON the photodetectors. That'll do it! You get the point. It is important to perform independent checks on the performance of the GTR TAC/SCA module to make sure that if there *were* triple coincidences, the GTR TAC/SCA module would record them.

Our use of the GTR TAC/SCA module is different from the GT and GR setups because for the GTR triple coincidence, we are employing the GATE input on the START circuitry. As indicated in Fig. 6.5, the idler photon pulse (gate pulse) is connected to the GATE input of the START circuitry, so that an idler photon will enable the START circuitry to register a START pulse from the transmission detector, which in turn allows a pulse from the reflection detector to register a STOP pulse and initiate TAC and SCA output pulses. We must be sure that this GATE input on the START circuitry is working properly. Also, we must be sure that the GTR SCA window is set properly to select a TAC pulse that corresponds to the actual time delay between a transmission detector pulse and a reflection detector pulse. We mentioned in Section II that we have inserted extra cabling in the transmission and reflection paths (10 ft and 20 ft, respectively) that results in a delay of ~15 ns for the transmission pulse and ~30 ns for the reflection pulse, relative to the gate pulse. That means that the reflection pulse should be delayed by ~15 ns relative to the transmission pulse. Hence we would expect to see GTR TAC pulses of ~ 3 V, and the SCA window should be centered at about 3 V.

Make Sure the GATE Input Works on the START Circuitry

Keep the gate pulse connected to the GATE input of the START circuitry and the transmission pulse connected to the START input of the GTR TAC/SCA module. However, disconnect the reflection pulse from the STOP input, and instead lead the transmission pulse through a 10 ft. cable from the START input to the STOP input (don't forget to terminate with 50 Ω). The 10 ft. cable will cause a ~15 ns delay (the electrical signals travel at about 8 inches/ns (2 x 10^8 m/s) in the coax cable). Connect the TAC output to the TRUMP PCI 2K card input, and switch the inhibit/out switch to "out" so that the TAC output is generated regardless of the SCA window. You should see the coincidence peak at about 15 ns. Also check to see that this GTT count rate is the same as the GT count rate. Replace the cabling to the original connections.

Make Sure the GTR SCA Window is Set Correctly

Disconnect the gate pulse from the GATE input of the START circuitry, and flip the associated switch to ANTI-coincidence. This effectively disables the GATE input on the START circuitry. No need to worry, we just checked to see that it works fine (see above). Now we want to set the SCA window to select TAC pulses initiated by simultaneous receptions of photons at the transmission and reflection detectors. We have already said (above) that we expect TAC pulses of about 3 volts amplitude. But of course we really don't expect to observe simultaneous receptions of photons at the transmission and reflection detectors! So how are we going to check the SCA window? Here's the trick. Keep the transmission detector cable connected to the START input, but reroute the gate (idler) photon fiber coupler to the transmission detector by switching the fiber cable connections at the fiber connector manifold on the optical table. Now the gate photon will go to the transmission detector, and the reflected photon will go, as before, to the reflection detector. If the SPDC source is working at all, we would expect coincident gate and reflection photons. Check it out! When you're finished with this procedure, replace the connections to their original configuration.

Measure $g^{(2)}(0)$

A typical measurement consists of 60 counting periods of 10 seconds each — a total of 10 minutes. Use your own judgment. You may want to make several attempts at this measurement. It may be useful to make simultaneous measurements of count rates and the TAC spectrum from the GTR TAC/SCA module.

By now you are probably an expert on the system, and you may want to think about performing a control experiment. You can see the need for a good control — we are trying to measure zero convincingly! The FPGA module should be the best data acquisition hardware for measuring $g^{(2)}(0)$ for a classical light source, but it may have some problems, as you will see below. Robert Kealhofer and Chris Gage (both HMC '13) have written guides for the use of the FPGA module, and these guides are available in the lab and on the course Sakai site. It would also be prudent to measure $g^{(2)}(0)$ for our single-photon source using the FPGA module and compare the results with those obtained with the NIM electronics. Kaew Tinyanont and Yantao Wu, in an Optics Lab tech report in spring 2014, attempted this comparison, and their results suggest that the FPGA timing windows may be miscalibrated.

6.3 Tests of Bell's Inequality

References

- "Entangled photon apparatus for the undergraduate laboratory," and "Entangled photons, nonlocality, and Bell inequalities in the undergraduate laboratory," two papers by D. Dehlinger and M. W. Mitchell, *American Journal of Physics* **70** (9) 898-902 and 903-910 (2002). These papers focus on tests of Bell's inequalities using very much the same experimental setup as our own. Hardcopies of these papers are provided in a 3-ring binder in the lab.
- "Quantum mysteries tested: An experiment implementing Hardy's test of local realism," by J. A. Carlson, M. D. Olmstead, and M. Beck, *Am. J. Phys.* **74** (3) 180-186 (2006). Excellent guide for performing Hardy's test with our experimental setup. A hardcopy is provided in a 3-ring binder in the lab.

6.3.1 Introduction

Recent work in Advanced Lab and Optics Lab has moved beyond tests of the quantum nature of light and has focused on tests of Bell's inequality, which compares the predictions of **local hidden variable theories** with those of quantum mechanics. The papers by Dehlinger and Mitchell (*Am. J. Phys.* 2002), especially the second one (pp. 903-910), are excellent guides to these tests. With our experimental setup, tests of Bell's inequality are implemented by exploiting the polarization state of the entangled photons produced in the spontaneous parametric down-conversion (SPDC) process. Initial work in Advanced Lab and Optics Lab employed Hardy's test of local realism as described in the paper by Mark Beck's group (*Am. J. Phys.* 2006). Hardy's test is generally considered the test of Bell's theorem which is easiest to understand. However, the entangled photon states produced in our experimental setup (and in most similar setups) are only "80% pure", and this fact led to many failed attempts to use Hardy's test to demonstrate the superior predictive capabilities of quantum mechanics over hidden variable theories. During the Fall of 2009, David Berryrieser and Rob Warren (HMC '10) showed that Hardy's test could be made to work, but eventually transitioned to the more general approach of Dehlinger and Mitchell. They successfully demonstrated that quantum mechanics describes nature accurately in situations where hidden variable theories cannot. Several workers in Optics Lab have since repeated and extended the results of Berryrieser and Warren. Recently we acquired a "pre-compensation" quartz crystal which should provide 95% pure entangled photon states and a substantial improvement in our ability to rule out hidden variable theories as explanations for our measurements. Initial attempts to use the crystal have not improved the entanglement purity as much as expected (see Anthony Corso's Optics Lab tech report, spring 2014); solving this puzzle is a worthy goal for this semester!

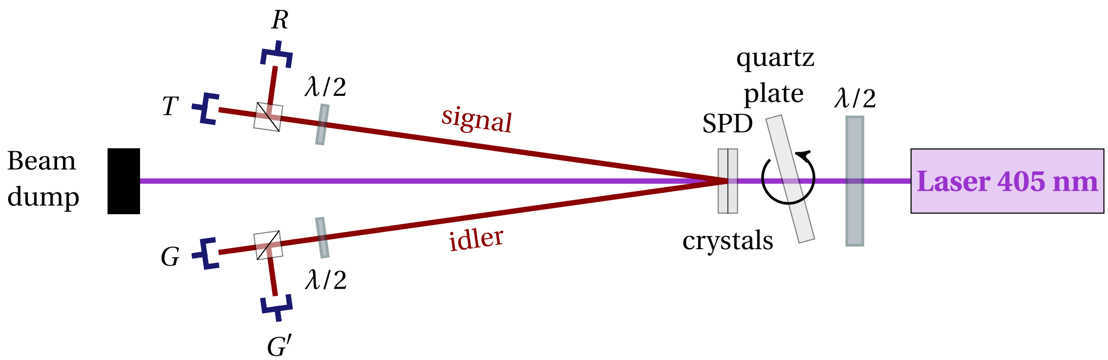

Figure 6.7: Top view of the experimental setup for performing tests of Bell's inequalities. SPD = spontaneous parametric down-conversion. The quartz plate can be rotated about a vertical axis.

6.3.2 The Experimental Setup

The experimental setup for performing tests of Bell's inequality is sketched in Fig. 6.7 (also see photo in Fig. 6.8). The entangled photon-pair source comprises a 50 mW violet laser (405 nm) illuminating a pair of β-barium borate (BBO) crystals cut to facilitate type-I spontaneous parametric down-conversion (SPDC). In this nonlinear process an occasional incident 405-nm photon is converted into a pair of 810-nm photons with linear polarization orthogonal to the linear polarization of the incident beam. The 405-nm half-wave plate provides a means for rotating the polarization of the incident beam so that roughly equal numbers of horizontally and vertically polarized 810-nm photon pairs are produced in the SPDC process. Conservation of momentum and energy imposes constraints on the two 810-nm photons, so that they are entangled in energy, momentum, and polarization. An 810-nm photon in the bottom path of Fig. 6.7 is often called an "idler" photon and is used as a gate for coincidence circuitry, while an 810-nm photon in the top path is called the "signal" photon. In our work in testing Bell's inequality, we may refer to idler photons as "gate" photons, and the signal photons may also be called "transmit" photons. The "gate" and "transmit" nomenclature is a remnant of using this setup for the test of the quantum nature of light. In actual fact, these two paths are on an equal footing in tests of Bell's inequality, and we simply take advantage of the coincidence circuitry to measure when an entangled photon pair is transmitted successfully through the two 810-nm half-wave plates and polarizing beamsplitters.

The pair of BBO crystals in Fig. 6.7 consists of two 0.5-mm-thick crystals rotated so that their crystal axes are effectively perpendicular, and then cemented together. The result is that a horizontally polarized 405-nm photon incident upon one crystal can generate a pair of entangled 810-nm photons with their polarization vertical, while a vertically polarized 405-nm photon incident upon the other crystal can generate a pair of horizontally polarized photons. A couple of meters downstream of the BBO crystals, where the polarizers and detectors are located, it is impossible to tell in which crystal the photon pair was created because, even in principle, there is insufficient depth resolution looking back at the BBO crystals to place the origin of the photon pair in one crystal or the other. Hence, the photons are entangled with respect to polarization as well as momentum and energy. The 405-nm laser emits horizontally polarized photons, so if the optic axis of the half-wave plate is oriented vertically (0°) (or for that matter, horizontally (90°)), a pair of vertically-polarized photons is generated. With the 810-nm $\lambda/2$ plates rotated to their 0° positions, the entangled photons will be reflected by the polarizing beamsplitters, leading to a minimum number of coincidence counts.

Why use both half-wave plates and polarizing beamsplitters, rather than polarizers to project the signal and idler photons into a particular basis? In fact, we used to use Glan-Thompson polarizers in this experiment. However, these polarizers are large and are much more likely to deviate the beams, causing a confusing decline in detection efficiency that is unrelated to polarization. By using the 810-nm $\lambda/2$ plates, you can rotate the polarization of the signal and idler photons before the polarizing beamsplitters, which reflect vertical polarization and transmit horizontal polarization. Note that each half-wave plate has a modest offset in its zero position (the idler at −2° and the signal at 4°) and that **the transmitted polarization rotates through 2ϕ when you rotate the wave plate by ϕ**.

The birefringent quartz plate in Fig. 6.7 provides a means of zeroing the phase φ in the QM state for the entangled photon pairs,

$$\left|\psi_{DC}\right\rangle = a|H\rangle_s|H\rangle_i + b\exp\left(i\varphi\right)|V\rangle_s|V\rangle_i \tag{6.12}$$

where normalization requires $|a|^2+|b|^2 = 1$, and $|a|^2$ is the probability that the photon pair is polarized horizontally and $|b|^2$ is the probability of vertical polarization. The optic axis of the quartz plate is oriented vertically, so a horizontally polarized photon pair will experience a different refractive index than does a vertically polarized photon pair, and hence a phase difference is introduced between the two polarizations. Rotating the quartz plate about a vertical axis changes the effective thickness presented to the 405-nm beam, thus varying the phase difference imparted to the two polarization states. This is the method used to set $\varphi = 0$ in Eq. (6.12).

For a more detailed description of the apparatus, see the papers by Dehlinger and Mitchell and by Mark Beck's group at Whitman College (hardcopies are available in the 3-ring binders in the lab).

6.3.3 Performing Tests of Bell's Inequality

The successful completion of a test of a Bell inequality involves mastery of a number of techniques: the quantum mechanical calculations involved in predicting count rates, the calibration of the two 810-nm half-wave plates, a thorough understanding of the coincidence electronics and data acquisition equipment, and a working familiarity with the operation of the 405-nm half-wave plate and the quartz plate. The goal of our work is to perform and document successful measurements that conclude that local hidden variable theories cannot explain our experimental results while the standard theory of quantum mechanics can!

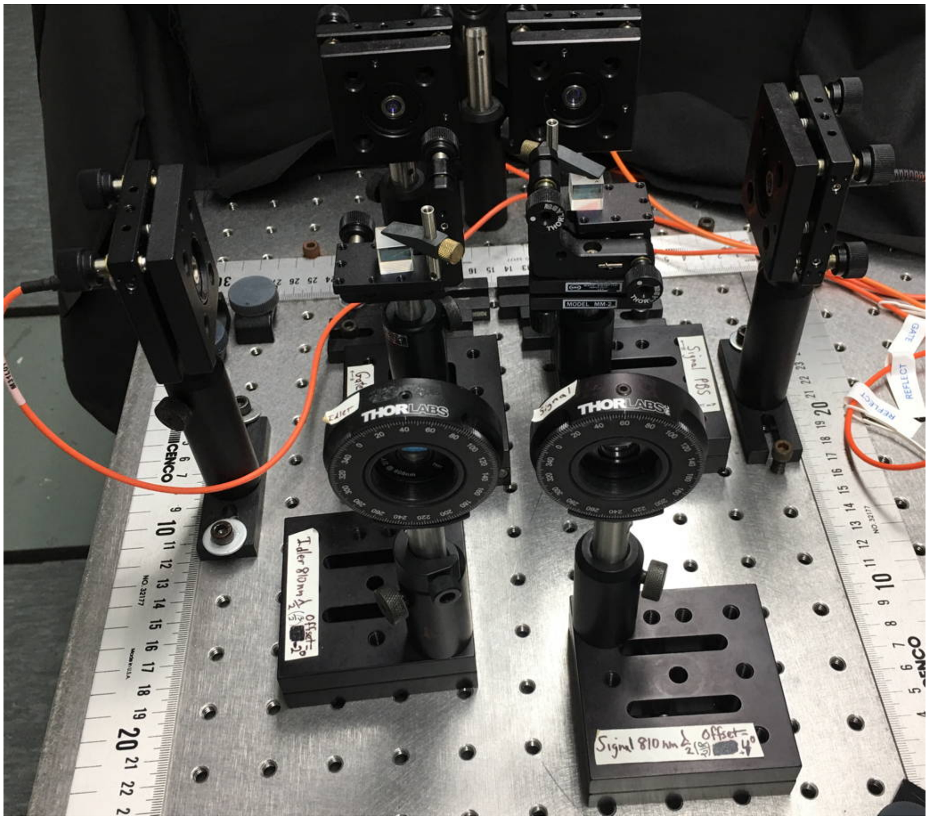

Figure 6.8: A photo of the half-wave plates, polarizing beamsplitters, and fiber couplers in the Bell inequality setup. The 405-nm laser, quartz plate, 405-nm half-wave plate, and BBO crystals (all not shown) generate 810-nm entangled photon pairs that propagate through the idler (gate) half-wave plate and polarizing beam splitter (shown on the left) and the signal (transmission) half-way plate and polarizing beamsplitter (on the right) and head toward their respective fiber couplers (face-on at the top of the photo). The 810-nm photons are carried by optical fiber to the silicon avalanche photon-counting detectors housed in the black box shown at the top of the photo.

Dehlinger and Mitchell (*Am. J. Phys.* **70** (2002) 903–910) describe in detail the procedure for performing a test of a Bell inequality first derived by Clauser, Horne, Shimony, and Holt, the so-called CHSH Bell inequality. You will need to read this paper carefully so that you understand the theory thoroughly and appreciate the motivation behind every step in their experimental procedure. A few words of advice should prove helpful and are included below.

You may want to begin by checking the orientation of the transmission axes of the signal (transmit) and idler (gate) half-wave plates. A simple method can be used to check on the settings of the two half-wave plates. With the optic axis of the 405-nm half-wave plate set vertically (actual rotation stage reading is $-1.5°$), and with the signal (transmit) half-wave plate set at 49° (45° away from its zero setting, so that it rotates vertical polarization to horizontal), rotate the idler (gate) half-wave plate while recording the signal-idler (GT) coincidence count rate. The maximum coincidence count rate should occur at 43° (45° away from its zero setting of −2°) on the idler half-wave plate. Then with both half-wave plates set to rotate vertical polarization to horizontal, rotate the 405-nm half-wave plate to check on the reading (−1.5° ?) that gives the maximum coincidence count rate. Then rotate the signal half-wave plate to achieve a minimum GT coincidence count rate. Does it correspond to its zero position of 4°?

Hereafter, I will speak of the polarization of the signal and idler photons, rather than the settings of the 810-nm *wave plates required to achieve them.* Now rotate the 405-nm half-wave plate to achieve linear polarization at 45° to the vertical. (This should be the case when the half-wave plate rotation stage reads 21°?) Check to see that the coincidence counts $N(0°,0°)$ and $N(90°,90°)$ are equal. Note that Dehlinger and Mitchell define $N(\alpha,\beta)$ to be the coincidence counts when the signal (transmit) polarizer is rotated to α (taking into account any offset in the rotation stage of the polarizer) and the idler (gate) polarizer is rotated to β.

Next tune the QM state to achieve $\varphi = 0$ in Eq. (6.12), resulting in the Einstein-Podolsky-Rosen state,

$$\left|\psi_{\text{EPR}}\right\rangle = \frac{1}{\sqrt{2}}\left[\,|H\rangle_s\,|H\rangle_i + |V\rangle_s\,|V\rangle_i\,\right] \tag{6.13}$$

This is accomplished by rotating the quartz plate until the measured coincidence counts $N(45°,45°)$ are maximized (about 30°?). You should perform the calculations to show that $\varphi = 0$ indeed corresponds to a maximum in $N(45°,45°)$. As a double-check, you might want to confirm both theoretically and experimentally that $N(-45°,45°)$ is a minimum when $\varphi = 0$ (looking for the minimum may be a more sensitive way to find $\varphi = 0$).

Finally, plan the sixteen measurements of coincidence counts that will allow you to evaluate S defined by (see Dehlinger and Mitchell):

$$S \equiv E(a,b) - E(a,b') + E(a',b) + E(a',b') \tag{6.14}$$

where

$$E(\alpha,\beta) \equiv \frac{N(\alpha,\beta) + N(\alpha_\perp,\beta_\perp) - N(\alpha,\beta_\perp) - N(\alpha_\perp,\beta)}{N(\alpha,\beta) + N(\alpha_\perp,\beta_\perp) + N(\alpha,\beta_\perp) + N(\alpha_\perp,\beta)} \tag{6.15}$$

and

$$a = -45° \qquad a' = 0° \qquad b = -22.5° \qquad b' = 22.5° \tag{6.16}$$

(note the misprint in Dehlinger and Mitchell, page 907, in which they erroneously say $b = 22.5°$ instead of $b = -22.5°$) and, for example,

$$\alpha_\perp = \alpha + 90° \tag{6.17}$$

You will probably find it useful to construct a table with all of the pairs of angles that you want to employ, taking account of the offsets in the readings of the rotation stages of the polarizers. Then methodically go through the sixteen measurements. Be sure to use a sample variance approach to determining your uncertainty — don't assume Poisson statistics as Dehlinger and Mitchell do, though that's probably not a bad assumption, just unnecessary!

According to the CHSH Bell inequality, $S \leq 2$, so if your calculated (measured) value of S is greater than 2 with statistical significance, then you have shown that local hidden variable theories cannot accurately describe the measurement you have performed, but presumably quantum mechanics can! The less-than-perfect purity of the state will lead to a value of $s < 2\sqrt{2} \approx 2.83$ which is the predicted value for a perfect EPR quantum mechanical state (see Eq. (6.13)).

6.4 Single Photon Interference and the Quantum Eraser

References

- "Comparing quantum and classical correlations in a quantum eraser," by A. Gogo, W. D. Snyder, and M. Beck, *Physical Review A* **71** (2005) 052103. This is an excellent paper from Mark Beck's group at Whitman College describing a quantum eraser experiment that also involves single photon interference. We should be able to repeat this experiment with our own advanced lab setup. A hardcopy of this paper is provided in a 3-ring binder in the lab.

6.4.1 Introduction

During the Fall of 2010, Advanced Lab students completed the assembly of the polarization interferometer described by Mark Beck's group in their 2005 paper (*Phys. Rev. A* **71** (2005) 052103). The interferometer was placed in the signal path of our experimental setup, and in early December, 2010, Aggie Szymanska (HMC '11) and Alex Baum (POM '11) were able to generate single photon interference fringes. Aggie and Alex did not have the benefit of motorized actuators to vary the path length difference for the two paths through the interferometer, so their achievement must be considered a true *tour de force*! They varied the path length difference manually, and in the process defined a new unit of small angular displacement, the "tiny turn"! Aggie and Alex made a valiant attempt to erase the fringes by rotating the 810-nm half-wave plate in the idler path, but the reduction in fringe amplitude was far from complete.

We now have a closed-loop motorized actuator that is capable of changing the path length difference in a precise, repeatable way, and the actuator has been installed on a kinematic mount holding the second of the two beam-displacing prisms comprising the interferometer in the signal path. During the Summer of 2011, Alex An (HMC '14) wrote a LabVIEW VI (virtual instrument) that incorporates control of the actuator into the acquisition of coincidence count rates using the NIM electronics. In Advanced Lab during the Fall of 2011, Robert Hoyt and Shaun Pacheco (HMC '12) performed some checks on the quantum eraser experimental setup, and then Susanna Todaro and Theo DuBose (also HMC '12) attempted to observe the presence or absence of single photon interference fringes to demonstrate the principles of a quantum eraser. They were unsuccessful — no fringes were observed.

In Optics Lab during the Spring of 2012, most activity focused on tests of Bell's inequality, but as a tech report project, Lucas Brady and Eric Anderson (HMC '13) took a shot at observing fringes with the quantum eraser setup. They too were unable to observe the expected fringes. Finally, in Advanced Lab during the Fall of 2012, Jesse Streitz (HMC '13) acted on a tip from Mark Beck who just happened to be visiting Mudd with his daughter. Mark suggested that the optical spectrum of the down-converted 810 nm entangled photon pairs may be broader than we thought, and hence the coherence length is shorter than we thought, so Jesse extended her search over a larger range of path length differences in the polarization interferometer in the signal arm. *Voilà!!*

Fringes were found! During the installation of the motorized actuator, the path length difference in the interferometer had been changed by about 1.5 mm, so a more aggressive scan was needed to reach the equal path length position of the interferometer. Jesse and later Robert Kealhofer (HMC '13) were able to rotate the idler 810-nm half-wave plate and significantly reduce the amplitude of the fringes, but like all their predecessors, the fringe amplitude was far from zero. In Optics Lab in the Spring 2013, the fringes were lost when the motorized actuator was bumped, but Alex An (HMC '14) and Carola Purser (HMC '13) managed to find them once again! Like researchers before them, Alex and Carola were not able to cleanly zero the fringes by adjusting the idler 810-nm half-wave plate. Clearly there remains a challenge to be answered, and the key may be in the relative numbers of horizontally versus vertically polarized entangled photon pairs. Alex An continued his work in the fall of 2013, and began to identify several polarization-sensitive elements in the beam path that may be responsible for the problem. We are close to a working quantum eraser, but still a bit of work to do! In the next section we will describe the experimental setup in more detail, and explain how the setup constitutes a quantum eraser!

6.4.2 The Experimental Setup

The experimental setup for generating single photon interference fringes is sketched in Fig. 6.9. The entangled photon-pair source is comprised of a 50-mW violet laser (405 nm) illuminating a pair of beta-barium borate (BBO) crystals cut to facilitate type-I spontaneous parametric down-conversion (SPDC). In this nonlinear process an occasional incident 405-nm photon is converted into a pair of 810-nm photons with linear polarization orthogonal to the linear polarization of the incident beam. The 405-nm half-wave plate provides a means for rotating the polarization of the incident beam so that roughly equal numbers of horizontally and vertically polarized 810-nm photons are produced in the SPDC process. Conservation of momentum and energy imposes constraints on the two 810-nm photons, so that they are entangled in energy, momentum, and polarization. An 810-nm photon in the bottom path of Fig. 6.9 is often called an "**idler**" photon and is used as a gate for coincidence circuitry, while an 810-nm photon in the top path is called the "**signal**" photon. In our work in producing single photon interference fringes, we may refer to idler photons as "gate" (G) or "gate-prime" (G') photons, depending on which detector receives them in the idler path. The signal photons may also be called "transmit" or "reflect" photons, depending on which detector receives them in the signal path. The "gate" and "transmit" and "reflect" nomenclature is a remnant of using this setup for the test of the quantum nature of light.

The pair of BBO crystals (SPDC crystals) in Fig. 6.9 consists of two 0.5-mm-thick crystals rotated so that their crystal axes are effectively perpendicular, and then cemented together. The result is that a horizontally-polarized 405-nm photon incident upon one crystal can generate a pair of entangled 810-nm photons with their polarization vertical, while a vertically polarized 405-nm photon incident upon the other crystal can generate a pair of horizontally-polarized photons. A couple of meters down-stream of the BBO crystals, where the detectors are located, it is impossible to tell where the photon pair was created because, even in principle, there is insufficient

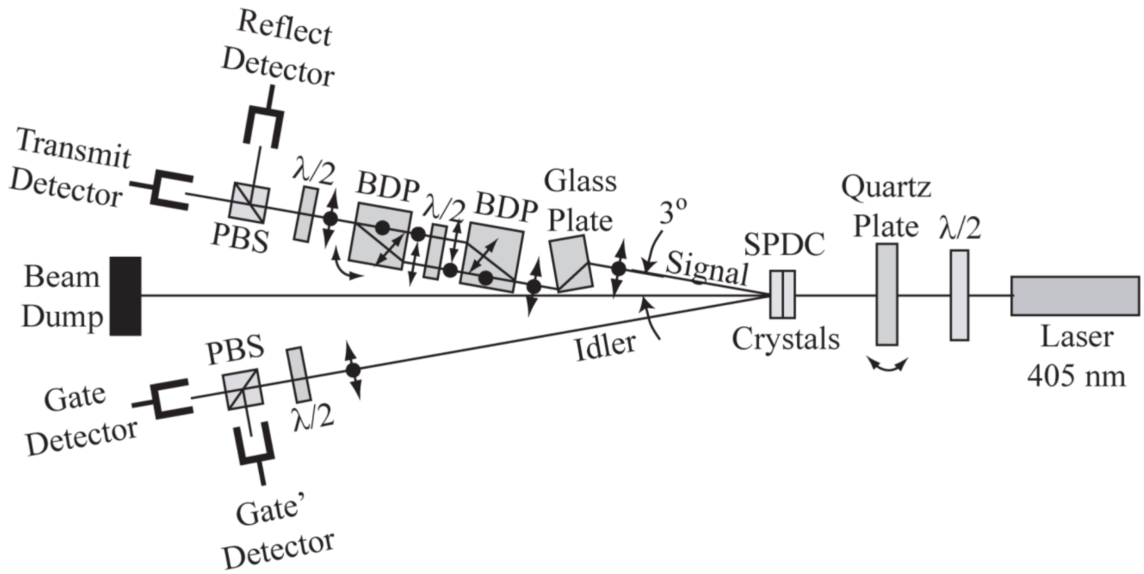

Figure 6.9: Top view of the experimental setup for generating single photon interference fringes and demonstrating the principles of a quantum eraser. The quartz plate can be rotated about a vertical axis to zero the phase φ in the QM state for the entangled photon pairs. SPDC = spontaneous parametric down-conversion. BDP = beam-displacing prism. The second beam-displacing prism (BDP) in the signal path can be rotated about a vertical axis to generate interference fringes. PBS = polarizing beam splitter.

depth resolution looking back at the BBO crystals to place the origin of the photon pair in one crystal or the other. Hence the photons are entangled with respect to polarization as well as momentum and energy.

The 405-nm laser emits horizontally-polarized photons, so if the optic axis of the 405-nm half-wave plate is oriented vertically (0°)—or for that matter, horizontally (90°)—a pair of vertically polarized 810-nm photons is generated. If the optic axis of the 405-nm half-wave plate is oriented at 45° so that the polarization of the incident laser is rotated to vertical, then a pair of horizontally polarized 810-nm photons is generated.

The birefringent quartz plate in Fig. 6.9 provides a means of zeroing the phase φ in the QM state for the entangled photon pairs:

$$\left|\psi_{DC}\right\rangle = a|H\rangle_s|H\rangle_i + b\exp\left(i\varphi\right)|V\rangle_s|V\rangle_i \tag{6.18}$$

where normalization requires $|a|^2+|b|^2=1$, and $|a|^2$ is the probability that the photon pair is polarized horizontally and $|b|^2$ is the probability of vertical polarization. The optic axis of the quartz plate is oriented vertically, so a horizontally polarized photon pair will experience a different refractive index than does a vertically polarized photon pair, and hence a phase difference is introduced between the two polarizations. Rotating the quartz plate about a vertical axis changes the

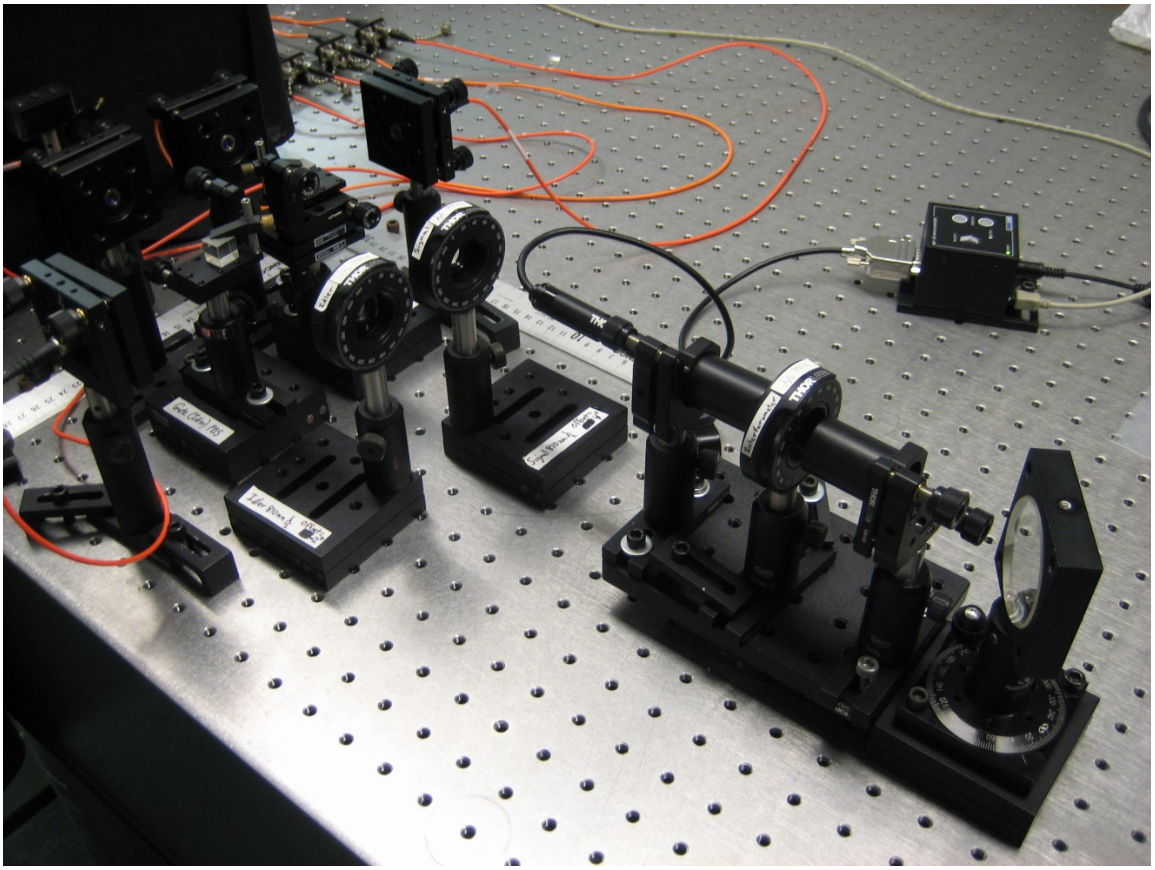

Figure 6.10: Photo of the idler (left) and signal (right) paths. The idler path consists of the 810-nm half-wave plate and the polarizing beam splitter (PBS) followed by the G (transmission) and G' (reflection) fiber coupler/photodectors. The signal path consists of the glass plate, the polarization interferometer (beam displacing prism, 810-nm half-wave plate, beam displacing prism), 810-nm half-wave plate, and PBS followed by the T (transmission) and R (reflection) fiber couplers/photodetectors.

effective thickness presented to the 405-nm beam, thus varying the phase difference imparted to the two polarization states. This is the method used to set $\varphi = 0$ in Eq. (6.18).

The polarization interferometer Two beam-displacing prisms (BDP) and an 810-nm half-wave plate form a polarization interferometer in the signal photon path. The first BDP encountered by a signal photon deflects horizontally polarized photons (denoted with a double-arrowed line in the plane of Fig. 6.10) so that they emerge from the prism at a spatially separated position from the vertically polarized photons (solid dot in Fig. 6.10). Next the 810-nm half-wave plate, whose optic axis is oriented at 45° from the vertical, converts the horizontally polarized photons to vertically polarized photons, and converts vertically polarized photons to horizontally polarized photons. As a result, the second BDP brings the two polarized beams back together again. The beams are now colinear, but cannot interfere because they are orthogonally polarized. The second 810-nm half-wave plate, if oriented with its optic axis at 22.5° from the vertical, will rotate the polarization of both beams by 45°. The polarizing beam-splitter (PBS) in the signal photon path will now select the vertical (horizontal) components of both beams and allow them to interfere on the reflect (transmit) detector.

The glass plate in the signal photon path introduces a displacement of the photons that compensates for the displacement introduced by the polarization interferometer. The net zero displacement allows the polarizing beam splitter and detectors to remain in the same positions they would occupy if the experimental setup is used to explore the quantum nature of light or to test Bell's inequality.

Generating single photon interference fringes If the polarization (horizontal vs. vertical) of the signal photon is unknown, even in principle, so that the signal photon takes both paths through the interferometer, then fringes can be generated by recording the coincidence count rate of the gate and transmit detectors (GT) as the second BDP is rotated about a vertical axis, thus changing slightly the path difference between the paths through the interferometer. Actually, the coincidence count rates GR or $G'R$ or $G'T$ could be recorded for the same purpose.

Which-way information and the quantum eraser If the 810-nm half-wave plate in the idler photon path has its optic axis rotated to 22.5° from vertical, then an incoming diagonally (antidiagonally) polarized photon has its polarization rotated to vertical (horizontal) before it hits the polarizing beam splitter. Thus the detection of a photon by the gate-prime (G') or gate (G) detector indicates that the idler photon was originally diagonally or antidiagonally polarized. This provides no information on the idler photon's polarization in the horizontal/vertical basis, and thus does not reveal whether the *signal* photon is horizontally or vertically polarized. Therefore, both paths through the interferometer will be explored. For this orientation of the idler half-wave plate, fringes will be observed in the records of the GT or GR or $G'T$ or $G'R$ coincidence count rates as the second BDP in the signal path is rotated about a vertical axis.

However, if the 810-nm half-wave plate in the idler path has its optic axis oriented vertically (or horizontally), then a count in the gate detector indicates horizontal polarization of the idler AND signal photons, and fringes will not be recorded. Similarly a count in the gate-prime detector indicates vertical polarization of the idler AND signal photons, and fringes will not be recorded.

Therefore, simply rotating the idler 810-nm half-wave plate by 22.5° will cause the fringes to appear or disappear, even though the G and G' detectors might, in principle, be located very far from the T and R detectors. When the idler 810-nm half-wave plate is oriented vertically, the signal photon polarization provides which-way information and no fringes are observed. When the idler 810-nm half-wave page is rotated by 22.5°, the which-way information is “erased” and fringes are recovered — in the other arm of the setup! This is the spooky action-at-a-distance exhibited by quantum correlations in these entangled photon states.

For a beautiful and somewhat more detailed description of the apparatus and its behavior as a quantum eraser, see the paper (Gogo et al. 2005) by Mark Beck’s group at Whitman College (hardcopies are available in the 3-ring binders in the lab).

6.4.3 Next Steps in Demonstrating a Quantum Eraser

Consult with your instructor to see where we are currently in acquiring data to demonstrate the complete removal of the single photon interference fringes. We suspect that a rotation of the 405-nm half-wave plate will change the relative numbers of horizontally and vertically polarized entangled photon pairs, and may make it possible to eliminate the fringes completely. We’ll see! Other ideas and insights are welcome!!

Experiment 7

Geometrical Optics

You will be introduced to ray optics and image formation in this experiment. We will use the optical rail, lenses, and the camera body to quantify image formation and magnification; this will require you to become familiar with image capture software. At the end of the experiment you will design a microscope or telescope.

This experiment is under development and thus we appreciate any and all comments as we design an interesting and achievable set of goals.

Equipment

Optical rail; one-inch lenses; 40D camera body; light-blocking attachment to camera body; computer; translation stage on which to mount the camera; calipers (for magnification measurement); connecting cable (camera to computer); memory card; powder-free latex gloves; business cards to image; and image capture software.

7.1 Image Formation and Focal Length

The focal length of an ideal lens, f, is defined as the distance beyond the lens at which rays coming from infinity are brought to a point, as shown in the left diagram of Fig. 7.1. Note that the rays coming from infinity are parallel at the lens. Given Snel's law and a lens made of a dispersive material (as they all are), can you see why we expect rays of different wavelength (color) to have different focal lengths? This phenomenon is known as chromatic aberration and is shown in the right diagram of Fig. 7.1.

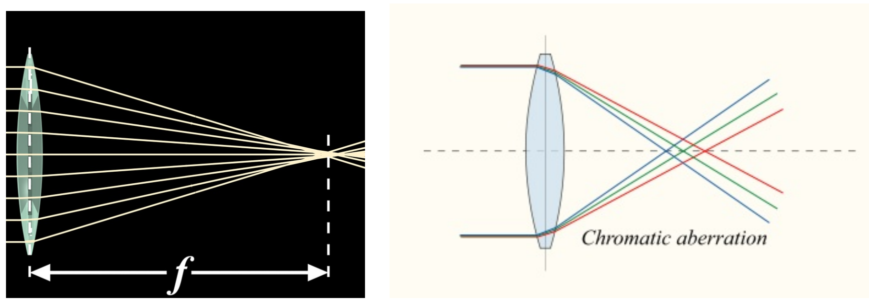

Figure 7.1: A lens focuses rays of light. When the rays are incident from very far away the lens forms an image at a distance from the lens equal to the focal length (left). Because the material from which a lens is made has slightly different values of the index of refraction for different colors; i.e., the lens is dispersive, the various colors of the incoming light come to focus at slightly different distances from the lens (right).

We can apply Snel's law to understand how lenses focus light, as shown in Fig. 7.2. Light is bent, or refracted, at both the front and the back surfaces of the lens, the front surface being the first surface the incident light encounters. Light incident at the front surface of the lens passes from a low n material (air) to a higher n material (glass) and, as described by Snell's law, is therefore bent toward the surface normal. Recall that θ is measured from the normal to the surface. Similarly, at the back surface of the lens, Snell's law dictates that the light is bent away from the normal. The combined effect of light entering and leaving the lens is that the light is focused.

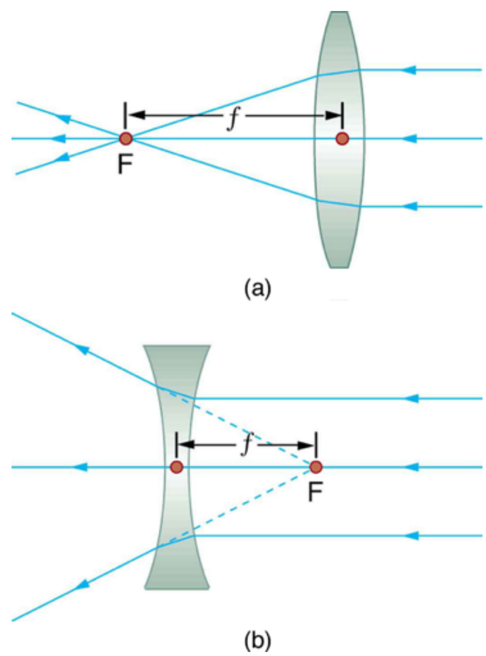

Figure 7.2: A converging lens and a diverging lens. Ideal converging lenses focus incident parallel light to a point downstream of the lens at the focal length (a), while an ideal diverging lens defocuses that same light as though it came from a point upstream of the lens at the focal length (b).

While converging lenses, such as those shown in Fig. 7.1 have a positive focal length, diverging lenses have a negative focal length. If we trace these diverging rays backward we find that they come to a point on the same side of the lens as that from which the light rays are incident. Note that unlike the example of the converging lens, with a diverging lens the light rays never actually cross at a single point. Further, for variety, rays in Fig. 7.2 are shown incident from the right side of the lens not the left.

Using the example of the converging lens in Fig. 7.3 we can derive an expression that governs image formation in thin-lens systems in the limit of small angles. This is often referred to as the "paraxial approximation". Recognizing similar triangles in Fig. 7.3 gives

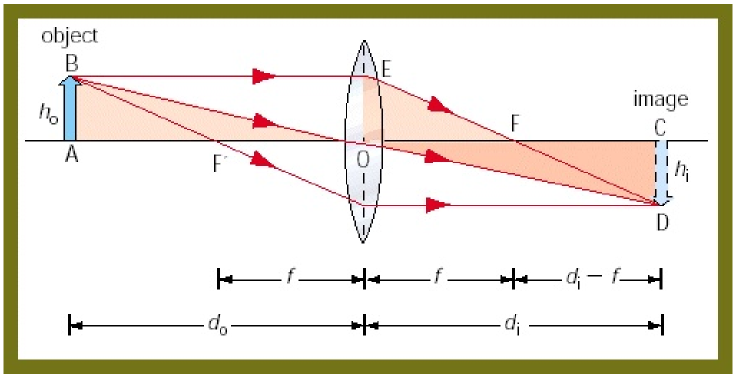

Figure 7.3: A single, thin, converging lens of focal length f forms an inverted image of an object.

$d_i/h_i = d_o/h_o$ and $h_i/(d_i - f) = h_o/f$, to arrive at the **thin-lens equation**:

$$\frac{1}{f} = \frac{1}{d_o} + \frac{1}{d_i} \tag{7.1}$$

The magnification, M, of a lens is given by

$$M = -\frac{h_i}{h_o} = -\frac{d_i}{d_o} \tag{7.2}$$

where the minus sign indicates that the image is inverted. With a bit more effort, you can arrive at the **lens maker's formula**, which is applied to a thick lens whose front and back surfaces have radii of curvature R_1 and R_2, respectively:

$$\frac{1}{f} = (n-1)\left(\frac{1}{R_1} - \frac{1}{R_2} + \frac{t(n-1)}{nR_1R_2}\right) \tag{7.3}$$

where n is the index of refraction of the lens material, t is the thickness of the lens as measured along the lens's center axis, R_1 is taken to be positive if the front surface (the first surface the light encounters) is convex, and R_2 is positive if the back surface is concave. The thin-lens approximation for this system would require that $t \ll |R_1|, |R_2|$, and under this assumption we would neglect the final term on the right side of this equation.

We can apply the thin lens equation to calculate the position of an image formed by a single lens, or multiple lenses. For instance, in the case of a two-lens imaging system, we start by using the thin lens equation to calculate the image position of the first lens, knowing the lens's focal length and the object distance. We then use this image position as the object position for the second lens. Knowing the object position and the focal length for the second lens, we can easily calculate the position of the image formed by the second lens. The magnification of the two lens system is the product of the magnifications of each lens, $M = M_1M_2$. For a more complicated optical system with N lenses, we calculate the final image position and magnification as above, daisy-chaining the object position of the N^{th} lens to the image position of the $(N+1)^{\text{st}}$ lens.

7.2 Image Formation and Ray Tracing for a Converging Lens

The thin-lens equation allows us to calculate the position at which an optical system will produce an image, in the thin-lens approximation. We can also calculate the image position using the ray method, which provides additional insight into how our optical system actually works. Using this method we find an image position by drawing three separate rays from our object through our thin lens. The rays are drawn:

1. parallel to the lens axis, from the top of the object to the lens, and then through the focal point on the far side of the lens;
2. from the top of the object, undiverted through the center of the lens, to the far side;
3. from the top of the object, through the focal point on the near side of the lens, and then exiting the lens parallel to the lens axis on the far side.

The image forms along a plane perpendicular to the lens axis where the three rays cross. Figure 7.4 shows the ray method for a converging lens. If used precisely, the ray method is as accurate as the thin-lens equation; in fact, you might notice that we used these same three rays in Fig. 7.3 to derive the thin lens equation. Note that the light rays “downstream” from the image are indistinguishable from rays that would be produced by a source at the location of the image. This generalization of an image to be the location from which the rays originate will be useful in the discussion of virtual images and virtual objects.

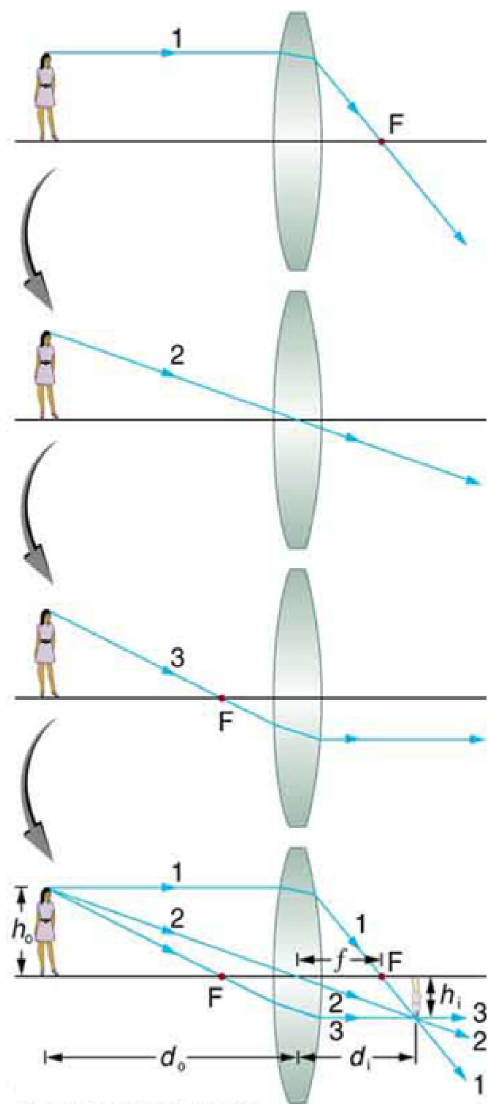

Figure 7.4: A demonstration of the ray tracing method for a converging thin lens.

As mentioned above, diverging lenses have a negative focal length. This implies a negative image distance for any positive object distance. The image that we would form using the diverging lens is not a real image; it’s what we call a virtual image—a mathematical construct that tells us where backward traveling rays would meet to form an image. This is equivalent to saying that the rays “downstream” from the lens are identical to rays that would be produced by a source of light at the position of the virtual image if the lens were not there.

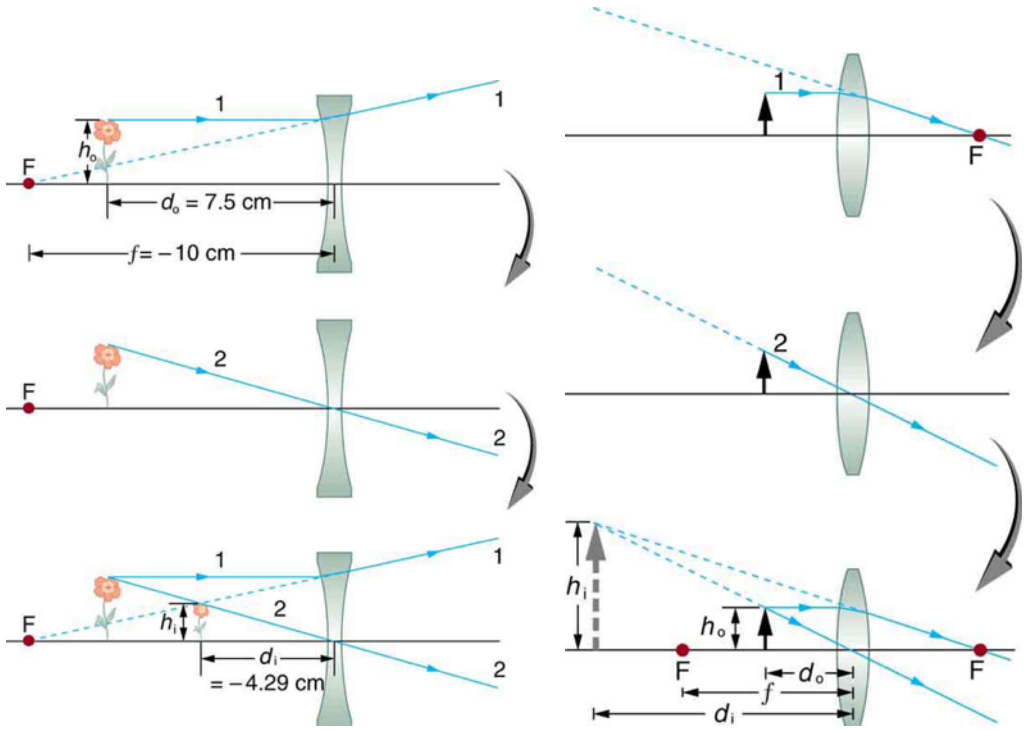

Figure 7.5: Virtual images. On the left, a virtual image is formed using a diverging lens and, on the right, a virtual images is formed using a converging lens.

The light does not actually travel backward to form that image, so we call it virtual, and we could not detect that image with a sensor. It's worth noting that if you place the object at a distance less than the focal length of the lens, a converging lens will also produce a virtual image (see Fig. 7.5).

Figure 7.6 uses the ray method to illustrate how a camera or an eye forms an image.

Let's summarize some results of the preceding discussion:

- $f > 0, d_o > f$: d_i is positive (the image is real) and M is negative;
- $f > 0, d_o < f$: d_i is negative (the image is virtual) and $M > 1$;
- $f < 0$: d_o is positive, d_i is negative (the image is virtual) and $0 < M < 1$;
- If $|M| > 1$ the optical system magnifies; if $|M| < 1$ the optical system demagnifies; and if $M < 0$, the image is inverted.

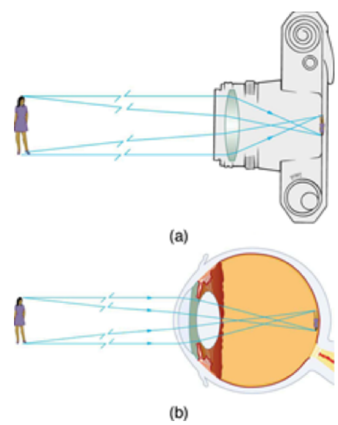

Figure 7.6: Rays demonstrate how an image is formed in (a) a camera, and (b) the human eye. Note that the eye contains a lens whose shape can be distorted by muscles to bring objects into focus.

- R_1 is taken to be positive if the front (upstream) surface is convex; R_2 is positive if the back (downstream) surface is concave. In the opposite cases, R is negative.

An alternate approach to summarizing the information about images and objects is to plot the thin lens equation in the form of $1/d_\mathrm{i}$ vs $1/d_\mathrm{o}$, as shown in Fig. 7.7. We start with the thin-lens equation,

$$\frac{1}{d_\mathrm{o}}+\frac{1}{d_\mathrm{i}}=\frac{1}{f} \qquad \Longrightarrow \qquad \frac{1}{d_\mathrm{i}}=\frac{1}{f}-\frac{1}{d_\mathrm{o}}$$

then realize what this says about a plot of $1/d_\mathrm{i}$ vs $1/d_\mathrm{o}$.

Now we can see that for any real object, a diverging lens will have a virtual object. For a converging lens, if $0 < d_\mathrm{o} < f$, then $1/d_\mathrm{o} > 1/f$, and the image will be virtual.

7.3 Aligning Optics

Finally, you should know the basics of caring for and aligning an optical system. In any optical system, such as your lenses or your camera,

- Make sure your optics are clean (please ask your instructor how to clean a lens so that you don't ruin the $50 lens), and use powder-free gloves when handling the lens;
- when setting up your imaging system be sure that each optical element is centered on the optical axis; you want light rays to hit your lens symmetrically both horizontally and

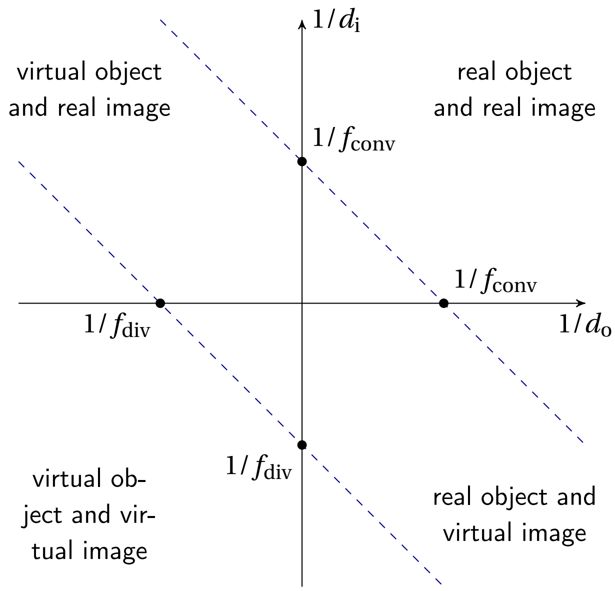

Figure 7.7: Plot of $1/d_\mathrm{i}$ vs $1/d_\mathrm{o}$.

vertically so that you don't introduce additional aberration to your image;

- it is important that the lenses are oriented so that they are perpendicular to the optical axis, otherwise you will introduce aberration in your image;
- the camera is one of your optical elements, so be sure that it is also centered along the beam axis (the sensor should be at the same height as the object and the lenses).

CAUTION: Any time you take the lens off of your camera, you are exposing your sensor to ambient air and dust and therefore the possibility of getting dirty. Dust sitting on your sensor will be noticeable in your exposures — much more so then dust on your lens — and is a big problem. Cleaning the sensor is problematic, so it's best to avoid getting dust or oil on the sensor in the first place. To this end, do not leave the lens off the camera any longer than is necessary, and try not to point the lens-less camera body up so as to avoid falling dust settling on the sensor. If you have any questions about camera care, please ask your instructor.

7.3.1 Image Capture Software

In this experiment you will need to use image capture software from Canon to transfer exposures from the camera to your computer over a USB interface. Canon supplies both a MacOS and a Windows version; install the version appropriate to your laptop.

MacOS

Warning: you need to follow these directions carefully. Do not double-click on the installer!

(1) Go to the Support & Driver section of Canon's website (found at `https://www.usa.canon.com/internet/portal/us/home/support/details/cameras/support-dslr/eos-40d?tab=drivers#Z7_MQH8HIC0L88RB0AMD0F1Q42K25`).
(2) Where it says **Enter Your Model Name**, put **EOS 40D** and hit Go.
(3) Drivers & Software should already be selected. Now enter your operating system and select Software below. You should now have many choices. Download the latest updater for **EOS Utility**.
(4) Unzip the download, open it, and drag the contents to your desktop.
(5) Right click on this and select Show Package Contents.
(6) Now, click on Contents, then Resources.
(7) Delete the file that says info.datx.
(8) Close the window and run the updater by double-clicking on the icon you dragged to your desktop (yes, now you can do it). You may get a message that says that the updater is damaged and cannot be run. If this happens, open system preferences, click on security and privacy and change it to allow apps downloaded from anywhere. Now run the updater and it should run like any other installer.

(9) If you are having trouble following this, there is a very helpful video at http://vimeo.com/72683307

Windows

Warning: you need to follow these directions carefully. Do not double-click on the installer!

(1) Go to the Support & Driver section of Canon's website (found at https://www.usa.canon.com/internet/portal/us/home/support/details/cameras/support-dslr/eos-40d?tab=drivers#Z7_MQH8HIC0L88RB0AMD0F1Q42K25).
(2) Where it says **Enter Your Model Name**, put **EOS 40D** and hit Go.
(3) Drivers & Software should already be selected. Now enter your operating system and select Software below. You should now have many choices. Download the latest updater for **EOS Utility**.
(4) Unzip the download, open it, and drag the contents to your desktop.
(5) Go to the start menu and type **regedit.exe**, then launch the editor.
(6) Click on **HKEY_LOCAL_MACHINE** and click on **SOFTWARE**.
(7) Right click on **Wow6432Node** and select **New Key**.
(8) At the bottom of the **Wow6432Node** folder there should be a folder that says **New Key #1**. Rename this **Canon**.
(9) Right click on this and select **New Key** and name it **EOS Utility**.
(10) You should now be able to run the download and it should install normally.

7.3.2 MATLAB Image Toolbox

You may need to use software to analyze properties of your exposure. For example, you may want to know how many pixels separate two bright spots in an exposure, or you might want to know the intensity count at a single pixel. To learn to do this please read through and become familiar with the "MATLAB Image Toolbox Tutorial". Or, you can use Igor Pro. Search the help system for information on image analysis.

7.3.3 Specifications for your Camera

The lens you are using with your camera has a focal length which can range from 28 mm to 135 mm, with minimum f-numbers of 3.5 and 5.6, respectively, depending on your zoom.

7.4 Notes on the apparatus

7.4.1 The Optical Rail and the Thin Lens Equation

In the exercise below, you may find it helpful to attach a light-tight snout to the camera body and/or cleverly place some black cardboard paper around the system to reduce the stray light that reaches your camera sensor. You might also put aluminum foil over the snout to further reduce stray light (create an approximately one-inch hole in the foil to let the desired light pass through to the sensor). Finally, you can adjust your lamp to increase or decrease the light incident on the objects you are trying to image.

7.4.2 Preliminary Exploration

Consider a single thin lens on your table and the thin lens equation. Image the business card at a variety of object distances from the lens and calculate the image positions that will result. (As an object, the dollar bill is even better than a business card; the dollar has lots of detail, interesting images and a surprising amount of color. It makes a rich target.) Check your calculations using the thin lens and the camera body (no lens attached) on the optical rail. Use Liveview in the EOS Utility so that you can see the image in real time. You'll probably want to run the camera in Av mode so that the shutter speed is automatically adjusted to the ambient light level.

Before you begin making quantitative measurements, you might want to play with the intensity and type of light that you use to illuminate your target. Does an incandescent light provide a different quality image than an LED? Do different lights create images with different colors? If you have a dollar bill as your target, does backlighting change the character of the image compared to front-side illumination?

Rotate slightly the lens in the post holder so that it is no longer perpendicular to the optical axis. Does the image distort? By how much do you have to rotate the lens before you affect the image?

Calculate and check the magnification of your system as well; does your calculated value match well with the value you measure? To determine the magnification of your optical system you might recall that the pixel on your sensor is square with sides of $5.7\,\mu\text{m}$ length.

Finally, place the camera's sensor along the rail at a distance away from the lens equal to the lens's focal length. What do you see?

7.4.3 Quantitative Measurements

Week 1: you should download the software and figure out how to use it. Then you should learn how to clean and mount lenses and work on aligning the optics. You should make at least one measurement of the focal length of a converging lens and check the magnification. With the knowledge of the first week you should be able to plan an efficient method of data collection for following weeks.

Week 2: plot a graph like Fig. 7.7 for a converging lens to determine its focal length. Notice that you need at least two quadrants sampled so that your value for the focal length is interpolated not extrapolated.

Week 3: repeat the measurements for a graph like Fig. 7.7 for a diverging lens. To test your acumen, optimize a system to make a telescope or a microscope. Then characterize the device.

7.4.4 Hints

1. The riders on the optical rail can give useful information about the image and object distances but you need to figure out how to go from the location of the rider on the rail to the distance between the optical elements. Use the calipers to measure the distance between the object and the lens to find the offsets for that part of the system. To find the relationship between the rider for the camera and its sensor, you might use the magnification of one arrangement of the system.
2. To work with virtual images and objects you will need more than one lens. With a bit of planning, you will not need to know the focal length of the "extra" lens.
3. The data in this experiment are very sensitive to small systematic errors in the image and object positions. Think about how to estimate the size of these and adjust the data within acceptable limits. It may be that using the magnification will give the most accurate way to find these offsets.
4. Ray diagrams are extremely useful in figuring out how to arrange the lenses to create real or virtual images. The concept of a virtual object will make much more sense if you draw the ray diagrams for the rays that created it.
5. Before the third week you will need to do a bit of research to decide what kind of telescope you wish to construct.

7.5 Warm up exercises to do if you wish

(1) For each of the following lens systems calculate the total magnification and use the thin lens equation to calculate the final image position. What is the physical significance of a negative magnification? A negative image position?

a. A 50-mm lens with an object distance of 100 mm. [Answer: 100 mm]

b. A 200-mm lens with an object distance of 120 mm. [Answer: −300 mm]

c. A −100-mm lens with an object distance of 300 mm. [Answer: −75 mm]

d. A 400-mm lens is placed 250 mm from a 75-mm lens and the object distance is 900 mm from the 400-mm lens. [Answer: ≈ 65 mm, as measured form the second lens]

e. A 150-mm lens is placed 500 mm from a −50-mm lens and the object distance is 400 mm from the 150-mm lens. [Answer: ≈ −42 mm, as measured from the second lens]

(2) Calculate the focal length of a lens for blue light and for red light, where the lens has a thickness of 5 mm, a front surface radius of curvature of 180 mm and a back surface curvature of -250 mm. You will need to look up the dispersive properties of the lens.

(3) Your camera's lens has a focal length ranging from 28 mm – 135 mm, the ratio of the maximum and minimum determines the "zoom" on your lens. Over this range of focal lengths, what is the range of magnifications if we take the object distance to be much greater than either the focal length or the image distance?
[Answer: $|M| = i/o$, and fro the thin-lens equation, $i = of/(o-f)$. Substitute this value of i into the expression for magnification to get $M = f/(o-f)$ which, for $f \ll o$, gives approximately $M = f/o$. We consider the object distance to be unchanging, therefore M changes by the ratio of the focal lengths: $135/28 = 4.8$]

(4) Draw the ray diagrams for a converging lens with a virtual object and a diverging lens with a real image.

Experiment 8

Fresnel Coefficients

References

- *Optics* by Eugene Hecht, Chapter 4
- *Introduction to Modern Optics* by Grant Fowles, Chapter 2
- *Principles of Optics* by Max Born and Emil Wolf, Chapter 1
- *Optical Physics, 4th edition* by Lipson, Lipson and Lipson, Chapter 5

8.1 Introduction

The ancients understood the law of reflection—that the angle of incidence was equal to the angle of reflection—but had a law of refraction that only worked near normal incidence. Willebrord Snel van Royen (1580–1626) was the first to figure out that $\sin\theta_1 \propto \sin\theta_2$, where the angles are measured with respect to the normal. Snel worked this out in 1621,[1] although he did not publish this result. René Descartes (1596–1650) gave the first published account in *La Dioptrique* (1637). In English-speaking countries, the relation

$$n_1 \sin\theta_1 = n_2 \sin\theta_2 \tag{8.1}$$

is called **Snel's law**; in the French-speaking world, it is known as **Descartes' law**. You will explore a number of routes to deriving Snel's law, including Fermat's principle and Maxwell's equations.

But Snel's law is only part of the story: it doesn't determine how the incident beam should divide its energy between the reflected and refracted beams. Figuring out that mystery was long delayed by Newton's incomparable stature as *the* scientist of his age. His corpuscular theory of light did

[1] M. Born and E. Wolf, *Principles of Optics*, 7th edition (Cambridge, 1999) xxvi.

not lend itself easily to this purpose. The way forward came from Etienne Louis Malus (1775–1812), who discovered in 1808 that light reflected from a glass plate at a certain angle is polarized. Shortly thereafter in 1815, David Brewster (1781–1868) worked out that when the angle between the reflected and refracted beams is 90°, the reflected beam is polarized with its electric vector perpendicular to the plane of incidence. The angle of incidence that achieves this condition is called **Brewster's angle**. Jean-Augustin Fresnel's (1788–1827) wave theory was able not only to account for diffraction—leading to the outrageous, but confirmed, prediction of the Poisson bright spot—but also how the reflected intensity depends on polarization.

In this experiment, you will use optical rails, a semicircular prism, a linear polarizer, two wave-plates, and two photodiode detectors to investigate the laws of Snel, Malus, and Fresnel. The main goals are:

1. To determine the index of refraction of a material using Snel's law.
2. To investigate polarization of light and the effects of half- and quarter-wave plates.
3. To investigate the polarization dependence of reflection and transmission coefficients for a dielectric-air boundary.

The procedure that follows is vague by design, to encourage you to develop skill in aligning optics and in designing your own approaches to confirming these theoretical relationships.

8.2 Theoretical Background

8.2.1 Snel's Law

Snel's law describes the refraction of light at an interface between two dielectrics with indices of refraction n_1 and n_2. If the angle the incident beam makes with the normal to the local tangent

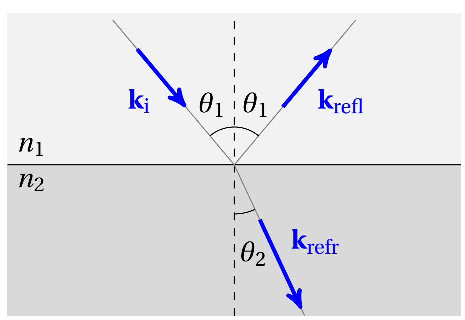

Figure 8.1: Geometry of refraction.

plane is θ_1 and the angle the transmitted beam makes with that normal is θ_2, as illustrated in Fig. 8.1, then the angles are related by Eq. (8.1).

Snel's law and the fact that the angle of incidence equals the angle of reflection are often introduced as facts of nature. To gain a deeper understanding of them, it is useful to examine four different approaches: the motion of wavefronts following Huygens' principle, a calculation using Fermat's principle of least time, the principles of quantum optics covered in Physics 51, and a derivation grounded in electromagnetic fields that applies boundary conditions at the interface between media that arise from Maxwell's equations. These approaches are all discussed in the reference in Hecht. The great advantage of the latter approach is that it incorporates the effect of polarization in a natural way.

You should understand the derivation of Snel's law from these different approaches.

8.2.2 Law of Malus

The law of Malus describes how the intensity of a linearly polarized beam of light traverses a perfect linear polarizer. The polarizer only transmits one component of the light wave's electric field, but since the intensity of the beam is proportional to the square of the electric field, the transmitted intensity is given by

$$I_{\text{trans}} = I_0 \cos^2 \phi \tag{8.2}$$

where ϕ is the angle between the pass axis of the polarizer and the electric vector of the incident beam.

8.2.3 Fresnel Coefficients

The Fresnel coefficients describe the amplitudes of reflected and transmitted electromagnetic waves at the interface between two dielectrics. The geometry is shown in Fig. 8.2. Recall that for an electromagnetic plane wave with angular frequency $\omega = 2\pi f$,

$$\mathbf{E}(x, y, z, t) = \mathbf{E}_0 \cos(\mathbf{k}\cdot\mathbf{r} - \omega t)$$
$$\mathbf{E}_0 \perp \mathbf{k}$$
$$\omega = \frac{c}{n}|\mathbf{k}| \qquad \Longrightarrow \qquad f\lambda = \frac{c}{n} \qquad \Longrightarrow \qquad f\lambda_0 = c$$

where λ_0 is the wavelength in a vacuum. Because electromagnetic waves are transverse, the electric and magnetic fields are perpendicular to the direction of propagation. Any arbitrary $\mathbf{E}_0$ can be resolved into two components with directions shown in Fig. 8.2. The key feature is recognizing that the direction of propagation and the normal to the surface between the materials determine a plane called the "plane of incidence". In the figure, one material is below the plane of the interface and one is above.

The reflection and transmission coefficients are determined by applying the electromagnetic boundary conditions at the interface. Since the boundary conditions for the electric field depend on the direction of the electric field, the reflection and transmission coefficients for $\mathbf{E}_{||,\text{inc}}$ and $\mathbf{E}_{\perp,\text{inc}}$ are different. **You should go through the derivation of the reflection and transmission coefficients for the two polarizations.** For the special case in which the materials are non-magnetic, so that $\mu_1 = \mu_2 = 1$, the results are

$$r_\perp = \left(\frac{E_{\perp,\text{refl}}}{E_{\perp,\text{inc}}}\right) = \frac{n_\text{i}\cos\theta_\text{i} - n_\text{t}\cos\theta_\text{t}}{n_\text{i}\cos\theta_\text{i} + n_\text{t}\cos\theta_\text{t}} = -\frac{\sin(\theta_\text{i}-\theta_\text{t})}{\sin(\theta_\text{i}+\theta_\text{t})} \tag{8.3}$$

$$t_\perp = \left(\frac{E_{\perp,\text{trans}}}{E_{\perp,\text{inc}}}\right) = \frac{2n_\text{i}\cos\theta_\text{i}}{n_\text{i}\cos\theta_\text{i} + n_\text{t}\cos\theta_\text{t}} = \frac{2\sin\theta_\text{t}\cos\theta_\text{i}}{\sin(\theta_\text{i}+\theta_\text{t})} \tag{8.4}$$

$$r_{||} = \left(\frac{E_{||,\text{refl}}}{E_{||,\text{inc}}}\right) = \frac{n_\text{t}\cos\theta_\text{i} - n_\text{i}\cos\theta_\text{t}}{n_\text{t}\cos\theta_\text{i} + n_\text{i}\cos\theta_\text{t}} = \frac{\tan(\theta_\text{i}-\theta_\text{t})}{\tan(\theta_\text{i}+\theta_\text{t})} \tag{8.5}$$

$$t_{||} = \left(\frac{E_{||,\text{trans}}}{E_{||,\text{inc}}}\right) = \frac{2n_\text{i}\cos\theta_\text{i}}{n_\text{i}\cos\theta_\text{t} + n_\text{t}\cos\theta_\text{i}} = \frac{2\sin\theta_\text{t}\cos\theta_\text{i}}{\sin(\theta_\text{i}+\theta_\text{t})\cos(\theta_\text{i}-\theta_\text{t})} \tag{8.6}$$

where we can use Snel's law to relate θ_i and θ_t.

Note that these equations describe the electric field *amplitudes*, which are not the same as the intensities of the reflected or transmitted beams.

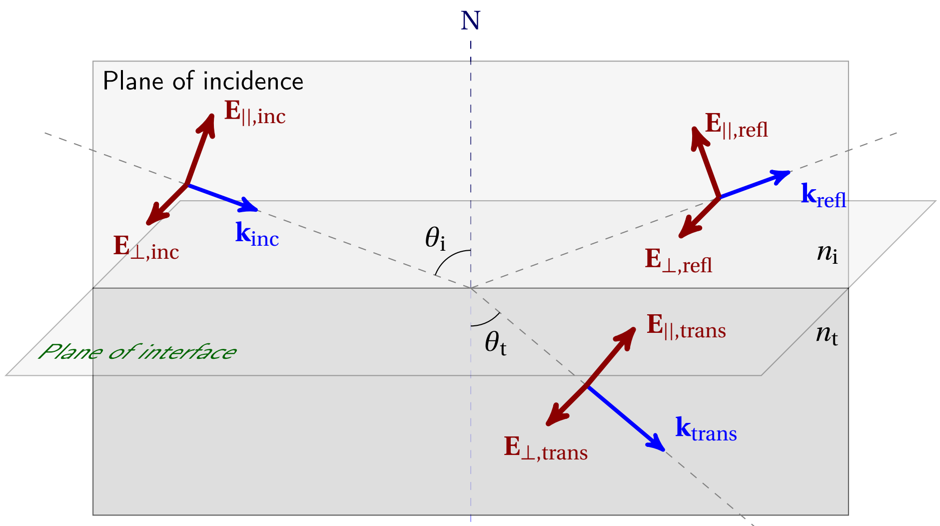

Figure 8.2: The geometry for the Fresnel coefficients. The incident electromagnetic wave can have polarization anywhere in the plane perpendicular to the direction of propagation. The incident field is thus a superposition of $\mathbf{E}_{||,\text{inc}}$ and $\mathbf{E}_{\perp,\text{inc}}$. In this figure, if the plane of incidence is the plane of the paper, then $\mathbf{E}_{\perp,\text{inc}}$ is out of the plane. Note: magnetic fields are not shown, but are orthogonal to both $\mathbf{k}$ and $\mathbf{E}$. Boundary conditions derived from Maxwell's equations require that components of $\mathbf{E}$ and $\mathbf{B}$ that are parallel to the interface must be continuous, as must be the parallel component of $\mathbf{k}$.

8.2.4 Brewster's Angle

Notice that the value for $r_{||}$ given in Eq. (8.5) goes to zero when $\theta_i + \theta_t = \pi/2$, which means that there is a particular angle of incidence where there will be no reflected light of the parallel polarization when that condition is met. This angle is called Brewster's angle.

8.2.5 Total Internal Reflection

If we examine Snel's law for the case that $n_1 > n_2$ then we see that there is a critical angle of incidence for which $\theta_t = \theta_2 = \pi/2$. At this condition, the transmission coefficients go to zero and all the light is reflected. What happens at larger angles of incidence?

8.2.6 Waveplates and Circular Polarization

In the discussion of Fresnel coefficients we resolved the incident electromagnetic wave into a superposition of linearly polarized components. Sometimes a more useful basis is that of left-hand and right-hand circularly polarized light. The action of a waveplate is to control the polarization of light and a waveplate can be used to change from linearly polarized to circularly polarized light or to change the orientation of linearly polarized light. The experimental setup includes a quarter and a half waveplate. Read about what these are and how they change the polarization of light.

8.3 Experimental Setup

The experimental setup is shown schematically in Fig. 8.3. It consists of a semicircular plastic prism on a rotation stage, a laser, two waveplates, a linear polarizer in a rotation mount and two photodiode detectors. These are mounted on a large board ruled with radial lines. The alignment procedure will be to ensure that the incident light hits the prism on the rotation axis. The prism is mounted on an *X-Y-R* stage so that it can be translated to make the alignment work. See Fig. 8.4.

Notice that the path of the light is most easily analyzed if the laser hits the flat face of the prism on the rotation axis and the center of the semicircle. Then the light refracted into the prism reaches the semicircular interface at normal incidence so does not refract on leaving the prism. The alignment procedure is designed to reach this position. One suggested process is detailed in Appendix A.

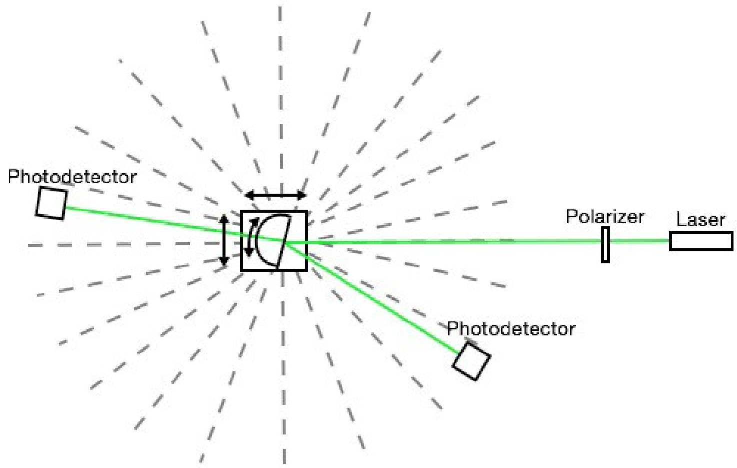

Figure 8.3: Schematic of the setup. The waveplates can be substituted for the polarizer or put in series with it. [Figure from Caleb Eades]

8.4 Qualitative Measurements

(to be answered with a combination of reading the specification sheets and using the equipment)

1. What type of detectors are supplied? How do they measure the intensity of the light? What do the scales on the top do to the signal?
2. What is the polarization state of the light from the laser?
3. Align the prism with the laser so the geometry for the rest of the experiment is convenient. Document the process you use and what you consider the figures of merit for a good alignment.

8.5 Quantitative Measurements

1. Determine if Snel's law applies to this system. If it does, then find the index of refraction of the prism. Observe total internal reflection and notice that a quick estimate of n can be found by making this one measurement.
2. Confirm that the detector and linear polarizer work as expected by taking measurements to confirm the Law of Malus.
3. Determine whether the quarter- and half-wave plates work as expected. At the end of these measurements you should be able to control the polarization of the laser beam.
4. Measure the reflected light from the prism as a function of incident angle for a couple of linear polarization directions. Analyze your data using the reflection coefficients to see if you

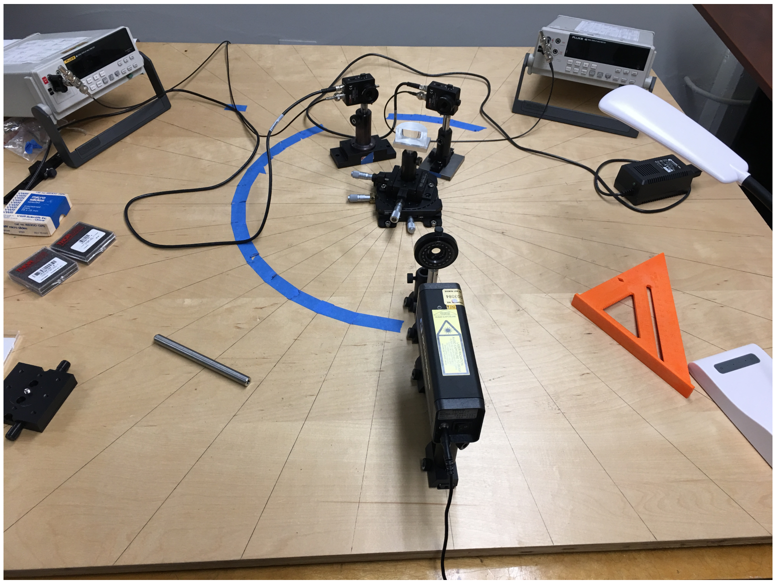

Figure 8.4: Photograph of the experimental setup.

have a consistent value for the index of refraction and if Equations (8.3)–(8.6) apply. Observe Brewster's angle.

5. Optional: Use another color of laser light to see if you can measure the dispersion in the prism. You can also investigate how well the waveplates work at this new wavelength.
6. Optional: Determine whether the transmitted intensities follow the predictions of Equations (8.3)–(8.6).

8.6 Appendix A: Alignment Suggestions

The following is slightly modified from the work by Caleb Eades.

We will now describe every step in the alignment procedure as it should be done sequentially when aligning the system.

1. The first step is ensuring that the laser beam (and hence the initial incident light) is going on a straight level line along one of the lines drawn on the table. The optimal way is to get a pair of irises on post mounts such that the irises are at the same height (note this can also be achieved using an index card in a card holder in a post mount with a dot on it with the dot centered over the post mount). Remove the prism temporarily and put one iris near the laser mounting strip and one far away, but make sure both are on the same line drawn on the table (the same one the laser will go on). Adjust the height of the laser mount and the positioning of the laser in the laser mount until the beam is going through the center

of both irises (or is hitting the dot on the index card in both the near and far field if using the index card). Use the set screw in the laser mount to adjust the positioning of the laser in the mount. Make sure that the laser is still at a height where it will hit the prism. If it is not, adjust the heights of the irises as appropriate and redo this step.

2. Put the polarizing optic in its mount on the same track as the laser diode and set it at a height such that the laser diode is roughly hitting the center of the optic (it should already be hitting the center horizontally based on step (i)). Twist the optic until the back reflection is into the laser diode as well as this can be arranged.

3. Place a stiff metal rectangular object of some width flat against the side of the square base of the prism-rotating stage. Barely unscrew the stage and then rotate holding the metal piece flat until the metal piece aligns exactly with the table line that is perpendicular to the table line the laser path is on (or the laser path line as it is a square). Screw the base back in. This ensures that the incident angle value read on the rotation stage has no offset (that is, the value you read is the actual incident angle value).

4. Put the prism in its mount and press it such that the flat face is against the flat part of the inset. Ensure that the rotation stage is set to 0° (that is, the flat face of the prism is perpendicular to the laser path). Now, use the micrometer perpendicular to the laser path to translate the rotation stage in the direction perpendicular to the path of the laser propagation until the beam is centered on the flat face of the prism. It is helpful here to use a neutral density filter to make the beam weaker and get a more precise centering. It is also helpful to look down the flat face of the prism and use the set screw hole to see where the laser should go (it should be centered on this hole as well).

5. (90°-90° test) One way to test whether the perpendicular position has been set correctly is to set the rotation stage to 90° and then look to make sure the beam is split in half, so if you hold an index card against the flat face of the prism, you should see half of the beam on the index card and half going onto the semicircular face of the prism. This should also be true when the rotation stage is set to 270°. If this is not the case, then try step 4 again.

6. (45°-45° test) Before this step, close the irises in front of the photodiode detectors all the way such that they have just a little hole. (Note you should adjust the height of the detectors such that the reflected beam is centered height-wise on the hole before continuing). Place the detectors on either side of the prism stage on the drawn line perpendicular to the laser path. Set the rotation stage (which should be at zero) to 45°. If the reflected light is not hitting one of the detectors exactly (to where the reflected beam is centered on the little hole), use the micrometer that is along the laser path to adjust the "z"-position of the stage until the beam is centered on the hole. Now set the rotation stage to 315°. If everything has been done properly, then the beam should be centered on the hole of the other detector. If the beam is not centered on the hole of the other detector, then something is off in the alignment. The potential issues are that the laser is not following the table line that it is mounted on, the square base of the rotation stage is not rotationally oriented properly, or

the beam is not hitting the center of the flat prism face. Repeat all the steps as necessary until the culprit is found.

If all these steps are done properly, then the data collected should be reasonably reliable (at least at the appropriate angles and with the center of the beam hitting the correct location on the center of the front flat face of the prism).

8.7 Appendix B: Sample Data for Fresnel Coefficients

Sample data for reflected light: A is the degree of polarization between 0 and 1. I fixed n and Origin happily found the polarization.

- Measure I_{refl} vs incident angle
- Fit with theta0 = −0.015 and nglass = 1.48
- Note that A = fraction of polarization
- thetat=asin(sin(3.14159/180*x+theta0)/nglass)
- r1=sin(3.14159/180*x+theta0-thetat)/sin(3.14159/180*x+theta0+thetat)
- r2=tan(3.14159/180*x+theta0-thetat)/tan(3.14159/180*x+theta0+thetat)
- y=I0*(A*r1^2+(1-A)*r2^2)+Ioff

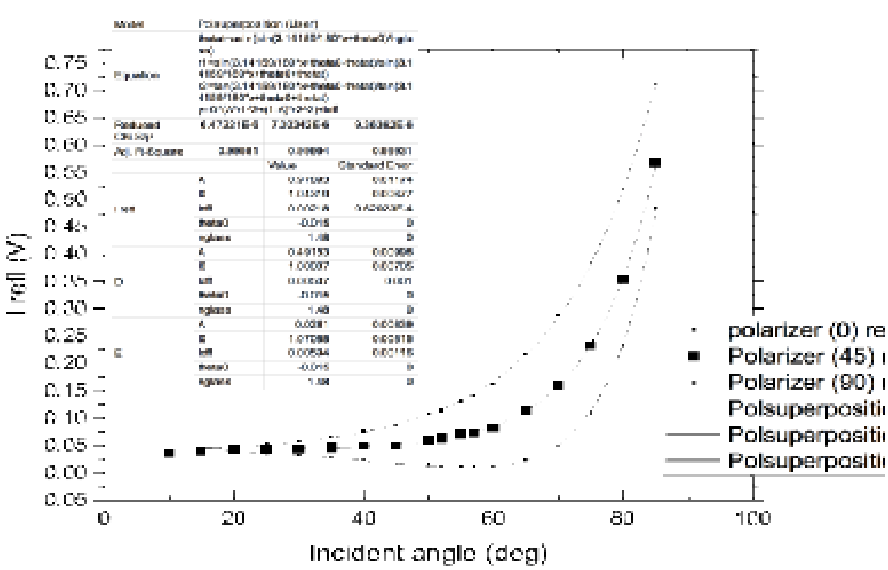

If we examine the fitting coefficients we see good agreement for the values.

		Value	Standard Error
I refl	A	0.97893	0.01174
I refl	I0	1.04319	0.00677
I refl	Ioff	0.00218	9.62023E-4
I refl	theta0	-0.015	0
I refl	nglass	1.48	0
D	A	0.49153	0.00996
D	I0	1.00007	0.00705
D	Ioff	0.00507	0.001
D	theta0	-0.015	0
D	nglass	1.48	0
E	A	0.0261	0.00839
E	I0	1.07088	0.00815
E	Ioff	0.00594	0.00116
E	theta0	-0.015	0
E	nglass	1.48	0

Appendix ***A***

Data Analysis Using Igor Pro in Windows or Mac OS X

Igor Pro is a data analysis and graphics package produced by Wavemetrics for Macintosh and Windows. Igor Pro includes a nonlinear least-squares fitting routine based on an algorithm by D.W. Marquardt (see Bevington and Robinson, Section 8.6). Igor Pro supports the use of Bessel functions and Fresnel integrals in fitting functions, so it can readily be used to fit diffraction data from both a circular aperture and a straight edge. Version 7 of Igor Pro is installed on the hard drives of the lab computers. The HMC Physics Department has a license which allows students in lab courses to download a copy of Igor Pro to their personal computers, and when launched Igor Pro. The URL for the download is `https://physics.hmc.edu/igor/` — each student enrolled in Optics Lab should be able to supply their name and email address and successfully download a copy of Igor Pro. We shall describe how to use Igor Pro to fit diffraction data from a circular aperture.

Log on to a Windows computer in the Optics Lab (or a Mac or PC in the computer labs on the HMC campus) and launch Igor Pro. To facilitate the discussion in this Appendix, we have placed our diffraction data in a text file on the Desktop named CircularMoore2004.txt (data donated generously by Chris Moore HMC '05), and we will use the LoadWaves feature of Igor to load our data. The data file CircularMoore2004.txt has three columns (see right): the first column contains the position of the detector (in mm), the second contains the intensity (in volts), and the third is the uncertainty in the intensity (in volts). The intensity and its uncertainty are actually the mean intensity and the standard deviation of the mean (standard error) deduced from five scans through the diffraction pattern.

From the **Data** menu select **Load Waves | Load Waves...** Select "Delimited Text" from the **File Type** popup menu, and check the boxes for **Make table** and **Read wave names**. Then click the **File...** button. We then switch directory levels (folders) to find the data file Circular-Moore2004.txt (look for Files of type "All Files"), and double-click on CircularMoore2004.txt. Finally, click the **Do it** button to open the data file.

The "Loading Delimited Text" dialog then opens, showing the top several lines of the data file along with the names Igor has identified for the three columns of data. Note that the first two have been changed from `x` and `I` to `xw` and `Iw`. This is necessary because both `x` and `I` have special meanings in Igor (`I` is the imaginary unit and `x` is the *x* coordinate of a data point). Click **Load** to complete the operation. A data table appears with the three columns of numbers. (Note that it is quite possible in Igor to load the data without producing any visible display; we see the data because we checked the ☒ Make table checkbox.)

The position values in CircularMoore2004.txt are in millimeters. To convert the values to meters, click into the command line (beneath the heavy red line) at the bottom of the screen in the "Untitled" window, and type the command

```
xW /= 1000 (or equivalently xW = xW/1000)
```

and press return. [Note that you can do all sorts of wave arithmetic this way.] Next, we assign the unit "m" (meters) to the data with the command

```
SetScale d 0,0,"m",xW
```

(type it into the command line and press return). Alternatively, you can find this command in the **Data | Change Wave Scaling...** menu. Then for practice, set the units for both `Iw` and `Iw_err` using the menus or with the command

```
SetScale d 0,0,"V",Iw,Iw_err
```

Here's a quick way to enter this command. Rather than typing the whole thing, press the up arrow once to highlight the previous command, then press Enter to copy the command to the command line. Now adjust the text of the latter portion to produce the new command.

Perhaps you are wondering what the two zeros are doing in this command? Me too. Let's ask what's going on. Select the word "SetScale" and right click (control-click on Macintosh). A contextual menu pops up from which you can select **Help for SetScale**. This is a handy way to find out what commands and functions do. In this case, it appears that the zeros are pretty worthless.

Plotting the Data

Now we plot the data using the menu command **Windows | New Graph...** and the ensuing dialog or with command

```
Display Iw vs xw
```

(You're probably getting the feeling that anything you can do in the menus, you can do straight in the command line. Learning Igor's magic words isn't too hard, since you can start with the menus/dialogs and then learn the commands that construct and execute, which are nearly always echoed in the history area above the command line.)

By default, Igor connects the data points. We would like to show discrete points and to plot error bars. The speedy way to manage this is from the HMC menu: **Fix Graph**. If you'd like to do things manually, then either right-click on a data point and select **Modify IW...** from the popup menu or use the menu bar command **Graph | Modify Trace Appearance...** to bring up a dialog to change the display. Select **Markers** for the Mode, and pick a marker you like.

Notice that the x axis is displayed in millimeters and the y axis in volts, since we have set units for the x and y waves. We'd like to change the label of the x axis to "Position (*unit*)". Double-click the label (`mm`) and enter in the Axis Label field:

```
Position (\U)
```

and click **Do It**. The `\U` is a code for the units. Now change the y axis label to "Intensity (\U)".

Fitting the Data

We now prepare to fit the data by defining constants to be used in the fitting function. Type the command

```
Variable lambda = 632.8e-9
```

into the command line. This creates a global variable named `lambda` having the value 632.8 nm, corresponding to the laser wavelength. While you're at it, create a variable `k` with the value 2π/lambda via

```
Variable k = 2*pi/lambda
```

and a variable `r0` (rzero) equal to 1.212 meters for the experimental setup of Chris Moore

```
Variable r0 = 1.212
```

(Note that `r` is reserved by Igor for a special purpose, so we have used `r0`.) Now define the fitting function by initiating a nonlinear fitting operation. From the menu bar, issue the command **Analysis | Curve Fitting...** Make sure that the **Function and Data** tab is selected, and click on the checkbox ☒ From Target. This restricts the choice of data to the waves present in the topmost graph (of course, that's our only graph at this point, but it can be quite helpful in general). Make sure that the **Y Data** menu displays `Iw` and the **X Data** menu displays `xW`.

Click the New Fit Function... button and enter a name for your fitting function (e.g., `DiffCirc`). Then select the **Fit Coefficients** box and enter the parameter names 'Imax','a','xzero', and 'Izero', putting one parameter on each line by hitting `Enter` after each parameter name. Then select the **Independent Variables** box and type `x` followed by `Enter`. At this point, the **Fit Expression** box should have the text "f(x) = " and the Status box should display "The coefficient `Imax` is not used in the fit expression." Enter the text of the fitting function so that the **Fit Expression** box reads as follows:

```
NVAR k, r0
Variable arg = k * a * (x - xzero) / r0
// Trap for the case where arg == 0, and substitute the value 1
Variable bess = arg == 0 ? 1 : Besselj(1, arg) / arg
f(x) = 4 * Imax * bess^2 - Izero
```

Then click the Save Fit Function Now button. If you have entered the text successfully, the function will compile and you will be returned to the **Curve Fitting** dialog. A short explanation is in order. The first line informs the fitting function of the global variables `k` and `r0`. The second line creates a local variable named `arg` and sets its value. The final line computes the value of the fitting function using the intermediate variable `arg` to simplify the expression.

Click the Data Options tab and select `Iw_err` from the Weighting menu, making sure that the button ⦿ Standard Deviation is selected.

Click the **Coefficients** tab to enter guesses for the parameters:
`Imax = 5`, `a = 1e-4`, `xzero = 0.013`, `Izero = 0.1`.
Click the Graph Now button to see if the calculated curve looks close to the data values. If so, click the Output Options tab. If not, check your work. Did you remember to define all three variables **lambda**, **k**, and **r0**?

In the Residual menu of the **Output Options** tab, select _auto trace_. You should also check the box ☒ Add Textbox to Graph. You can customize the automatic content of the fit results box by clicking the Textbox Preferences... button. For example, we checked the ☒ Fit Function Name box. Finally, click the Do It button.

The fit should converge properly. Click OK in the **Curve Fit** dialog box, and the fitted values for the parameters will be added to the graph in a text box. From the HMC menu select the command Add ChiSq Information. Then click the button Move Fit Info near the top of the graph to move the fit information from the bottom of the graph to the right side. You should get a graph like this:

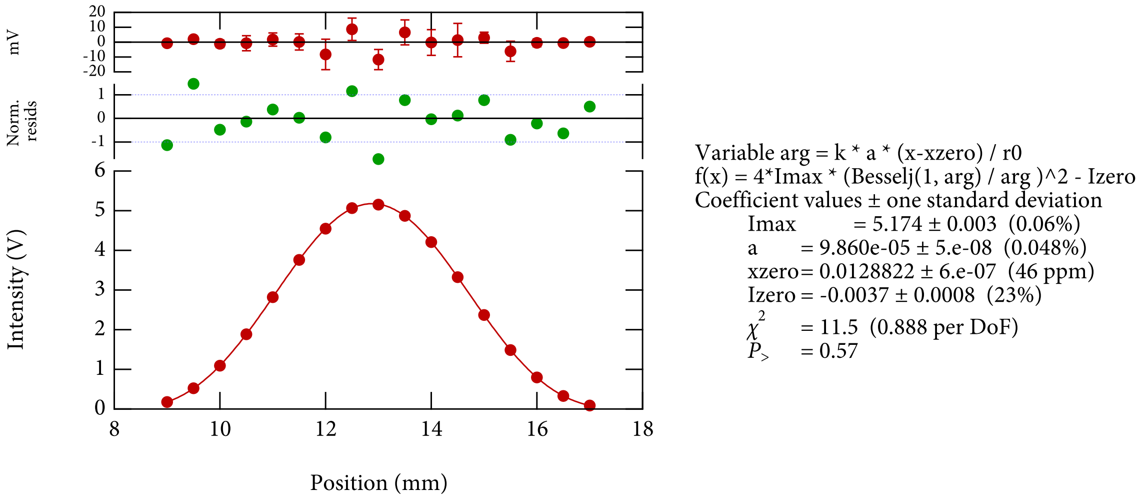

Note that the fit information, as modified by the **Add ChiSq Information** command adjusts the display of uncertainties to provide both absolute and relative uncertainties, and reports both χ^2 and reduced χ^2, as well as the probability that one would obtain a value of χ^2 at least this large on repeating the experiment with the same number of data points.

Fitting Straightedge Diffraction Data

Because Igor can calculate the Fresnel sine and cosine integrals, it is straightforward to fit your Fresnel diffraction data in a similar way to that described above for Fraunhofer diffraction data. An example is shown in the figure below.

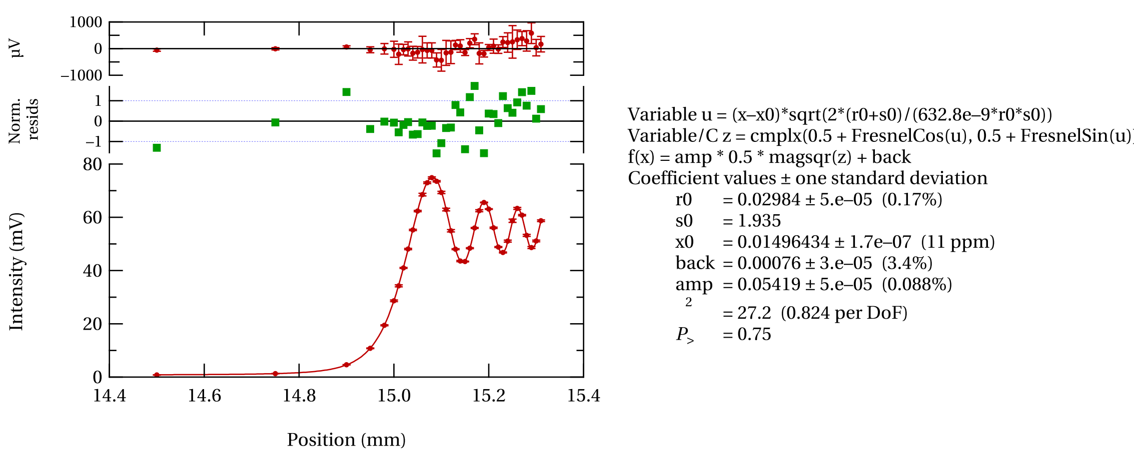

This figure was made using the data taken by Candace Church and Joe Checkelsky (both HMC '04) available in the file candace_joe.dat on the PC in the lab. The three columns in this text file hold position, intensity, and uncertainty for 37 data points. After loading the data into Igor and renaming the waves, I set their units and magnitudes with the following commands:

```
SetScale d 0,0, "m",Position
SetScale d 0,0,"V",Intensity,Intensity_unc
Position /= 1000
Intensity /= 1000
Intensity_unc /= 1000
```

to take advantage of Igor's automatic SI prefixing mechanism. I then created the plot with

```
Display Intensity vs Position
```

and used the command **Fix Graph** from the HMC menu.

To perform the fit, start the Fitting dialog from the **Analysis** menu as usual, and click the **New Fit Function...** button to define the fitting function for Fresnel diffraction from a straightedge. As you can see from the information at the right side of the plot, rather than trying to write the whole function in a single expression, I found it much more convenient to define a pair of intermediate variables. The first one is defined by

```
Variable u = (x - x0) * sqrt(2*(r0+s0)/(632.8e-9*r0*s0))
```

and represents the argument to the Fresnel sine and cosine integrals. The second is defined by

```
Variable/C z = cmplx(0.5 + FresnelCos(u), 0.5 + FresnelSin(u))
```

The **/C** switch tells Igor to make **z** a complex variable, whose real part is set to $\frac{1}{2} + \mathscr{C}(u)$ and whose imaginary part is set to $\frac{1}{2} + \mathscr{S}(u)$. The final line of the fitting function specifies the actual value returned:

```
f(x) = amp * 0.5 * magsqr(z) + back
```

It uses the **magsqr** function to compute the squared magnitude of the complex number **z**.

Note from the figure that the deduced values for the fitting parameters are expressed in the base SI values (m and V); to get the fit to converge properly, it was necessary to check the ☒ Hold box next to parameter **s0** (why?) and to enter initial guesses close to the right values. I usually have to try a few different values, clicking the **Graph Now** button to see how close my guesses are until the curve is fairly close to the data.

Exporting the Graph for a Report

You can print your graph at this point. If you wish to export it for inclusion in a report, there are a few options, all available from the **File | Save Graphics...** command.

- You can just copy and paste into a Word document. This produces a platform-dependent picture (either a windows Metafile or Macintosh picture). As long as you don't transfer to the other platform you should be fine.
- For a platform-independent graphic, you can use **File | Save Graphics...** and save a PNG file at 2x or 4x screen resolution.
- For use in LaTeX, select a PDF file (for pdflatex) or an encapsulated PostScript (EPS) file if you are using a traditional latex compiler. This command produces a vector graphics copy of your graph that will scale properly to any size. You can then include it with a standard LaTeX command, such as `\includegraphics[width=4in]{filename}` .

Appendix B

Data Analysis Using MATLAB

MATLAB is a software package for scientific computation and visualization and is produced by The Math Works, Inc. At HMC, MATLAB is used on PCs, Macs, and Unix/Linux workstations. MATLAB's Optimization Toolbox includes a routine LSQCURVEFIT for nonlinear least-squares fitting. While the default fitting algorithm is a "subspace trust-region method based on the interior-reflective Newton method", the Levenberg-Marquardt algorithm is available as an option. It is reassuring to note that both algorithms give identical results for the Checkelsky-Church data (see below). Fabio Rojas and David Painter (both HMC '96) and Kevin Moore ('99) wrote a MATLAB graphical user interface (GUI) called MatFit that facilitates the fitting of straight edge data to the standard function involving Fresnel sine and cosine integrals. The GUI is really just a collection of "M" files, so if you are familiar with MATLAB you can extend the GUI to fit circular aperture data to an expression (Eqn. (1-1)) containing the first Bessel function.

MATLAB 2011a is available on all of the computers in the lab, in particular the computer associated with the diffraction setup. Before you begin fitting your data in MATLAB, you will want to perform two file manipulations. First, create a text data file (but give it the extension .dat rather than .txt) and copy it to the working subdirectory c:\matfit. Your data file should consist simply of three columns of numbers: position, intensity, and uncertainty in intensity. Example data collected by Candace Church and Joe Checkelsky (both HMC '04) are contained in the file candace_joe.dat. (See the plot below.) Second, you will want to edit the file razorfun.m to set the distance s from the razor to the detector equal to the value appropriate to your setup. Candace and Joe used s = 1935 mm. To edit razorfun.m, just locate the file icon in c:\matfit and double-click on it. Wait *patiently* for the MATLAB editor to load and then perform the editing and save

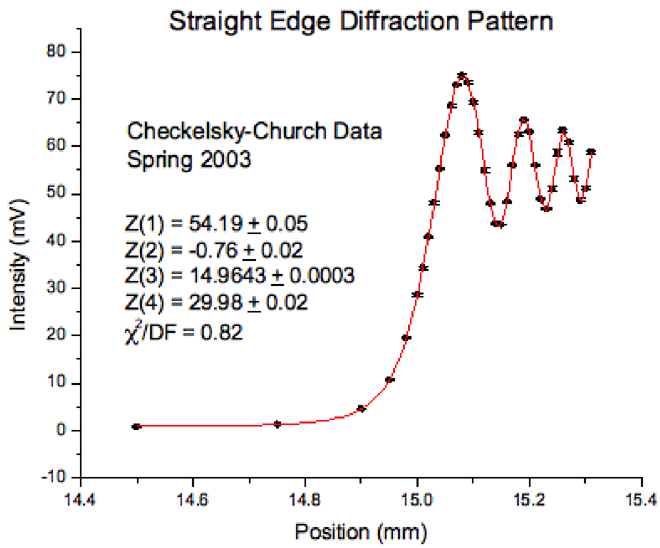

the edited file. More will be said below about the file razorfun.m.

To begin your MATLAB fitting session, select Start—All Programs—MATLAB R2011a or double-click on the MATLAB 2011a shortcut on the desktop. Now set the default directory to c:\matfit by typing into the MATLAB command window:

cd c:\matfit

Now run the MatFit "M" file to enter the MATLAB GUI environment written by Rojas/Painter/-Moore. Type into the MATLAB command window:

MatFit (Caution: case-sensitive!)

A plot window appears with a number of menus laid out across the top of the window.

Data File—Load Datafile Click on the "Data File" menu and highlight the "Load Datafile" menu item. Find your data file in the pop-up directory window, then double-click on it. Your data should now be plotted in the plot window.

Fitting—Fit Data Click on "Load Function File" and double-click on the file razorfun.m in the "Files" list. Also click in the "Initial Values for Fitting Parameters:" box, and type, for example, "Z = [55 0.5 15 30]". (That's a *capital* Z! See below for a discussion of these initial values.) Click on "Start Fit".

At this point a few words of explanation are in order. The file razorfun.m defines the fitting function:

f(x) = Ifinal * 0.5 * ((C+0.5)^2 + (S+0.5)^2) + Izero where C and S denote the Fresnel cosine and sine integrals with argument

arg = (x-xzero) * sqrt(2/lambda * (1/s + 1/s_prime))

The fitting parameter s_prime is the distance between the spatial filter aperture and the razor blade - Candace and Joe measured this to be 30 mm. The fitting parameters are contained in the vector Z = [Ifinal Izero Xzero s_prime], so you should enter their initial values in the appropriate order.

After a few seconds the Marquardt algorithm will converge (assuming your initial values make sense), and the fitted curve will be added to the plot. (Move the MATLAB R2011a window around to see the MatFit v1.0 window.) You can monitor the progress of the fitting procedure in the MATLAB R2011a window. The column labeled “f(x)” contains the value of chi-square at each iteration. When convergence is achieved, you are asked in the command window to name your plot of the residuals which will appear in a separate window. Enter, for example, "Normalized Residuals." Next enter a label for the x-axis of the plot of residuals, e.g., “Position (mm).” Then enter a label for the y-axis, "(Fitted Point - Data Point)/sigma".

Back in the MatFit v1.0 window, add some information to the plot of the data and the fit.

Plot Options—Show Fitting Results The final values of the fitting parameters, their uncertainties, and chi-square/degree of freedom will be pasted into the plot. Just move the cross-hairs to the point on the plot where you want the upper-left corner of the text box to be, and then left-click with the mouse.

Plot Options—Change Plot Settings You can label the axes and add a title. Click in the “Title” box and type “Straight Edge Diffraction Pattern”. Click in the “x-Axis Label” box and type “Position (mm)”. Click in the “y-Axis Label” box and type “Intensity (mV)”. If you wish, you can add a comment in the “Placeable Text” box, e.g., your name and date. Click on “Done”. Then position the cross-hairs where you want the upper-left corner of your “placeable text”, and left-click with the mouse.

Plot Options—Print Plot You can obtain a hardcopy of your plot on the Scandal_DeskJet6940 printer located in Jacobs B121.

In the Figure No. 2 window,

File—Print Use the standard MATLAB utilities to print a hardcopy of your plot of the normalized residuals on the Scandal_DeskJet6940 printer located in Jacobs B121.

Of course you can always use the standard MATLAB utilities to save the plot of the normalized residuals as a jpeg or bitmap or other graphic format. Unfortunately that is not true of the plot of the data with fitted curve because that plot is not a standard MATLAB figure. An alternative is described below.

During the fitting procedure, MatFit saves the fitted curve to a file named “FittedPoints.txt” in the c:\matfit directory. The file “FittedPoints.txt” may be readily imported into Origin as a single ascii file, and you may then combine the data for the fitted curve with your experimental data points. When you have combined all of this data into a single Origin worksheet, you may reproduce in Origin the plots you created in MATLAB, both data plus fitted curve and also the plot of normalized residuals. These plots can then be copied and pasted into a Word document. Below we simply used standard MATLAB utilities to save a .jpg version of the Normalized Residuals plot in Figure No. 2, and then inserted the figure here:

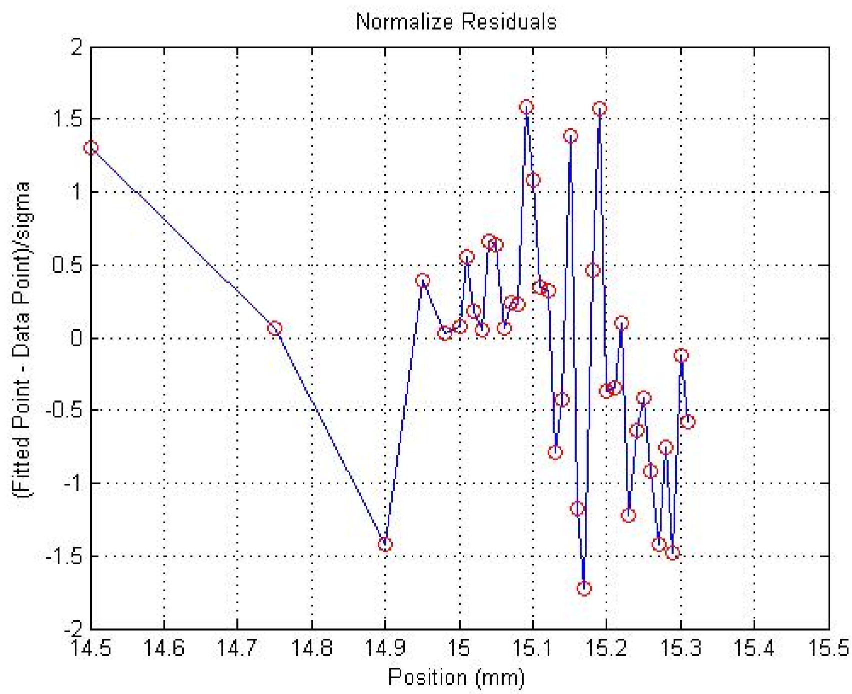

To exit the program, return to the MatFit 1.0 window and select Quit—Quit MATLAB.

Appendix C

Data Analysis Using Origin on a PC

Origin is a data analysis and graphics package produced by OriginLab for the Microsoft Windows environment. Origin includes a nonlinear least-squares fitting routine based on an algorithm by D.W. Marquardt (see Bevington and Robinson, Section 8.6). Origin supports the use of Bessel functions in fitting functions, so it can readily be used to fit diffraction data from a circular aperture. Version 9.0 of Origin is installed on the hard drives of the lab computers, and when run, these installations obtain a license from an HMC server. We shall describe how to use Origin 9.0 to fit diffraction data from a circular aperture.

x	I	sigI
9	0.176	7.07107E-4
9.5	0.5222	0.00132
10	1.094	0.00245
10.5	1.886	0.0051
11	2.82	0.00447
11.5	3.76	0.00548
12	4.546	0.0103
12.5	5.064	0.00748
13	5.154	0.00678
13.5	4.87	0.00837
14	4.208	0.0086
14.5	3.326	0.01122
15	2.372	0.00374
15.5	1.484	0.00678
16	0.7944	0.0026
16.5	0.3302	0.00102
17	0.0862	3.74166E-4

Table C.1: data

Log on to a Windows computer in the Optics Lab (or in the computer labs on the HMC campus) and launch Origin 9.0. When the main Origin window appears, you will probably want to maximize the Book 1 worksheet window and type in your diffraction data or load it from a text file. To facilitate the discussion in this Appendix A, we have placed our diffraction data in a text file named CircularMoore2004.dat (data donated generously by Chris Moore HMC '05) that resides on our computer's hard drive, and we will use the Import feature of Origin to load our data into the Worksheet. Our data file CircularMoore2004.dat has three columns (see Table C.1): the first column contains the position of the detector (in mm), the second contains the intensity (in volts), and the third is the uncertainty (in volts) in the intensity. The intensity and its uncertainty are actually the mean intensity and the standard deviation of the mean (standard error) deduced from five scans through the diffraction pattern.

File—Import—Single ASCII That is, click on “File” to pull down the File menu, then slide the mouse down to “Import”, then slide the mouse over to “Single ASCII...” in the Import submenu.

We then switched directory folders on our computer’s hard drive to find the data file CircularMoore2004.dat; and double-clicked on CircularMoore2004.dat to open it.

Because our data file has headings on the columns, the import filter creates data columns with those headings. If you create a data file without headings, you can label the columns simply by double-clicking on the heading of the column and typing in a name. Our columns are labeled “x”, “I”, and “sigI.” You can also add units for each column. (If “####” is displayed instead of a data value, just broaden the column width by grabbing the right vertical boundary line and moving it to the right. That will provide enough space in the column to display the full value in scientific notation.)

The position values in CircularMoore2004.dat are in millimeters. To convert the values to meters, highlight the x column (click on the heading) and then

Column—Set Column Values Type “col(x)/1000” and then click “OK”. The values in the x column should now be in meters.

This is a good time to type into the row titled “Units” the appropriate units for each column. Origin will then automatically label graphs with the units appropriate for each data column. We typed in the units “meters”, “Volts”, and “Volts”, respectively.

Next we tell Origin that the sigI column contains uncertainties for the I column. Highlight the sigI column and then

Column—Set as—Y Error The sigI column should now have (yEr±) behind its name.

To plot the data with error bars, highlight all 3 columns by clicking on the name of one column and dragging the mouse across the tops of the other 2 columns, then

Plot—Symbol—Scatter A plot will be created. (The System Theme is fine — click OK.) In order to see the error bars on the plot, we had to reduce the size of the data symbol from 9 points to 5 points — double-click on the data symbol in the legend and select the font size you want.

To change the label on the y-axis, double-click on the current label (“I (volts)” in our case) and replace it with your choice of label. Similarly for the x-axis.

We now prepare to fit the data by defining constants to be used in the fitting function.

Window—Script Window Type “lambda=632.8e-9” and then hit Enter. A semicolon will be appended to the line. (The wavelength of the laser is 632.8 nm.)

Type “k=2*pi/lambda” and hit Enter. (k is the wavenumber.)

Type “r=1.212” and hit Enter. (The distance from aperture to detector was 1.212 meters in Chris Moore’s experimental setup.)

We now define the fitting function.

Analysis—Fitting—Nonlinear Curve Fit—Open Dialog...

In the NLFit window, click on the "f(x)" icon to create a new function (left-center on the screen).

In the Fitting Function Builder window, type "DiffCirc" into the Function Name box.

In the Description box, you might want to type in "Fit circular aperture diffraction pattern with Bessel functions".

Click on "Next" and in the Parameters box, type "Imax, a, xzero, Izero".

Click "Next" and in the large Function Body box, type the fitting function as an expression:

"4*Imax* (J1(k*a*(x-xzero)/r)/(k*a*(x-xzero)/r))^2 + Izero"

Now in the Parameters table, enter the initial values for the fitting parameters. Just double-click on the space where the value is to be entered, and type in the value. We entered 5.2 for Imax, 1e4 for a, 0.013 for xzero, and 0.001 for Izero. Note that an initial guess of zero for any parameter may give the nonlinear fitting routine trouble when it tries to calculate the derivative of χ^2 with respect to that parameter — it will not be clear what step size to use in the derivative.

You can now click "Finish", or simply click "Next" repetitively through the next few windows until you are forced to click "Finish". You will be dumped back into the NLFit window.

Next click on "Data Selection" (in the Settings tab of the NLFit window) and in the Weights box, select "Instrumental" which will weight the data with the values in the sigI column.

Now click on the button which is roughly in the middle of the window. The Messages tab will display the calculated value of (about 48,000 for Chris Moore's data and our initial guesses). The fitted curve will be superposed on the plot of the data — just move the NLFit window to see it.

Click on the "1 Iteration" button just to the right of the button. The Messages tab will display the new value after the single iteration (about 8000 for Chris Moore's data and our initial guesses).

Click on the "Fit until converged" button (just to the right of the "1-Iteration" button) and look for the results in the Messages tab and for the new fitted curve on the plot of the data (just move the NLFit window to see it).

Click "OK" and say "No" to the report sheet. You will be dumped into the "Graph1" window with the plot of the data and the fitted curve superposed, and the results box pasted onto the plot. You can click on the results box and drag it to a convenient place on the plot. The same is true of the legend box. See our plot of the fit to Chris Moore's data on the next page. You can always return to this "Graph1" window by double-clicking on the "Graph1" icon at the left-center of the Origin screen, or just use the Window menu at the top of the Origin screen.

If you click on the "Project Explorer" tab on the left side of the screen, and double-click on the "CircularMoore2004" icon (the name depends on the name you give to the data), you will return to the original data window (or you could have used the Window menu at the top of the Origin screen) which now has two additional tabs accessed at the bottom of the window. If you select the "FitNL1" tab, you can explore the results of the fit. If you select the "FitNLCurve1" tab, you will see a table of the fitted curve and residuals.

While viewing the "FitNLCurve1" window, "copy (full precision)" the column of residuals and paste them into the main datasheet tab in a new column. To create new empty columns in the main datasheet, go to

Column—Add New Columns Make two new columns, one labeled "Residuals" and one labeled "NormResid" into which you can place the normalized residuals.

After you have pasted the residuals into the "Residuals" column, create the normalized residuals by clicking on the remaining empty column and using

Column—Set Column Values Set the new column values equal to col(residuals)/col(sigI).

Plot NormResid versus x. This is your plot of the normalized residuals!

You can get a hard copy of the plot of the data with fitted curve (click on the graph and choose File—Print) or copy the plot to the clipboard (Edit—Copy Page) and then paste it into a document (as we have).

Our value of 0.89 for χ^2 per degree of freedom ($17-4=13$ degrees of freedom) indicates that our fitting function provides a fit to the data with a 55% chance of being exceeded if the measurements were repeated.

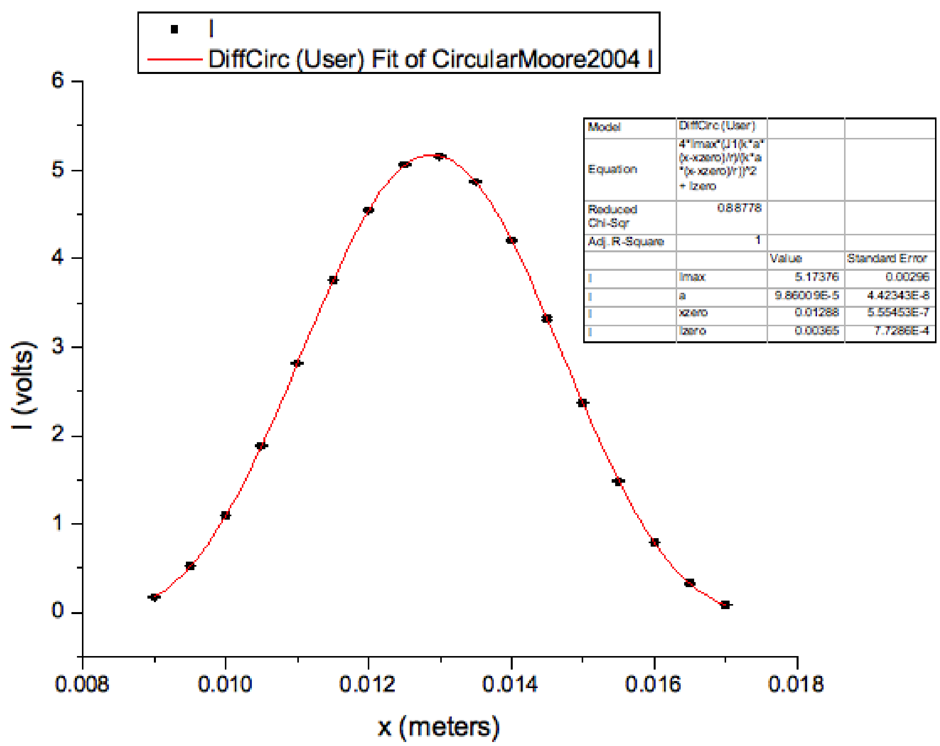

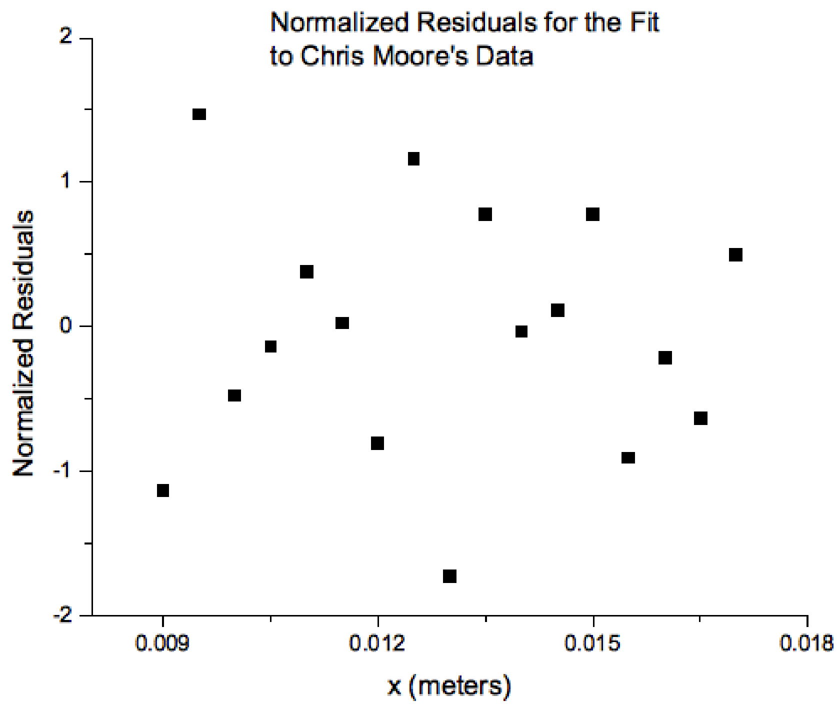
Normalized Residuals for the Fit
to Chris Moore's Data
Normalized Residuals
x (meters)
2
1
0
-1
-2
0.009
0.012
0.015
0.018